UNIVERSITÀ DELLA CALABRIA

Facoltà di Scienze Matematiche, Fisiche e Naturali

Dottorato di Ricerca in Scienze della Terra
XXIII CICLO – Settore Geo-01 – Geo-02

Tesi di Dottorato

Carbonate Deposition in Tufa Systems: Processes and Products

Tutor
Dott. Edoardo Perri

Coordinatore
Prof. Franco Russo

Co-Tutor
Prof. Maurice Tucker

Dottoranda
Dott.ssa Elena Manzo

Preface

Tufa is a category of freshwater limestone that occurs at spring sites, waterfalls and in fast-flowing streams, where waters are in a supersaturated condition with respect to the mineral phase that precipitates. The products that originate from these systems are commonly low Mg-calcite-deposits, with various crystal fabrics, formed by the calcification of microbial biofilms, bryophytes and plant remains. Different research topics related to this type of deposit are currently being examined in academia and industry: as palaeo-proxies in Quaternary palaeoclimate reconstructions, as potential biomarkers in geomicrobiology and biogeochemistry studies, and finally as potential hydrocarbon reservoir rocks.

The object of this PhD research project has been the study of the precipitation processes involved in active tufa systems, occurring in different climatic and depositional settings (NW Calabria- NE England). In particular the research has focused on the role of microbial communities in the precipitation process, in order to understand the relation between microorganisms, metabolic processes and mineral precipitation products. In the literature, although the study of biochemical processes leading to carbonate precipitation in modern microbial communities has been pursued in the field and in the laboratory, the mechanisms of crystal nucleation and mineral growth structures, such as the final texture of the deposits, are less investigated. Furthermore, if microbial communities have been well studied in some marine domains, calcifying freshwater biofilms that create tufa deposits, essentially remain unknown. Investigations of mineralizing biofilms and mats are mainly based on the measurement of bio-chemical parameters, whereas the study of the mineral component (fossil and modern precipitates) is often limited to the traditional thin-section, petrographic approach. Only recently, with the use of high-powered scanning electron microscopes has it been possible to start investigations on the ultra-structure of the organo-minerals, both at the interface with the organic components that induce their formation in living systems, and for discerning their mechanisms of formation in ancient microbialites.

In this project traditional study methods have been used, including fieldwork, sampling of the depositional facies, and petrographic and geochemical analyses, coupled with high-powered scanning electron microscope (SEM-ESEM) techniques for the micro-morphological and nano-structural study of the organic and mineral components. Moreover, to investigate the nano-structures of the tufa neo-precipitates formed in association with organic matter under the SEM, a combination of fixation and dehydration techniques have been used to avoid alteration of the organic tissues and the possible modification of the delicate mineral ultra-structure.

The thesis starts with an introductory chapter (Chap.1) on the existing knowledge of modern tufa environments reported in the literature, followed by 10 chapters divided into 2 parts:

- the first part (Chap. 2 to Chap. 7) illustrates the general climatic and geological context of the studied tufa sites. In particular, the sedimentological, petrographical and geochemical features of tufa deposits forming in different depositional environments have been examined, together with the characterization of the chemical properties of tufa-depositing waters. The analyses of the data collected have allowed sedimentary models to be defined for the studied tufa systems; these have been compared with the models reported from similar climatic settings.

- the second part (Chap. 8 to Chap. 11) reports the study of the micro and nano-structural features of tufa neo-precipitates, formed in association with microbial biofilms. In order to understand the relation of mineral product and organic matter, some field experiments have been performed at selected tufa sites. Tufa neo-formed crusts and already existing naturally-formed deposits have been observed with different microscopic techniques, with a view to obtaining useful information to understand the mechanisms of crystal nucleation (at the nano-scale) and growth mineral structures, such as the final texture of such organo-minerals. Results provide new insights into the interpretation of the origin of the minerals in terms of biotic and abiotic processes.

Acknowledgments

I would like to show my gratitude to my supervisors: Edoardo Perri and Maurice Tucker. Edoardo supported me in a number of ways from the initial to the final level of this experience; with his patience, he taught me how to be rigorous towards the research, encouraging me with precious advices. Prof. Tucker with his charisma, inspiration, and great enthusiasm for the Geology, enriched my passion towards the research.

I'm grateful to all people and institutions made the work presented here possible; in particular I would to thank: The University College staff, my friends Juan, Sarbani and Robert, as well as and the Master and Vivienne, that, during my visiting period in Durham, with their kind and friendly hospitality made this experience truly memorable. A special thank to Mariano Davoli, Valentino Pingitore, Carmine Apollaro, Mike Mawson and Leon Bowen for their great helpfulness.

At the end of this 3-years study period I'm once more grateful, to my parents, my brother and my grandfather, that still encourage me to pursue my interests, even if could mean they would take me away from them. Finally, many thanks to two special friends, Marco and Barbara, that, during the infinite times that I stressed them with my "paranoie", encouraged me to follow my dreams.

TABLE OF CONTENT

RIASSUNTO *p. v*

1. CONTINENTAL CARBONATE DEPOSITS: TUFA **» 1**

1.1. TERMINOLOGY » 1
1.2. CLASSIFICATIONS » 2
1.3. PETROGRAPHY AND FABRICS » 6
1.4. DIAGENESIS » 8
1.5. ENVIRONMENTAL MODELS AND FACIES ASSOCIATIONS » 9
1.6. PRECIPITATION PROCESSES » 19

PART I
TUFA DEPOSITIONAL ENVIRONMENTS

2. STUDY SITES **» 25**

3. METHODS **» 28**

4. TUFA ENVIRONMENTAL SYSTEMS **» 31**

4.1. BARRAGE SYSTEMS » 31
4.2. TERRACED SLOPE SYSTEM » 41
4.3. TUFA OVERHANGING LOBES » 45

5. WATER CHEMISTRY **» 48**

6. TUFA DEPOSITIONAL FACIES **» 56**

6.1. MINERALOGY AND GEOCHEMISTRY » 56
6.2. PETROGRAPHY AND MINERAL FABRICS » 64
6.3. FABRIC OCCURRENCE IN TUFA DEPOSITIONAL FACIES » 67

7. FACTORS CONTROLLING TUFA DEPOSITIONAL SYSTEMS: DISCUSSION **» 73**

7.1. TUFA ENVIRONMENTS AND FACIES ASSOCIATION » 73
7.2. WATER CHEMISTRY » 76
7.3. GEOCHEMISTRY » 77
7.4. ORIGIN OF PETROGRAPHIC FACIES » 81

PART II
NEO-PRECIPITATED MINERALS AND ASSOCIATED BIOFILM COMPONENTS

INTRODUCTION **» 83**

8. BIOTA **» 85**

9. THE BIOFILM STRUCTURE **» 88**

9.1. NANO-SCALE FEATURES OF NEO-PRECIPITATES IN THE ACTIVE DEPOSITIONAL ZONE » 90

9.2. PETROGRAPHIC FEATURES OF NEO-PRECIPITATES » 94

10. BIOFILM MEDIATION IN MINERAL GENESIS: DISCUSSION **» 97**

10.1. BIOTIC VERSUS ABIOTIC INTERPRETATION OF THE PETROGRAPHIC COMPONENTS » 101

11. CONCLUSION **» 105**

REFERENCES **» 108**

Riassunto

L'oggetto della ricerca è lo studio sedimentologico, geochimico e geomicrobiologico di sistemi attivi di *tufa* calcarei, in diversi contesti ambientali e deposizionali, finalizzato alla comprensione dei processi che determinano la formazione di questa particolare tipologia di carbonati continentali.

I *tufa* (o travertini meteogenici) sono depositi carbonatici di acque dolci, principalmente formati dalla mineralizzazione di biofilm microbici (composti da batteri, funghi ed alghe eucariotiche), briofite e resti vegetali. Tale processo avviene in acque sovrassature rispetto alla calcite, che è il principale costituente di questi depositi. In letteratura sono stati proposti alcuni processi per spiegare la formazione dei tufa, che si basano su meccanismi diversi: da esclusivamente fisico-chimici (abiotici) ad unicamente legati ad attività biologiche (biotici), con varie posizioni intermedie. Nella prima visione i tufa sono depositi carbonatici inorganici, mentre nella visione opposta i tufa sono depositi organogeni, microbiologicamente prodotti, pertanto definibili microbialiti. Il principale fattore abiotico alla base della precipitazione del minerale è il degassamento di CO_2 dell'acqua, che porterebbe ad una calcificazione passiva dei substrati organici ed inorganici presenti; mentre i fattori biotici che porterebbero alla formazione di minerale sono principalmente la fotosintesi dei cianobatteri e secondariamente le altre attività metaboliche dei microrganismi eterotrofi, legate alla degradazione della materia organica.

I tappeti ed i biofilm microbici che producono depositi microbialitici sono stati studiati in dettaglio in alcuni contesti marini, mentre quelli che sviluppano in acque dolci (come quelli associati ai *tufa*) sono in parte sconosciuti. In questi sistemi, le metodologie di studio applicate per la comprensione dei processi di precipitazione, sono principalmente basate su misure dei parametri biochimici (CO_2, DIC, pH etc.), alla macro e microscala, nell'interfaccia biofilm/deposito. Inoltre lo studio della componente minerale (fossile e neo-precipitata) è spesso analizzata attraverso un tradizionale approccio petrografico in sezione sottile, che permette di distinguere la micrite, microsparite e sparite, che sono, di fatto, i prodotti più comuni delle microbialiti marine e non marine. In generale, è accettata un'origine biotica solo per i precipitati neoformati (micrite), mentre la neoformazione di sparite (cemento) è considerata abiotica. Recentemente, lo studio in microscopia elettronica degli organominerali ha suggerito che l'ultra struttura dei cristalli può essere utilizzata per discriminarne l'origine biotica o abiotica. Infatti, l'approccio metodologico seguito nella ricerca ha integrato le metodologie di studio sedimentologiche, geochimiche e petrografiche "classiche", con tecniche di microscopia SEM ultrastrutturale, abbinate a protocolli istologici di campionamento e preparazione campioni, per lo studio dell'interfaccia componente organica-minerale nei siti di nucleazione dei cristalli.

Ai fini del progetto, sono stati campionati e studiati dei depositi di *tufa* che attualmente si formano nel settore NO della Valle del Corvino in Calabria settentrionale e in diverse aree dell'Inghilterra nord-orientale. In queste aree sono stati individuati e campionati tre sistemi

deposizionali: sistemi fluviali a barriere (fiume Parmenta- NO Calabria e fiume Thornley NE Inghilterra), sistemi su pendii a gradinata (Barnard Castle- NE Inghilterra) e lobi sospesi in prossimità di sorgenti (Sunderland e Barnard Castle, NE Inghilterra).

In tutti i sistemi deposizionali studiati, indipendentemente dalla dimensione dei depositi, sono state individuate due principali macro-morfologie deposizionali: le dighe, che si sviluppano come barriere sinuose e/o irregolari, che originano pozze di acqua quasi stagnante; e i lobi, protendenti dalle pareti di valle delle dighe, o sospesi sul versante a formareo protuberanze concave verso il basso. E' stato osservato che la frequenza, dimensione e forma delle barriere e dei lobi, sono determinate dalla interazione delle caratteristiche litologiche, giaciturali degli strati, ed inclinazione del substrato sottostante.

Le facies deposizionali osservate nei sistemi studiati, sono rappresentate principalmente da depositi autoctoni e secondariamente da depositi alloctoni. Il primo gruppo include croste stromatolitiche, *framestones fitoermali* (sensu Pedley, 1990), formati da muschi incrostati e micro-lobi formati dell'alga *Vaucheria,* e tufa fitoclastici (sensu Pedley, 1990) formati da resti vegetali incrostati; il secondo gruppo è formato da pisoidi e "cave pearls". Le osservazioni suggeriscono che la suddivisione tra framestone fitoermali e tufa fitoclastici, termini comunemente usati in letteratura, non è applicabile ai casi in esame, poichè queste facies deposizionali "estreme" non sono state osservate singolarmente a formare morfo-facies significative. Infatti, le facies individuate sono state costantemente trovate associate a formare depositi porosi, come per esempio i muschi incrostati, i micro-lobi a *Vaucheria* e i tufa pustulari, che possono essere chiamati complessivamente depositi di tufa vacuolari.

In tutte le suddette facies deposizionali sono stati riconosciuti identici componenti petrografici: micrite e microsparite, che sono spesso associati a formare fabrics peloidali, afanitici, laminari e dendrolitici e sparite, che si può presentare in livelli composti da cristalli botroidali isolati o coalescenti a formare croste continue. In generale i fabrics osservati nelle diverse facies studiate, sono organizzati in livelli che si ripetono ciclicamente. Questa caratteristica è ben visibile sia nei depositi laminati alloctoni e sia in quelli alloctoni (tufa stromatolitici, croste laminate e pisoidi). Persino nei tufa pustulari, in cui sono presenti diverse fasi cristalline (livelli ricchi in manganese, calcite fibrosa, microsparite afanitica), è visibile questa ciclicità.

Nonostante la variabilità dei sistemi di tufa studiati in termini di composizione geochimica delle acque, condizioni climatiche, geologia del substrato drenato, tutti i depositi sono composti da calcite a basso contenuto di magnesio (Mg 1.0 - 3.5 moli %). La distribuzione degli elementi minori, quali Sr, Mn, Fe, S è variabile. La calcite nei depositi del Parmenta è caratterizzata da un contenuto di magnesio comparabile con i valori riportati in letteratura mentre è arricchita in stronzio (0.5 - 0.8 moli%). I valori del magnesio sono attribuibili alle variazioni stagionali di temperatura dell'acqua del fiume Parmenta (8°-17°). La presenza di evaporiti (solfati) e dolomie

ricche in Sr nel substrato, influenzano la quantità di Sr presente nella calcite. Nei depositi che si formano nel fiume Thornley, la calcite a basso contenuto di magnesio è arricchita anche in Mn (0.2 – 1.8 moli%), Fe (0.2 – 1 moli%) and S (1.1 – 2.4 moli%). La presenza di tali elementi minori rappresenta una fase carbonatica di transizione tra la “normale” precipitazione di calcite a basso contenuto di magnesio ed i livelli formati da fasi cristalline manganesifere non carbonatiche (probabilmente organominerali), che seguono una possibile variazione delle condizioni di Eh-pH dell’acqua del fiume. Inoltre, la composizione chimica del fiume Thornley, che appartiene ad una facies idrochimica di origine bicarbonatica-solfatica-calcica, influenza l’arricchimento di S nella calcite. L’origine degli ioni solfato potrebbe derivare dalla degradazione della materia organica nei suoli e/o dall’ossidazione della pirite presente nel substrato non carbonatico che costituisce il bacino idrogeologico del fiume Thornley.

L’osservazione in microscopia elettronica a scansione (SEM-ESEM) delle croste neo-formate, ha mostrato che la precipitazione del carbonato avviene più o meno costantemente all’interno di una zona deposizione (active depositional zone ADZ), che si estende per poche centinaia di micron attraverso la superficie esterna del deposito. La precipitazione è attribuita alla presenza di un esteso biofilm (presente in tutti i siti di studio) che vive all’interno della ADZ e ne determina la formazione. Il biofilm è generalmente composto da cianobatteri filamentosi endolitici ed epilitici, alghe verdi, procarioti unicellulari, Actinobatteri e funghi, con una quantità variabile di sostanze polimeriche extracellulari (EPS). Quando il biofilm è assente, non si osserva precipitazione e questo suggerisce che le attività biologiche del biofilm sono cruciali, sia in presenza di microrganismi viventi e sia con materia organica non vivente. L'ADZ è caratterizza da micro-colonne di dimensioni comprese tra i 50 ed i 150 µm, separate da cavità interstiziali ed è presente in tutte le stagioni. La precipitazione del minerale avviene sia sulla superficie esterna dell’ADZ e sia all’interno delle cavità. Ulteriori punti di precipitazione sono presenti lungo i ciuffi dei cianobatteri filamentosi, che si estendono al di sopra della superficie di deposizione.

I neo-precipitati osservati sono rappresentati da nano-cristalli sub-sferici (nao-sfere) di 10-20 nm di diametro. Essi generalmente si formano sostituendo e replicando micro-particelle di materia organica in degradazione (qualunque tipo), ed in punti ristretti lungo la superficie esterna dei filamenti di cianobatteri. Essi pertanto sono organominerali. Le nano-sfere si aggregano a formare per prima aggregati cristallini a ”bastoncino” (100-200 nm), che evolvono in triadi di fibre di calcite e successivamente dopo un'apparente aggregazione casuale, formano solidi disfenoidali. Sia le triadi di calcite (tozze e lunghe), sia i solidi disfenoidali, si uniscono a formare cristalli più grandi (principalmente tetraedri di una decina di micron di diametro) che rappresentano i "mattoni" per la costruzione delle micro-colonne. Pertanto, i depositi di tufa studiati sono da considerarsi totalmente prodotti da processi di mineralizzazione biotici.

Il confronto tra le caratteristiche petrografiche e le nano-strutture dei tufa neo-formati osservate nel monitoraggio effettuato per circa un anno nel fiume Parmenta, ha mostrato che ogni componente petrografico, nonchè la sua ultra-struttura in termini di aggregati cristallini primari, è legata alle variazioni stagionali di temperatura. Nel periodo più freddo, abbondano microcristalli di disfenoidali, che nel periodo intermedio vengono gradualmente sostituiti da triadi tozze e, successivamente, nel periodo più caldo da triadi lunghe. Questi tre aggregati cristallini primari corrispondono, in termini petrografici, rispettivamente a: sparite, microsparite e micrite. Tali termini acquisiscono quindi un significato solo descrittivo nell'ambito dei tufa, e probabilmente in tutti i depositi microbialitici, senza alcuna implicazione genetica nella loro origine abiotica o biotica.

1 CONTINENTAL CARBONATE DEPOSITS: TUFA

1.1. Terminology

Calcareous tufa or *meteogene trevertine* is a category of continental limestone that forms in a range of freshwater settings, including streams, lakes, springs and paludal environments, without the influence of marine water.

The terminology adopted for this category of carbonates is controversial because of the mixed use of descriptive and genetic terms, together with the common usage of the alternative term travertine, mainly adopted in Spain, USA and parts of Europe, whereas the term tufa is used mainly in English-speaking countries and generally throughout northern Europe (Pedley, 2009).

According to Pedley (1990), Ford & Pedley (1996) and Pedley (2003), the terms tufa and travertine should be utilized separately to distinguish two categories of continental carbonates. In fact, they propose the term *tufa* for carbonate precipitated under cool-water conditions (near ambient temperature) and the term *travertine* for carbonate deposits derived from $CaCO_3$ precipitation in thermal water.

A typical feature of tufa deposits is the presence of the high content of encrusted plant tissues and microbial biofilms, that produce distinctive porous fabrics (Pedley, 1992, 2000). By contrast, travertine deposits are less porous because of a minor amount in plant material, since vegetation growth is disadvantaged by the water temperature, and generally they are characterized by well-cemented laminites (Pedley, 1990).

A further terminological distinction can be based on the different geochemical proprieties of the depositional environment, as proposed by Pentecost (1993), Pentecost & Viles (1994) and Pentecost (2005). According to these authors the main distinguishing factor for a genetic subdivision is the origin of the dissolved CO_2 in the water. This is either derived from soil or thermal sources and they recommend use of just one term, travertine, with the addition of the terms *meteogene* and *thermal* respectively, as appropriate.

In the *meteogene* deposits the origin of the CO_2 derives principally from carbon dioxide fixed from the atmosphere in terrestrial vegetation and associated soils. These carbonates form typically in cold-water springs and streams in regions underlain by carbonates or occasionally evaporites (gypsum). Moreover, according to Pentecost (2005) *meteogene travertines* can be divided into two categories: *evasive* where carbon degassing leads to travertine deposition, and *invasive* where the reverse process leads to deposition. Both can be further subdivided into *ambient meteogenes*, the most frequently encountered where the water is at ambient temperature, and the *superambient meteogenes* where through deep circulation the water rises at a temperature above that of ambient, and often as hot springs (>37°C).

In *thermogene travertines* the origin of the carbon dioxide derives from thermal processes within or even below the Earth's crust. These carbonates have a restricted distribution in comparison with the meteogene deposits, because usually they are associated with regions of volcanic or tectonic activity. Although in many cases the source water is hot, the term thermogene is referred to the source water rather than the exit temperature of the water.

1.2. Classifications

In the literature various criteria have been used to classify calcareous tufa, and these consider different aspects such as: the abundance and type of the biota, the sedimentological setting and/or the facies and microfacies association (Table 1.1).

Many of the early schemes, based on deposits in southern Germany, used a botanical approach, classifying the deposits in terms of the presence and type of the main biota incorporated in the deposits, as algal tufa, moss tufa and inorganic calc-sinters (Irion & Müller, 1968). A flora-based classification was also used by Pentecost & Lord (1988) in their study of tufa and travertine from Yorkshire, England. They recognized several cyanobacterial tufa, named after the dominant genera (e.g., *Homeothrix, Schizothrix, Rivularia* and *Scytonema*); bryophyte tufa (in the same way named after the dominant genera, such as *Rynostegium, Cratoneuron, Gymnostomum* and *Eucladium*) and unconsolidated tufa or 'spring chalk', which often forms around the base of wetland plants such as *Carex* and *Juncus*.

Several alternative schemes of classification were based on general sedimentological or geomorphological criteria. Buccino et al. (1978), working on ambient temperature deposits (tufa) in central Italy, introduced and developed the use of prefix terms, such as 'phytoherm' and 'phytoclast' to distinguish autochthonous from allochthonous deposits and provided generalized petrological identifications. A comparable, facies-based approach was developed by Ordóñez & Garcia del Cura (1983) for the tufa deposits within the Madrid Basin, Spain. Here, a distinction was made using three levels of classification: macrostructure, controlled by the position relative to the water-table and topography; mesostructures controlled by the ecology, distinguishing autochthonous 'vertical-tube facies' (phytoherms) and allochthonous or 'detrital tufa facies'; and microstructure, controlled by the efficiency of degassing.

Pedley (1990), later refined by Ford & Pedley (1996) attempted to rationalize earlier tufa terminologies to produce an overview in which existing terms were redefined and expanded into an outcrop-based tufa classification scheme. Their classification, mainly based on the petrological and sedimentological observations of Buccino et al. (1978), Chaftez & Folk (1984) and Ordóñez & Garcia del Cura (1983), divided tufa lithotypes on the basis of genetic origin of the mineralized

components and of the fabric types, into: autochthonous and clastic deposits. Two types of deposit were recognized as autochthonous: *Phytoherm framestone* and *Phytoherm boundstone* that correspond to phytoherm tufa and stromatolitic tufa of Buccino et al. (1978).

- *Phytoherm framestones* are characterized by a primary framework constituted by living hydrophytes and semi-aquatic macrophytes, frequently colonized by a dense and often felted microbial biofilm. A diverse fauna inhabits these structures and commonly includes annelids, ostracodes, insect larvae and molluscs. These are cemented by thick fringes of low-Mg calcite isopachous cements. Voids filled of phytoclastic, micritic (often peloidal), and detrital tufa are common.

- *Phytoherm boundstones* are represented by in-situ calcified bacteria. This tufa type is dominated by skeletal stromatolite and consists entirely of cement fringes formed in intimate associated with Oscillatoriacean cyanobacteria. Coarse detrital intraclastic tufa and oncoids generally occur with these phytoherms. Both these types of autochthonous deposit are considered freshwater reefs (Pedley, 1992; Pedley 2000) in which mainly prokaryotic and eukaryotic microorganisms play an active role in the precipitation of the carbonate minerals (see session 1.6).

In the category of clastic deposits, authors included the following tufa types:

- *Phytoclast tufa* (corresponding to phytoclast tufa of Buccino et al., 1978 and crossed-tube facies of Ordóñez & Garcia del Cura, 1983) generally consist of allochthonous, cement-encrusted plant fragments. Typically, this is composed of leaves and transported branch fragments forming a "grain-support fabric". Phytoclasts are cemented together after deposition, though some earlier cement development around phytoclasts may have occurred prior to or during their transport.

- *Cyanolith 'oncoidal' tufa* (oncolites of Ordóñez & Garcia del Cura, 1983) are composed of a cyanobacterial-cement fringe association. The shape of these oncoids is determined by prevailing levels of environmental energy. Generally the highly spheroidal forms dominate in rivers, whereas strongly oblate spheroidal forms are typical of sluggish flow regimes, and free-form growth-forms (mammilated to irregular branching) of static conditions. Detrital woody fragments often form the nuclei to these cyanoliths and are rolled along as cylinders. Generally they form a grain-supported fabric associated with smaller tufa intraclasts or even micrite.

- *Intraclast tufa* (detrital tufa facies of Ordóñez & Garcia del Cura, 1983) are dominated by silt and sand-grade detrital tufa fragments derived from breakup of phytoherm frameworks. These can be deposited as grain-supported fabrics in fluvial channels or can accumulate around phytoherm frameworks in static water bodies, where supporting frameworks have decayed.

- *Microdetrital tufa* comprise *micritic tufa* and *peloidal tufa* that generally in thin section are characterized by a “grumose texture”.

- *Palaeosoils* may be associated with tufa and are a function of the variations of the water-table. Generally the lowest horizon consists of degraded tufa including tufa cobbles, whereas, the upper horizon is humus-rich and often contains pulmonate gastropods.

Glover & Robertson (2003) studying a mid-Late Quaternary palustrine-lacustrine tufa environment in NW Turkey and using the classification proposed by Pedley (1990), recognized two further types of clastic deposits: *pisolith tufa* (inorganic deposits) occurring as clusters of hard, nearly spherical, pea-like balls (c. 0.5 cm in size), commonly forming small cross-bedded lenses; and *tufa breccia* composed of intraformational reworked tufa, made of angular, poorly-sorted fragments of phytoclast and phytoherm tufa in a matrix of silt- and sand-grade detrital tufa.

Based on the origin of the components of tufa deposits, Pentecost & Viles (1994) in a review of travertine classification, classified deposits based on three main criteria: geochemistry, microfabric and morphology. According to this scheme meteogene and thermogene travertine can be represented by eleven categories, divided into two sub-groups. The first sub-group, with eight categories contains all of the autochthonous deposits associated with springs, streams, rivers, lakes and marshes. In these deposits they differentiated three main types of microfabric: microbial tufa that include different 'stromatolitic' forms, as oncoids, shrubs, algal tufts (e.g. *Vaucheria*); bryophyte tufa represented by mosses and liverworts; and inorganic tufa characterized by sinter, mainly in thermogene travertine and pisoids. The allochthonous deposits comprise the clastic travertines.

More recently, Carthew et al. (2006) working on active and Quaternary tufa deposits in northern Australia expanded the classification reported by Pedley (1990) and proposed a scheme for the common tufa facies in tropical monsoonal environments. According to the authors autochthonous facies comprise:

- *microphytic facies* (corresponding to the phytoherm boundstone of Pedley, 1990) that include four subtypes, termed: brain, spongy, thrombolitic and compact;

- *larval facies* characterized by calcified dwelling tubes formed by a variety of insect larvae, net-building caddis flies and moths;

- *macrophytic facies* (corresponding to the phytoherm framestone of Pedley, 1990) and characterized by calcite-encrusted bryophyte stems and leaves (bryophyte facies) and calcified roots (root-mat facies);

- *calcite raft facies* consisting of calcite sheet crusts;

- *microdetrital facies* consisting of micritic mud;

- *shell facies* containing articulated mollusc shells in life position and often associated with macrophytic root-mat or microdetrital facies.

Pedley (1990)		Pentecost and Viles (1994)		Glover and Robertson (2003)		Carthew et al. (2006)	
Facies type	*Description*	*Facies type*	*Description*	*Facies type*	*Description*	*Facies type*	*Description*
Autochthonous							
Phytoherm boundstone	In situ stromatolitic build-ups (cemented Oscillatoriacean cyanobacteria)	Microbial	Oncoids, bacterial scrubs, stromatolites, algal tufts (e.g. Vaucheria)	Phytoherm boundstone	In situ stromatolitic build-ups	Microphytic -brain -spongy -thrombolitic -compact	In situ calcification of prokaryotes-eukaryotes biofilm
Phytoherm framestone	In situ cemented plant material (hydrophytal and semi-aquatic macro-phytes)	Bryophyte	Encrusted mosses and liverworts	Phytoherm framestone	In situ cemented plant material (hydrophytal and semi-aquatic macro-phytes)	Macrophytic -root-mat -bryophyte	In situ calcification of roots and mosses
X		X		X		Larval	In situ calcification of insect larvae
X		Inorganic	Calcite raft	X		Calcite raft	Floating calcite crusts
X		X		X		Microdetrital	Structureless to clotted micrite *sensu* Pedley (1990)
X		X		X		Shell	Mollusc shells in life position
X		Inorganic	“Sinter”, most pisoids	X		X	
Clastic allochthonous							
Phytoclast tufa	Allochthnous, cemented-encrusted plant fragments	Clastic		Phytoclast tufa	Allochthnous, cemented-encrusted plant fragments	Phytoclast	Allochthnous, cemented-encrusted plant fragments
Cyanolith “oncoidal” tufa	Sub-spherical stromatolites			Cyanolith “oncoidal” tufa	Sub-spherical stromatolites	Oncoidal	Sub-spherical stromatolites
				Pisolith tufa	Finely laminated, inorganic, spherical balls.		
Intraclast tufa	Reworked deposits dominated by silt- and sand-size fragments	Intraclast		Intraclast tufa	Silt-and sand-size detrital material, rich in plants	Intraclast tufa	Sand to boulder-size detrital tufa, re-cemented together
Microdetrital -Micritic tufa -Peloidal tufa	Structureless to clotted	Peloids		Microdetrital -Micritic tufa -Peloidal tufa			
X		X		Tufa breccia	Detrital origin		
		X		X		Lithoclastic	Non-tufa clasts
Paleosols	Soil profiles resulting from variation in water table	X		Paleosols	Moderately developed, carbonate-rich	X	

Table 1.1. Classification schemes and common features of authochthonous and allochthonous tufa deposits.

In the allochthonous deposits they distinguished four different types including:

- *lithoclastic facies* formed by detritic clasts cemented together by tufa crusts;

- *phytoclastic facies* consisting of calcified plant leaves, stems, branches and bark and containing abundant voids preserving the location of this decayed material;

- *intraclastic facies* formed by eroded tufa deposits successively re-cemented together, that can range in size from sand to boulder;

- *oncoidal facies* composed of nodules formed from calcified cyanobacteria.

1.3. Petrography and fabrics

Calcareous tufa is basically constituted by low-magnesian calcite, which precipitates from the water body on all exposed surface. The calcite crystal-sizes commonly occur are: micrite, less than 4 microns in size, and sparite, in excess of 62 microns (Pedley, 1992) and only locally microsparite, 4-62 microns (Arp et al. 2001a).

According to Pedley (1992) micrite can form fringes or peloids. Micrite fringes are constituted by optically dense micrite of 20-200 μm in thickness. They may have a clotted appearance, which may give the outer surface of the fringe an undulate appearance upon which a subsequent spar fringe may develop. Peloids, single or aggregated, vary in size from 4 to 70 μm reaching 100 μm in diameter in multi-nucleate peloids. Nuclei adhere directly together without growth of a further acicular calcite spar coating, though a spar coat commonly collectively entombs peloid aggregates. Micrite locally can have a structureless fabric or can develop on cyanobacterial filaments to form a filamentous micritic zone.

Encrusted filamentous bacteria are widely reported in various tufa deposits (Ordóñez & Garcia del Cura, 1983, Freytet & Plet, 1996; Feytet & Verrecchia, 1998; Jassen et al., 1999; Arp et al., 2001a; Kano et al 2003; Carthew et al., 2006). This fabric can be compared with the "algal bushes" of Love & Schafetz (1988) that is characterized by bushes formed by radiating structures, as cyanobacterial tufts, that directly control the growth of the crystals (Pentecost, 2005). The dominant species forming these micro-structures is the *Phormidium incrustatum*, even if it is commonly associated with other prokaryotic species such as *Rivularia, Schizothrix, Lyngbya and Scytonema*, as well as various eukaryotic algae such as *Cymbella, Gomphonema and Navicula*, that can influence the fabric of single laminae (Freytet & Plet, 1996; Freytet & Verrecchia 1998).

According to Pedley (1992) spar fringes that commonly are found alternated with micritic fringes, consist of narrow (30-500 μm) fringes of clear, sparry calcite. From active tufa deposits in Belgium, Jassen et al. (1999), reported more or less continuous layers of sparry calcite fans, from

500 µm to 1 mm in thickness, that typically are characterized by sweeping extinction under crossed polars.

Concerning the origin of the micro-scale lamination commonly found in tufa deposits, several different hypotheses have been suggested to explain their origin in term of primary fabrics: 1) a combination of seasonal changes in microbial growth (biological), 2) primary organically induced precipitation of sparry calcite crystals around cyanobacterial filaments (reported for specific species of cyanobacteria such as. *Rivularia haematites* and *Phormidium foveolarum*- Freytet & Plet., 1996), 3) changes in the rate of calcification (inorganic), and 4) diagenetic modification (see below) (e.g. Irion & Muller, 1968; Pedley, 1992; Freytet & Plet, 1996; Freytet & Verrecchia, 1998; Janssen et al., 1999; Arp et al., 2001a; Kano et al., 2003).

The first explanation of micrite-sparry couplets in term of primary products (combined biotic/inorganic processes) is that the micritic layers (laminae and peloids) are the product of biological mediation associated with a procaryotic-microphytic biofilm, whereas the bladed-spar fringes are inorganic precipitates (Pedley, 1992). According to this author the cyclicity can be explained as follows: during the spring-summer cyanobacterial-diatoms blooms are more abundant and lead to the development of a sub-millimetre biofilm at the substrate-water interface. Here, water exchange rates are sluggish or even static on account of the felted intergrowth of cyanobacteria, bacteria and diatoms. Further CO_2 intake by attached prokaryotes and microphytes, in the presence of organic matter and decomposition products, triggers the precipitation process, resulting in the precipitation of a micrite fringe characterized by a clotted or peloidal texture. Successively, during the autumn-winter interval, death of procaryotes and microphytes together with an increase of the water flow favour the development of a bladed-spar fringe resulting from inorganic precipitation on to the micritic lamina formed in the summer.

Although in the above described hypothesis the micritic layer, mainly described as a continuous fringe or peloidal, is produced through biofilm mediation, there is no explanation for the origin of the "filamentous micritic zone" that is well documented in other tufa localities. As mentioned above, the common cyanobacterial species forming these bush-like micro-structures is the *Phormidium incrustatum* that usually is the main component comprising the porous micritic laminae.

Freytet & Plet (1996) working on modern *Phormidium*-stromatolites in France proposed that bush-like cyanobacterial growths dominated by *Phormidium incrustatum* α (arranged as radiating filaments) were lightly calcified in the interval from May to December (spring-summer-winter) whereas cyanobacterial growths dominated by *Phormidium incrustatum* β (densely arranged parallel filaments) formed dark (dense) micritic texture in the interval from January to April (winter-spring).

A similar seasonal pattern has been recognized in specimens collected in England and Belgium, and has been attributed to seasonal change in cyanobacterial growth (Pentecost & Spiro, 1990; Janssen et al., 1999). In an active fluvial tufa system in Germany, Arp et al. (2001a) observed that the fabric of laminated tufa crusts reflected the temporal alternation of porous microsparitic *Phormidium incrustatum-Phormidium foveolarum*-diatom biofilms in spring, micrite impregnated *Phormidium incrustatum-Phormidium foveolarum*-diatom biofilms in summer-autumn, and detritus-rich non-calcified diatom-biofilms in winter.

In southwest Japan, Kano et al. (2003), instead, reported a laminated pattern characterized by densely calcified summer laminae where calcite (micrite) thickly encrusts cyanobacterial filaments and pore spaces, and more porous, weakly calcified laminae form in winter. The authors proposed that the lamination pattern is primarily controlled by seasonal changes in calcite precipitation which correlates positively with dissolved $CaCO_3$ concentration and water temperature. An increase in dissolved $CaCO_3$ in summer-autumn results from elevated underground pCO_2, which originates from the diffusion of CO_2-rich soil-air and limited ventilation.

Another common feature of many laminated European tufa and tropical tufa (Carthew et al., 2003; Carthew et al., 2003), are bands of hollow tubes alternating with cyanobacterial bushes. The tubes appear hemispherical (typically convex-upward) in cross-section and are usually between 0.5 and 5 mm long, 0.2 and 0.5 mm high; individual tubes can be traced up to 15 mm in hand specimen. These tubes are attributed to living and feeding burrows of chironomid (midge) and Trichoptera (caddis fly) larvae (Irion & Müller, 1968; Freytet & Plet, 1996; Janssen et al., 1999), formed during the spring before the larvae pupate, and preserved when covered by summer/autumn calcification of cyanobacterial micrite and/or sparry calcite fans (e.g. Janssen et al., 1999). The presence of larval tubes may be the best unequivocal indicator of spring laminae, although water flow and warmth are probably the primary controls on larval abundance (Andrews & Brasier, 2005).

1.4 Diagenesis

The main diagenetic modifications that can occur in tufa deposits are related to the effects of meteoric diagenesis, in which the major processes are carbonate recrystallization, dissolution and the formation of soils (Tucker, 2001).

Recrystallization is a process that involves changes in the mineralogy and/or fabrics of the sediments. The process of replacement and recrystallization between one mineral and itself or a polymorph, is termed *neomorphism*, that can be distinguished in aggrading and degrading type

(Tucker, 2001): the first type leads to a coarser mosaic of crystals whereas the second results in a finer mosaic of crystals.

Effects of aggrading neomorphism are reported in different inactive tufa sites (Jassen et al., 1999; Freytet & Verrecchia, 1999; Arp et al. 2001a). Comparing recent and sub-fossil tufa deposits, Jassen et al. (1999) concluded that the effects of diagenetic modifications can be attributed to the disappearance of the organic matter due to natural decay, which causes recrystallization and cementation of micritic cyanobacterial bushes, changing them into sparry crusts with the formation of new calcite crystals in which the traces of filaments gradually disappear.

Similarly, Freytet & Verrecchia (1999) recognized that two types of recrystallization form can develop: (1) isodiametric (equant) crystals, resulting from either the recrystallization of micrite or microsparite, or primary sparite (mainly on *Rivularia, Dichothrix,* diatoms, *Scytonema* and coccoid felts); and (2) radial palisade crystals (often with micro-lamination) with sweeping extinction when seen under crossed polars.

Dissolution occurs when deposits become exposed to an undersaturated solution with respect to a carbonate mineral, such as direct rainfall and soil-percolation water. This may lead to karsification and the dissolved products may be capable of re-precipitating. This may be the mechanism by which stalactites and flowstones are formed within old tufa/travertine caves (Pentecost, 2005).

Finally, although a possible primary inorganic origin for sparry layers and fringes in many modern tufa deposits has been proposed in the literature, at the same time it has been agreed that these layers can be generated through diagenetic modification, and this can start immediately after deposition.

1.5. Environmental models and facies associations

One of the first tufa depositional models was described by Golubić (1969) focused on fluvial and lacustrine settings in tufa-filled gorges in Plitvice National Park, Croatia. Successively, Chafetz & Folk (1984) used a morphological criterion to classify travertines in Italy and USA, recognizing the following types: waterfall or cascade deposits, lake-fill deposits, steeply sloping mounds, fans or cones, terraced mounds, and fissure ridges.

As already mentioned, a list of tufa types, classified according with their environmental setting, has been provided by Pedley (1990) and successively reviewed in Ford & Pedley (1996). They grouped tufa depositional environments into five basic models: perched spring-line, cascade, fluvial, lacustrine and paludal. These models were based on the geometry and profile details together with information on typical bed associations and characteristic facies, and derived from

fieldwork carried out on Quaternary and recent deposits that occur in temperate, semi-arid, tropical and arid settings. Below follows a brief description of the characteristics of each model, together with the main variations proposed by further authors.

- *Perched springline model*.

This type of tufa commonly develops in hilly country and typically on steep valley sides. The slope travertine system of Violante et al. (1994) directly compares with this model, as do travertine fans (Chafetz & Folk, 1984), cliff-drape tufas (Viles & Goudie, 1990a) and partially with the terrace morphology of Kano & Fujii (2000).

Perched spring-line deposits are fan-shaped in plan and wedge-like in profile (Chafetz & Folk, 1984), with the thickest deposits located close to the spring (Pedley, 1990) (Fig. 1.1). This model is composed of two elements: proximal and distal deposits.

Proximal deposits (generally point-sourced) develop close below resurgence points. Mature deposits typically show lenticular to wedge-shaped down-slope facing lobate profiles. The upper surface is often gently convex, although mature examples tend towards being extremely flat. Descending, lobate step-like terraces often typify this region and develop on slopes which can exceed 30°. The terraces are decimeters in width, measured parallel to flow, and are typically flat bottomed without a raised rim, even if cascades are locally developed. Some paludal ponds may occur above the terraces, depending of the position of the water table.

Distal deposits are composed of intraclast tufa (Pedley, 1990), which is carried beyond the proximal deposit and deposited on the lower valley slopes as a distally fining, thin detrital tufa spread; these may be incised by channels and contain intercalated palaeosoils. Perched spring-line tufa lies precariously on hill slopes and fluctuations in water-table levels critically control their development (Martin-Algarra et al., 2003).

Terrace tufa morphology reported by Kano & Fujii (2000) consist of a series of stair-like terraces of 30-70 cm in height and 20-100 cm in width, characterized by a raised rim around the edge and a slightly depressed plane towards the back (Fig. 1.2). Their external morphology is similar to rimstone pools forming in caves.

Violante et al. (1994) described four sedimentary environments in spring-line systems; shallow ponds and pool-terraces are located on gentle slopes in the proximal zone, whereas slope and waterfall deposits may be identified on higher inclination slopes in the lower part of the tufa.

Evans (1999) suggested that the preservation potential of the microterraces is low, as they are not present in the Eocene Chadron Formation (South Dakota, USA). However, their absence may simply indicate that these features only form under certain hydraulic conditions, which were not present at this site.

Although not mentioned by Pedley (1990) and Ford & Pedley (1996), tufa stalactites (Viles & Goudie, 1990b) or hanging curtains (Chafetz & Folk, 1984) may form where a cave is present at the base of the hillslope or cliff.

Under temperate conditions, the dominant flora in proximal spring-line deposits consists of bryophytes extensively colonized by cyanobacteria and diatoms (Ford & Pedley, 1996); moulds of leaves may also be identified (Violante et al., 1994). Freshwater and pulmonate gastropods, insect larvae, worms and ostracods are common, particularly in the microterraces and ponded areas around the spring (Pedley, 1990; Violante et al., 1994).

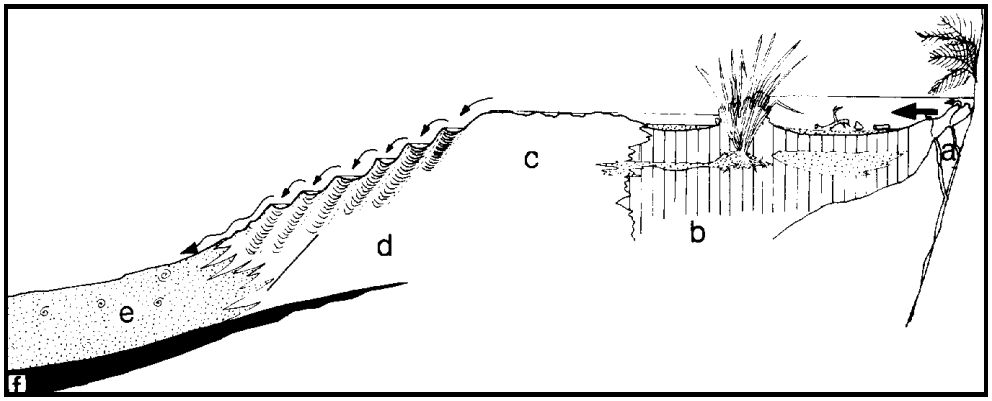

Fig 1.1. Perched spring-line tufa model proposed by Pedley (1990) and Ford & Pedley (1996): a) resurgence point associated with sinter deposits; b) local paludal environment in the vicinity of the spring; c) massive bedded proximal terrace; d) terraced gutter development, e) massive bedded microdetrital tufa containing an extensive pulmonate gastropod fauna; f) palaeosol. Adapted from the Cozzo Marotta tufa deposits, southeastern Sicily.

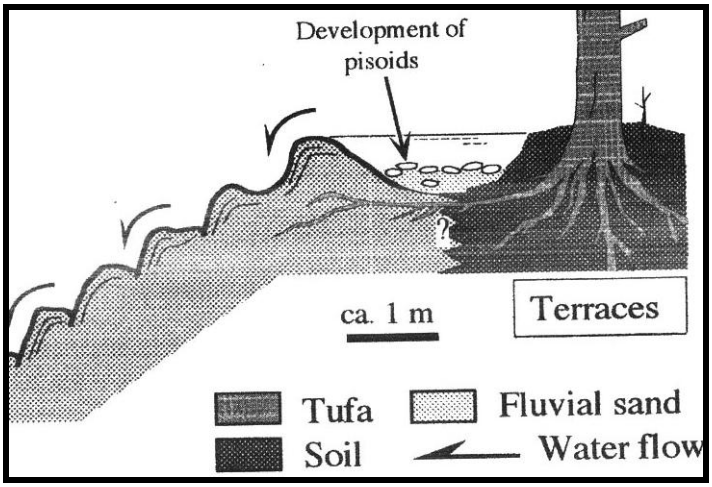

Fig 1.2. Terraces model proposed by Kano & Fujii (2000). Terraces are characterized by a stair-like relief where mosses and secondarily cyanobacteria abound. Pisoids form in weakly flowing water. Based on an active tufa system in Shirokawa, SW Japan.

- *Fluvial models.*

Two end types are recognized: braided fluvial model and barrage model.

- *The braided fluvial model* predominates in areas of unimpeded active fluvial flow, and is similar, but on smaller scale, to that of siliciclastic braid-plain deposits. This model is dominated by cyanolith and intraclast tufa (Pedley, 1990) (Fig.1.3). Commonly cyanoliths with ostracods and charophyte grains are contained in thin tabular or lenticular channel-fill beds.

Small irregularities and living vegetation (phytoherm) obstructions on the channel floor may become the focal point for the development of fluvial stromatolites; these consist of low-relief domes (microherms) which often show preferential thickening of laminae on their downstream faces.

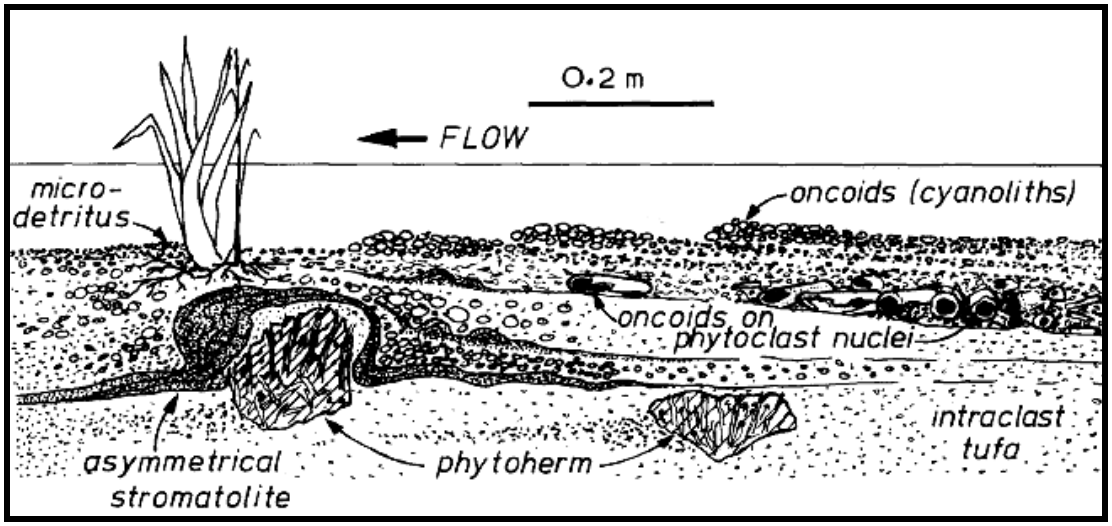

Fig 1.3. Braided fluvial tufa model and related facies association, based on the Ippari valley travertine, southeastern Sicily (Pedley, 1990).

- *The barrage model* generally develops in low gradient water courses and often in gorge settings. The two main features of this model are barrages and pools. Barrages are natural dams that usually form transverse to the watercourse and create pools and lakes behind each barrier (Pedley, 1990; Ford & Pedley, 1996).

Different barrage-pool morphologies and facies associations are reported from different active and fossil examples in diverse climatic regimes (Table 1.2) (Fig. 1.4).

In the cool temperate conditions of NE England, several barrage sites are reported as arcuate buttresses (J-shaped) built of downstream-facing tabular sheets constituted by calcified bryophytes-mosses (phytoherm framestones) (Pedley 1990; Pedley et al 1996; Pedley & Rogerson, 2010).

Pools are shallow and filled by lithoclasts, phytoclasts and microdetrital tufa whereas the marginal areas are dominated by stromatolic deposits, varying from laminar to low relief or oncoidal (Fig. 1.4A).

In warm semi-arid conditions, in the Ruidera National Park of Spain (Pedley et al., 1996; Pedley & Rogerson, 2010), barrages develop as vertical, narrow rimmed arcuate structures, which commonly alternate with deep lakes, both upstream and downstream (Fig. 1.4A). Barrages are broader in the direction of the flow because of the development of a broad ramp-like buttress of inclined tabular bedded tufa on the downstream side of the core areas (Ordóñez et al. 2005). Barrages are characterized mainly by phytoherm framestones and secondarily by phytoherm boundstone, which also compose the steep overhanging carbonate buildups that develop in the marginal area of the lakes.

Pentecost et al. (2000) studying an active barrage tufa system in Gloucestershire (SW England), described barrages ranging in width from 1 to 10 m characterized by a slightly curved crest and a drop wall (wall on the downstream side) convex that commonly overhangs below water level. Here barrages are mainly made of calcified *Vaucheria* tufts forming small keel-shaped mounds, while pools are filled with fine calcareous mud and loose eroded tufa fragments.

In tropical sites of active and fossil barrage systems, Carthew et al. (2003) and Carthew et al. (2006) reported a diverse range of barrage profiles, differing in the wall style (Fig. 1.4B). Rear walls can be characterized by an upper stream-dipping ramp while the drop walls can occur with a downstream-overhanging crest where tufa domes or tufa stalactites can develop, and with a downstream-dipping ramp similar to the J-shaped buttresses previous described. Barrages are reported to be characterized by diverse types of autochthonous and allochthonous deposits (sensu Carthew et al., 2006) that comprise: microphytic, larval and phytoclastic facies, whereas macrophytic facies (phytoherm framestones sensu Pedley 1990) is common in inter-dam pools or on inactive dams. In the pools are also present calcite rafts and microdetrital tufas where there is static water; locally shell facies and stromatolitic-like reefs (phytoherm boundstones sensu Pedley, 1990) characterized by a bulbous morphology, can be present (Carthew et al. 2003).

In the Naukluft Mountains, Namibia, Viles et al. (2007) reported inactive and recent fluvial tufa systems forming along the Tsondab River and the Brandfontein River respectively. In the last tufa develops as a series of large barrages which culminate in a large cascade feature at the mountain front. The main morphologies are reported as downstream prograding barrages, with forward-dipping fronts where, encrusted mosses abound (moss-tufa facies) on the whole faces of the barrages. Moreover, the rear of the barrages in slack-water areas are dominated by laminated and reed tufa facies.

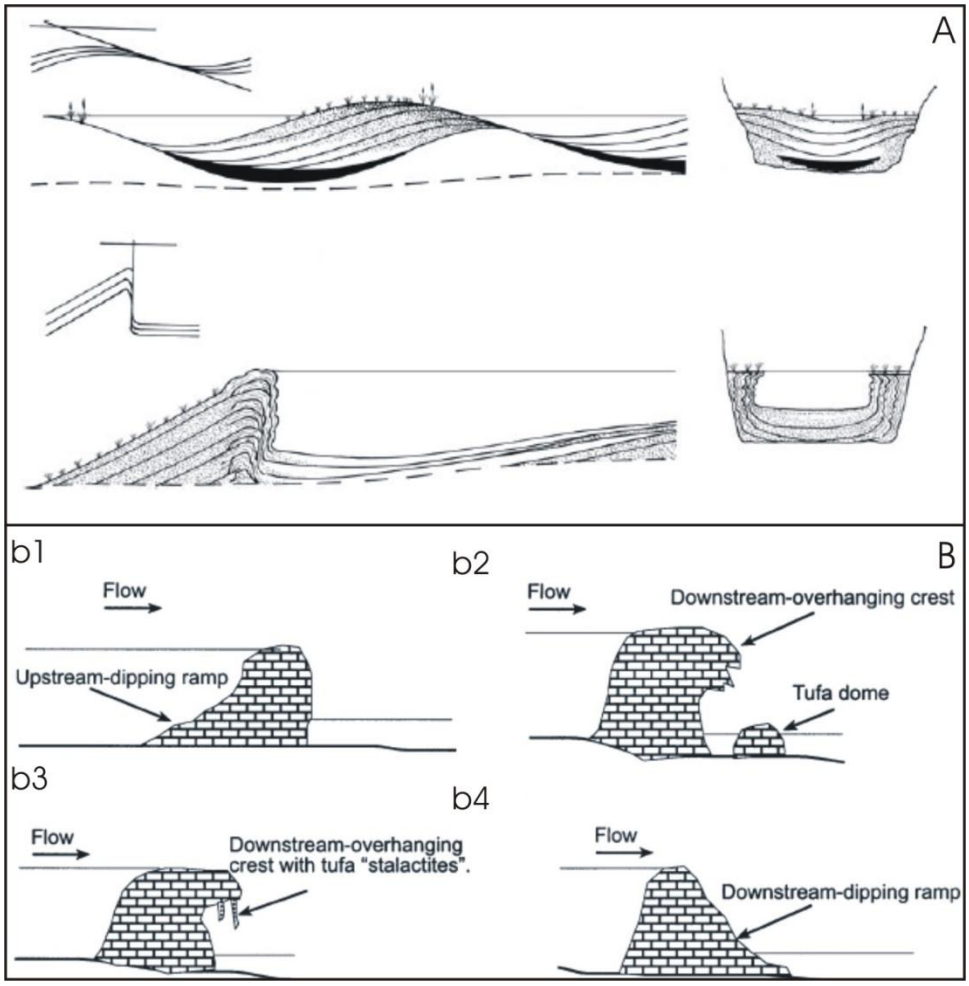

Fig 1.4. Barrage macro-morphologies and associated pools in different climatic regimes. A) Profiles of barrage tufa constructions proposed for cool-humid climates (upper sketch) and warm, semi-arid climates (lower sketch) (from Pedley et al., 2010). In the first case barrages show strong progradation and weak aggradation, resulting in the development of shallow pools upstream whereas in the second case barrages develop almost vertically, mainly due to the aggradation of stromatolites (laminated symbol). This mode of barrage accumulation involved progressive deepening of the upstream pools. B) Common profiles of barrage tufa of Gregory River, Australia (Carthew et al., 2003): b1) rear wall characterized by an upperstream-dipping ramp, b2) drop wall occurring with a downstream-overhanging crest where tufa domes or tufa stalactites (b3) can develop and downstream-dipping ramps (b4) similar to J-shaped buttresses described in cool-temperate conditions.

- *Cascade model.*

Cascades commonly develop wherever vertical surfaces are available, e.g. the periphery of perched spring-line lobes, barrage overflow points and bare-rock gorges. Their external morphology is similar to a barrage tufa, but they are distinguished by the absence of upstream lake deposits (Pedley, 1990; Chafetz et al., 1994). The cascade morphology may be wedge-shaped when discharge rates are high (erosively-shaped deposits) or downstream convex when discharge is less (Pentecost & Viles, 1994) (Fig. 1.5a,b). Overhangs and moss curtains are common on the downstream side, resulting in the formation of tufa caves often containing speleothems (Ford &

Pedley, 1996). Hemispherical moss cushions are locally present beneath the cascades, but these elements are uncommon in many areas (Pedley, 1990). Strings of calcite beads may be found in active cascades (Viles & Goudie, 1990b), and they have also been identified in fossil deposits (Arenas et al., 2000).

Pentecost (1993, 2005) reported two other less common cascade sub-types: 1) keeled cascade, where the water flows along a narrow slot before plunging in a meteogene travertine nose (Fig. 1.5c). (e.g. Caldon Canal, Staffordshire, England) and 2) hummocky well-vegetated cascades, characterized by low water discharge, with a succession of boggy hollows and moss bosses (Fig. 1.5d). These structures have been originally described in Belgium as "crons" and represent a transition between cascades and barrages.

Bryophytes and algae dominate on cascades, as the steep slopes prevent colonization by larger plants (Arenas et al., 2000; Kano & Fujii, 2000). Phytoclasts are periodically washed over the rim of the waterfall and incorporated into the deposit (Pedley, 1990); however, cylindrical cavities preserving evidence of encrusted macrophytes are rare if compared with barrage tufas (Ordóñez & Garcia del Cura, 1983).

Internally, cascade tufa is laminated (Kano & Fujii, 2000), with the orientation of each layer closely related to the shape of the hillslope and steeply inclined at the front of the deposit (Pedley, 1990).

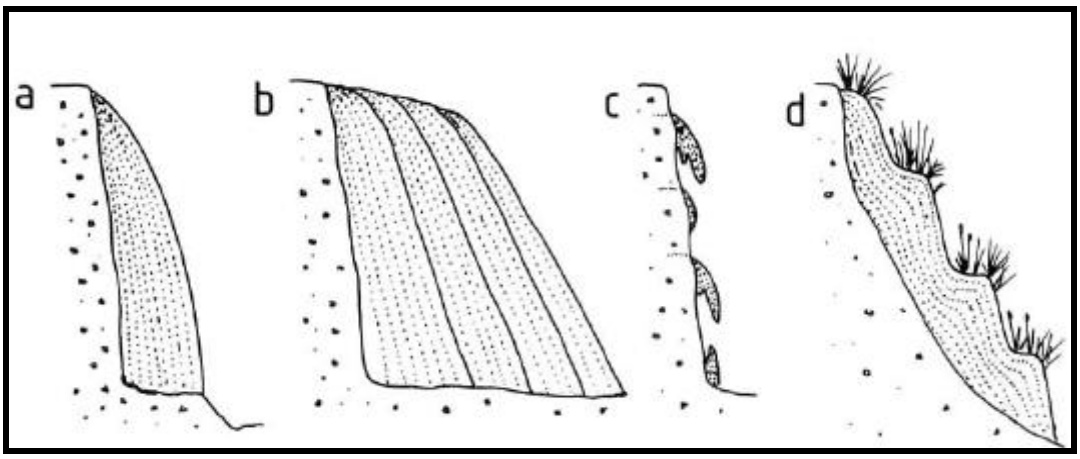

Fig 1.5. Categories of cascade macro-morphologies: a) erosively-shaped deposits, b) prograding type, c) keeled cascade, d) cron. (from Pentecost & Viles, 1994)

Typesite	Ruidera National Park, Spain (active and Quaternary) (Pedley et al., 1996)	N Walles and Derbyshire, UK (active and Quaternary) (Pedley et al., 1996)	Gloucestershire, UK (active) (Pentecost et al., 2000)	NW Australia (active and Quaternary) (Carthew et al., 2003; 2006)	Naukluft Mts, Namibia (active and Quaternary) (Viles et al., 2007)
Climatic context	Semi-arid r.<490mm pa-amwt 18°C	Temperate r.c.1000mm pa-amwt 9°C		Tropical r.535mm pa-amat 25°C	Arid r.200mm pa-amat 20°C
Macro-morphology					
Barrages	Vertical, narrow rimmed arcuate structures. Fast vertical growth	Wide crests, arcuate buttresses built of downstream-facing tabular sheets. Slow vertical growth	Slightly crests with convex dropwalls overhanging below water level.	Diverse barrage profiles, with upstream-dipping ramps common	Downstream prograding barrages with forward-dipping fronts
Pools/Lakes	Deep lakes up and downstream	Shallow upstream pools	Shallow up and downstream pools	Pools and waterholes	Shallow pools
Facies association					
Barrages	Phytoherm framestone Phytoherm boundstone, (sensu Pedley, 1990)	Phytoherm framestone (sensu Pedley, 1990)	Vaucheria tufa (sensu Pentecost and Viles, 1994)	Microphytic Macrophytic Phytoclastic	Tufa moss facies (Phytoherm framestone, sensu Pedley, 1990)
Pools/Lakes	Stromatolitic deposits and oncoids developing in the marginal areas	Lithoclast Phytoclast Microdetrital Stromatolitic deposits and oncoids developing in the marginal areas	Fine calcareous mud and tufa fragments	Microphytic Macrophytic root-mat Lithophytic Phytoclastic Intraclastic Calcite raft Microdetrital Shell Oncoidal Larval	Laminated and reed tufa facies

Table 1.2. Common barrage morphologies and related facies associations, reported in different climate settings.

- *Lacustrine model.*

Lacustrine tufa depositional models comprise elements from shallow marginal areas, where tufa stromatolites, oncoids and intraclast tufa facies are common, through to the profundal zone, where deposition of microdetrital tufa occurs (Fig. 1.6). Lake margin reefs develop on all hard substrates and, once established, grow vertically towards the light; their height is controlled by the water/air interface but many also accrete laterally (Pedley, 1990). A series of flat-topped reefs develop by this process around the lake margins, and can coalesce to form a flat-topped shoreline carbonate rim, which overhangs the deeper parts of the lake. Pinnacle stromatolites may develop in the shaded zone immediately below these overhangs. Away from the lake-margin reef walls, the lake floor slopes gently to depth. In the brightly sunlit zone algae, especially stands of Chara, form carpet-like colonies. Superficial carbonate encrustations of these algae contribute locally to the proximal lake-floor sediments. These deposits grade from unsorted muddy to sand grade detrital tufa surrounding the phytoherms to fine lime muds towards the lake depocentre.

Fauna may include molluscs, ostracods, gastropods, small crustaceans, insect larvae, bivalves, beetles, fish and turtles (Pedley, 1990; Evans, 1999; Arenas et al., 2000).

Arenas et al. (2000) described a Quaternary fluvial-lacustrine system in Spain, according to the distribution of the facies associations, and proposed the following interpretation for the studied model: macrophyte and bryophyte facies developed along the margins of ponded areas that corresponded in part to fluvial streams. Bryophytes formed small mounds and `pillows' that, in places, grew from macrophyte barriers along stream banks, and also in wet areas very close to springs. Oncolites and coated grains formed in shallow ponded areas, where phytoclasts and other debris accumulated.

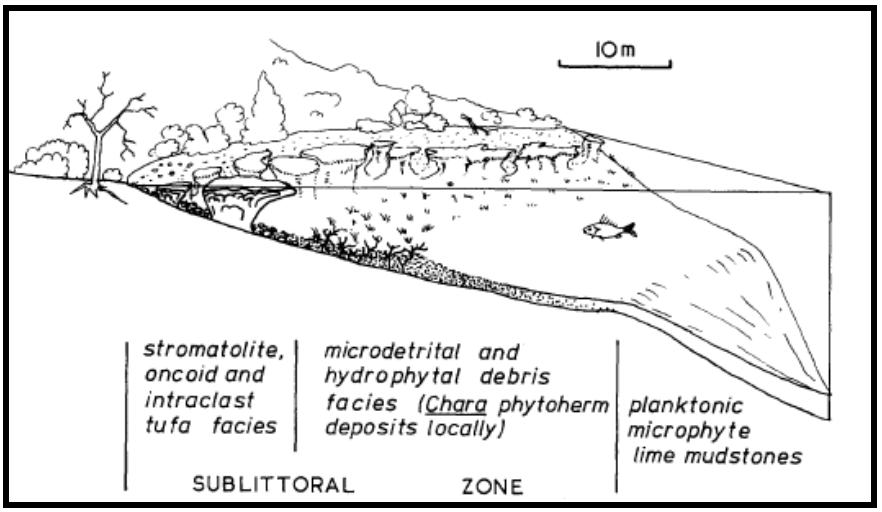

Fig 1.6. Facies distribution in the lacustrine tufa model. In the shallower areas stromatolitic tufa is common, associated with oncoids and phytoclastic sediments. These deposits pass to micro-detrital and hydrophyte tufas whereas in the distal areas lime mudstones accumulate. (from Pedley, 1990)

- *Paludal model.*

Paludal tufa is typically developed on low-gradient and valley-floor sites. Deposits can occupy the full width of a valley and extend for kilometres in length. The most diagnostic feature of this model are phytoherm cushions of grasses (sensu Pedley, 1990) and rushes; sapropels and peats may be also common (Pedley et al., 2003) (Fig. 1.7).

Paludal sites are often confused with barrage tufa. It is therefore important to note that paludal deposits contain no developments of transverse phytoherm barrages and lakes (e.g. Pedley et al., 1996), although such deposits can be succeeded by paludal tufa in the later stages of valley infilling.

Typical paludal deposits develop in water depths of little more than a decimeter down to wetted surfaces controlled by slow continuous water seepage. Nevertheless, the continued development of precipitates demands that an open hydrological system existed with a constant supply of lime-rich water.

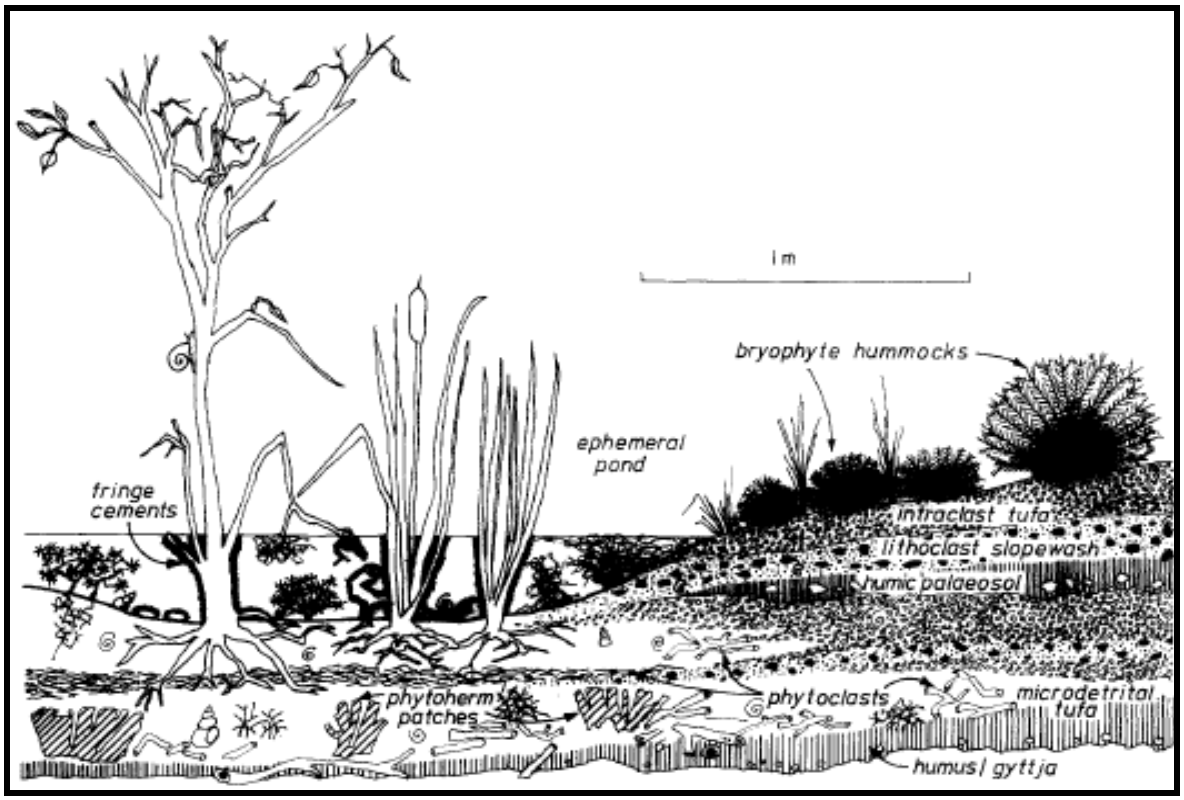

Fig. 1.7. Facies distribution in the paludal tufa model. Pond sediments range from micro-detrital tufa to intraclast tufa, and locally oncoids. Typical features are encrusted macrophytes that produce characteristic "horizontal and vertical tube facies" fabrics. (from Pedley, 1990)

1.6. Precipitation processes

In the literature it has been suggested that the basic condition for tufa formation is the supersaturated state of the water with respect to calcite, which requires a high concentration of dissolved $CaCO_3$ (Merz-Preiß & Riding, 1999; Arp et al., 2001a). The chemical parameter that combines the carbonate alkalinity and the availability of free calcium, is the saturation index, defined as:

$$SI = \log (IAP/K_{sp})$$

where IAP denotes the ion activity product (i.e., $\{Ca^{2+}\}\times\{CO_3^{2-}\}$) and Ksp, the solubility product of the corresponding mineral (Stumm & Morgan, 1996). The solution is supersaturated when IAP>Ksp, although, experimental evidence has shown that when SI>0.8, $CaCO_3$ can precipitate spontaneously (Kempe & Kazmierczak, 1994). Arp et al. (2001b) suggested that SI>1 (i.e., a 8-10-fold supersaturation) is a pre-requisite for spontaneous carbonate precipitation.

Various processes can increase carbonate alkalinity, either in the macro-environment (acting in the depositional setting) and in the micro-environment (acting within biofilms), and both indirectly promote carbonate precipitation. These processes can be driven by extrinsic factors (e.g. evaporation, degassing, alkaline water input) or intrinsic factors (e.g. photosynthesis, respiration). When alkalinity changes resulting from physicochemical processes in the macro-environment, the precipitation is extrinsically driven. When alkalinity is controlled by microbial communities altering their immediate microenvironment through their metabolism, the precipitation is intrinsically driven (Dupraz et al., 2009).

In freshwater settings, such as in fast-flowing streams, the common physicochemical process considered to lead to carbonate precipitation, is the removal of CO_2 through degassing occurring at turbulent sites (i.e., springs, waterfalls). This raises the carbonate level within the system towards saturation. (Ford & Pedley, 1996; Merz-Preiß & Riding, 1999; Arp et al., 2001b; Pentecost, 2005).

Although it has been suggested that tufa precipitation is basically driven by a physicochemical process, at the same time the importance has been emphasized of microbial communities, which are always associated to the growing surface of these deposits, in the calcite precipitation (Pedley, 1990; Pedley, 1992; Pedley 2000).

Microbial communities are commonly organized in well developed biofilms, that represent a unique micro-ecosystem in which microorganisms, through their metabolic activities and/or products, can induce or influence the precipitation (and dissolution) of $CaCO_3$ (Barabesi et al., 2007). Biofilms, similar to microbial mats, can be considered as "geochemical bioreactors" (Dupraz et al., 2009) with two fundamental components: (1) the microbial communities, that through their metabolic activities alter the geochemical environment and (2) the EPS (extracellular polymeric substance) matrix, produced by microorganisms, that provide mineral nucleation sites

and influence with their properties, the mineral shape and composition, producing various crystal morphologies and mineralogies (Hardikar & Matijevic, 2001; Braissant et al., 2003; Chekroun et al., 2004; Bosak & Newman, 2005; Ercole et al., 2007; Lian et al., 2007; Rodriguez-Navarro et al., 2007).

Basically, activities of microorganisms have two effects: organic carbon production, mainly through photosynthetic CO_2 fixation; and/or organic carbon mineralization/decomposition. Several major functional groups of microorganisms participate in these activities: (1) photolithoautotrophs (i.e. primarily the cyanobacteria that carry out oxygenic photosynthesis); (2) aerobic heterotrophs (that carry out CO_2 respiration), (3) fermenters, (4) anaerobic heterotrophs (primarily sulphate-reducing bacteria), (5) sulphide oxidizers, (6) anoxyphototrophs (i.e. purple and green sulphur bacteria), and (7) methanogens (Decho, 2010). Certain microbial metabolic activities create carbonate alkalinity and therefore promote precipitation, whereas other activities increase dissolved inorganic carbon (DIC) and/or produce organic acids that could lead to a pH decrease and net carbonate dissolution (Dupraz et al., 2009) (Fig. 1.8).

Microbially-mediated precipitation in nature occurs in a wide range of environments, both in marine and non-marine settings (Burne & Moore, 1987; Riding, 1991; Arp et al., 1999; Garcia-Pichel, 2002; Bontagnoli et al., 2008; Shiraishi et al., 2008a,b; Spadafora et al., 2010).

Freshwater microbialites, such as tufa stromatolites, are examples of *in situ* biofilm calcification when approximately an 8- to 10-fold calcite supersaturation in the macro-environment is exceeded (Kempe & Kazmierczak, 1990; Arp et al., 2001b). Here, carbon assimilation by autotrophs, such as cyanobacteria, is considered to be the major factor in shifting the carbonate equilibrium that consequently increases $CaCO_3$ supersaturation, because oxygenic photosynthesis drives the pH away from an unstable neutral point and shifts the carbonate equilibrium to promote precipitation in carbonate-saturated water (Soetaert et al., 2007; Shiraishi et al., 2008a,b; Bissett et al., 2008). Organic carbon derived from photosynthesis can also be oxidized anaerobically by sulphate-reducing microorganisms, and this would result in precipitation (Visscher et al., 1998).

However, one question always arises in studies of environments where water already has a high supersaturation for $CaCO_3$: Is biofilm calcification biologically-induced (active precipitation) or biologically-influenced (passive precipitation)?

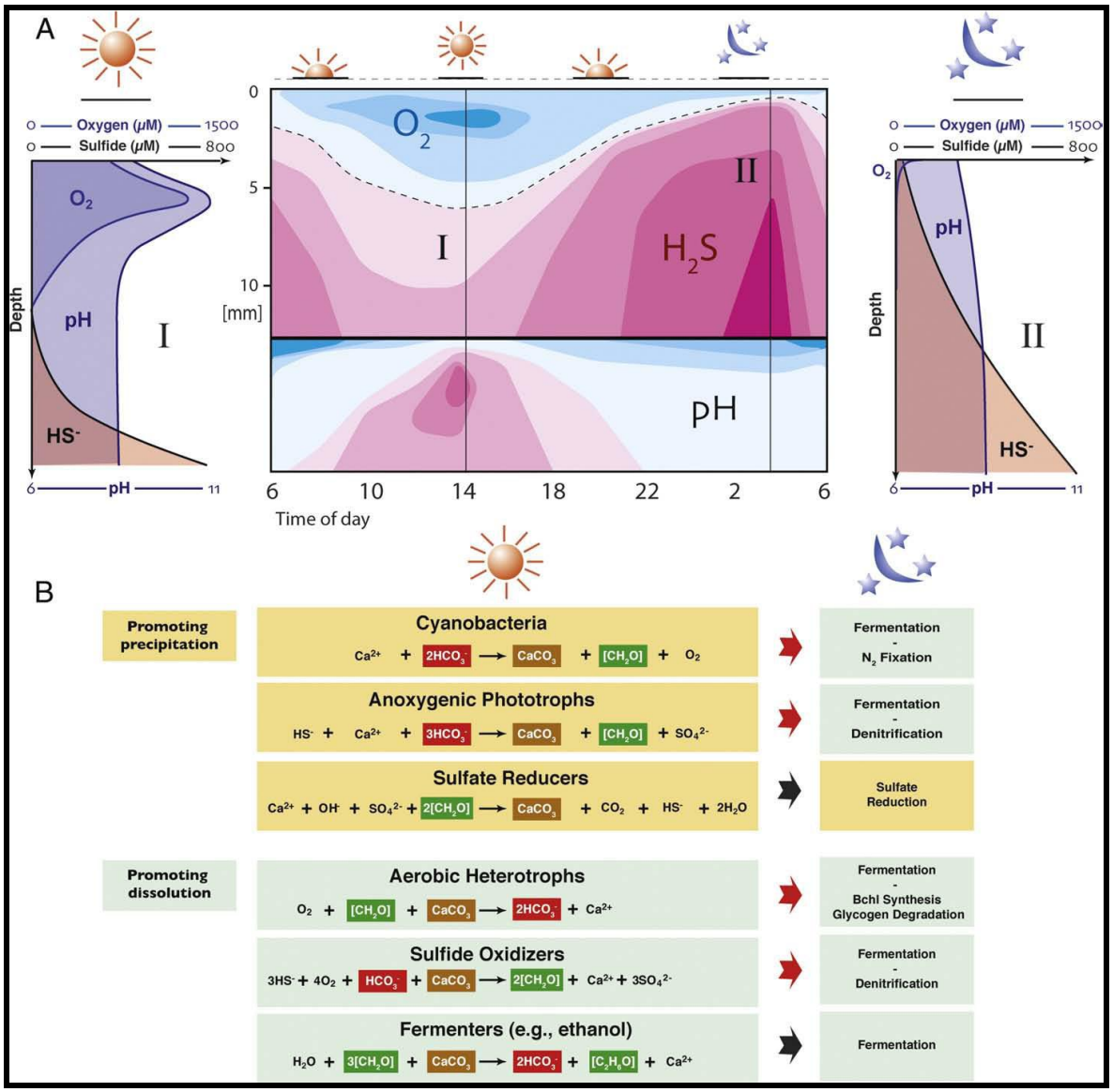

Fig.1.8. Daily fluctuations of vertical geochemical gradients in a microbial mat and combined metabolic–geochemical reactions leading to carbonate precipitation and dissolution. (A) The variation in oxygen, sulphide and pH within a microbial mat over a 24 h period. Profiles I and II represent geochemical differences in depth profiles between day and night. During the night, the photosynthesis ceases and the mat turns completely anoxic because of rapid O_2 consumption by aerobic heterotrophs. (B) The six major guilds of microorganisms that compose a typical microbial mat are arranged by their respective effects on the precipitation process. Photosynthesis and sulphate reduction are known to increase alkalinity (promoting carbonate precipitation), whereas aerobic respiration, sulphide oxidation and fermentation are more likely to induce dissolution. When oxygen-depending metabolisms stop during the night, anaerobic heterotrophy such as sulphate reduction prevails. The net carbonate precipitation depends on the balance between the different metabolic activities as well as their temporal and spatial variations. (from Dupraz et al., 2009)

In freshwater environments, microbial deposits often show carbonate precipitation around cyanobacterial sheaths or cells (Merz, 1992; Freytet & Plet, 1996; Freytet & Verrecchia, 1998). Precipitation of $CaCO_3$ associated with the cyanobacterial sheath is believed to be a result of CO_2 uptake during photosynthesis (Thompson et al., 1997; Freytet & Verrecchia, 1998, 1999; Merz-Preisß & Riding, 1999; Riding, 2000). The increase in alkalinity in the cell's microenvironment leading to precipitation is attributed to an exchange of HCO_3^- and OH^- through the cell-membrane. Since pH ranges generally from 7 to 10, most of the dissolved inorganic carbon (DIC) is comprised of HCO_3^- ions. HCO_3^- is transported into the cyanobacterial cell as a source of inorganic carbon for photosynthesis and converted to CO_2 by the carbonic anhydrase enzyme (Merz, 1992; Verrecchia et al., 1995; Badger, 2001). When cyanobacteria convert HCO_3^- into CO_2, OH^- is released in the exopolymeric sheath environment, which results in an increase of carbonate in solution. When Ca^{2+} is present, calcium carbonate can nucleate within the cyanobacterial sheath, which consists of exopolymeric substances similar to EPS.

Carbonate precipitation associated with cyanobacterial sheaths through photoautotrophy can lead to two different forms of calcification that reflect the degree of influence of the cyanobacteria (Merz, 1992): encrustation and impregnation. In the first, carbonate crystals nucleate on the outside of the sheath surface, forming a carbonate tube with an inner diameter reflecting the diameter of the filament. According to Merz (1992) and Merz-Preisß & Riding (1999), this process is dominant in freshwater tufa formation, where environmental factors such as CO_2 degassing or an increase in temperature, lead to precipitation. In the impregnation of the sheath, carbonate crystals are precipitated completely within the sheath, as a result of the physiological activity of the cyanobacteria. The outer diameter of the resulting tube corresponds to the outer diameter of the filament, while the inner diameter might have the same or a larger diameter than the trichome.

In a recent review of the carbonate precipitation processes in modern microbial mats and biofilms, Dupraz et al. (2009) proposed a distinction between two main types of bio-mediated mineral products: those formed by biologically-induced processes and those biologically-influenced processes, both responsible for the production of organominerals, the primary constituents of microbialites (*sensu* Burne & Moore, 1987).

In the biologically-induced process, the mineral precipitation is the direct result of bacterial activities and requires the activities of living cells whereas in the biologically-influenced mineralization external parameters, both biogenic (partial microbial consumption) or abiotic (UV, temperature, salinity) in origin, rather than microbial activities, are responsible for creating the conditions for mineral precipitation and the presence of living organisms is not required.

A key component in both processes is the presence of the extra-polymeric substances (EPS), which have specific intrinsic (i.e., physicochemical) characteristics. EPS within a microbial mat

can exist in a continuum of physical states, ranging from particulate to dissolved, or from a 'cohesive gel' to a 'loose slime' to a 'dissolved solute' state. The physical state is largely a function of the EPS concentration (or the water activity), and the abundance and types of bonds or interactions between individual EPS molecules. These molecular-scale interactions may influence the 'availability' of functional groups to bind ions (Dupraz et al., 2009).

Moreover, the physicochemical properties of the polymer matrix, such as the acidity or functional group composition, are important factors in the metal-binding potential (initially inhibiting calcium carbonate mineral formation), and biotic and abiotic degradation or alteration of the EPS (favouring calcium carbonate precipitation) (Dupraz & Visscher, 2005).

In order to precipitate calcium carbonate minerals within a microbial mat, the Ca-binding capacity of the EPS matrix has to be greatly reduced. This can be accomplished through biologically-induced mineralization (active precipitation) in which EPS is modified by microbes or biologically-influenced mineralization (passive mineralization) (Dupraz et al., 2009).

In marine and hypersaline environments it has been observed that an important factor controlling the biologically-induced processes is the degradation of the EPS matrix, mainly by aerobic and anaerobic heterotrophic bacteria. These can increase the calcium concentration and the alkalinity and consequently facilitate carbonate precipitation (Decho, 1990; Visscher et al., 2000; Reid & MacIntyre, 2000; Paerl et al., 2001; Dupraz & Visscher, 2005; Vasconcelos et al., 2006).

The biologically-influenced mineralization takes place through two fundamental mechanisms: 1) supersaturation of the cation-binding sites or 2) diagenetic alteration of EPS, i.e., organomineralization sensu stricto (Trichet & Défarge, 1995).

The binding capacity of EPS can be saturated when a continuous supply of cations are available. When all the functional groups of the polymer are occupied with bound cations, a combination of local alkaline conditions and the presence of free Ca^{2+} ions can lead to nucleation of calcium carbonate on the EPS matrix (Arp et al., 1999).

The organomineralization process sensu Trichet & Défarge (1995) is defined as mineral formation mediated by non-living organic substrates in soils and sediments. According to the authors' model, the acidic macromolecules in microbial biofilms are randomly distributed throughout the EPS-matrix. Rearrangement of these acidic sites through diagenetic processes provides an organized nucleation template for complete biofilm organomineralization (Reitner, 1993; Reitner et al., 1995; Trichet & Défarge, 1995).

Although the origin of organomineral products can be different (intrinsic/extrinsic), bacterial cells and/or their extracellular matrix serve as physical substrates for carbonate precipitation and control the mineral shape and composition of the crystals (Dupraz et al., 2009). Micrite, rhombs, dumbbells, needles and spherulites are examples of organominerals.

Lab experiments using silica gel provide insight into the importance of the gel-like properties of EPS in the precipitation process. Although silica gel differs fundamentally from EPS, this environmentally unusual medium can also produce various types of carbonate minerals (e.g., Fernandez-Diaz et al., 1996; Chekroun et al. 2004; Braissant et al., 2003).

Variations in [Mg^{2+}] when supersaturation is reached produce distinct morphologies such as spheres, dumbbell-like, wheat-sheaf- like bundles or rhombs (Fernandez-Diaz et al., 1996). Similar morphologies are also observed in physicochemically-forced precipitation of carbonate minerals within an EPS matrix with (Chekroun et al., 2004) or without bacterial cells present (Braissant et al., 2003). Regardless as to whether organic (EPS) or inorganic (silica gel), the gel properties of the matrix in which precipitation occurs influence diffusion processes and adsorption/complexation of Ca, both of which affect the mineral product.

The experiments with inorganic gel matrices indicate that spherulites or dumbbell shapes in the fossil record do not necessarily represent organomineralization (Chekroun et al., 2004). Therefore other criteria, such as organic and inorganic biomarkers, have to be considered to determine conclusively a biotic mineral origin.

In addition to influencing mm-scale properties of minerals, EPS also affects the nano-scale structure of carbonate precipitates. In natural microbial mats, precipitation often involves replacement of the EPS matrix with small carbonate nanospherulites (e.g., Sprachta et al., 2001; Dupraz et al., 2004).

The initial precipitation of calcium carbonate in microbial mats (Zavarzin, 2002) can be summarized by the following steps: 1) a local increase in alkalinity and pockets of supersaturation within microdomains of the EPS matrix; 2) formation of an amorphous calcite gel; 3) production of nanospheres from a mixture of amorphous calcite and acidic EPS macromolecules, and 4) nanospheres acting as seeds for further carbonate crystallization. The crystals exhibit various shapes, from anhedral to euhedral, as a result of the physicochemical constraints of the organic matrix on crystal growth. Organic molecules can attach and poison specific crystal faces, thereby inhibiting a part of the crystal growth, which leads to the formation of spherulite, dumbbell or smooth rhombic crystals.

PART I

TUFA DEPOSITIONAL ENVIRONMENTS

2. STUDY SITES

Five sites of actively-forming tufa, located in northern Calabria (Italy) and in north-east England (Fig. 2.1) have been the subject of this study.

In northern Calabria, along the western coast, tufa deposits form within a small stream, named Parmenta, a side-stream of the Corvino River (Fig. 2.1A). Along the stream, tufa deposits are scattered and form a series of irregular barrages, developing transverse to the watercourse (see Section 4.1). The stream flows in a narrow steep-sided wooded valley draining an area of Upper Triassic carbonates (Fig. 2.1A). They are characterized by dolomitized peritidal cycles, belonging to the platform domain of the Dolomia Principale Fm and this overlies Carnian-Norian shelf carbonates (Perri et al., 2003). The succession has been affected by widespread intense tectonic deformation, as a result of the Alpine-Apennine orogeny, which in the study area, mainly resulted in west-verging thrust-related folds.

From the climatic point of view, the area is influenced by a typical Mediterranean climate, characterized by high temperatures in the summer months, which decrease progressively in the autumn-winter interval, resulting in an annual average temperature between 25° and 11°C (historical series data 1929-2008) (Fig. 2.2A). In particular during the summer the average diurnal range is between 17°-35°C while in winter it is 2°-19°C. The major rainfall events occur between November and January reaching the monthly average value of about 135 mm, whereas during the summer months (June-August) precipitation decreases to an average monthly value of 21 mm (Fig. 2.2A).

In NE England, studied sites are located in the areas around the cities of Gateshead, Barnard Castle (two sites, indicated as A and B) and Sunderland (Fig. 2.1B). Tufa deposits form in a moderate flow-stream in the form of barrage tufa, as in Calabria, near Gateshead, but also occur locally where springs are emerging, forming overhanging lobes (Barnard Castle B and Sunderland) or on drained slopes, where they develop with step-like macro-morphologies (Barnard Castle A) (Fig. 2.1C).

The geological setting of the area is characterized by Carboniferous strata, that extend from Durham County to northern Northumberland, and by a Permian succession which crops out to the south-east, along the coast (Fig. 2.1B). The lower-middle Carboniferous is represented by mixed clastic-carbonate cycles (Yoredale cycles), characterized by a lower limestone unit and an upper coarsening-upward clastic succession of mudrocks to sandstones (Tucker et al., 2009), whereas the youngest Carboniferous strata that crop out in this sector, are represented by the Pennine Coal Measures Formation, consisting of sequences of interbedded grey mudrock, siltstone, sandstone and coal. The Permian strata, cropping out along the coast, are characterized by a carbonate-evaporite succession (Fig 2.1B) (Zechstein Group) deposited from marine and hypersaline waters (Tucker, 1991).

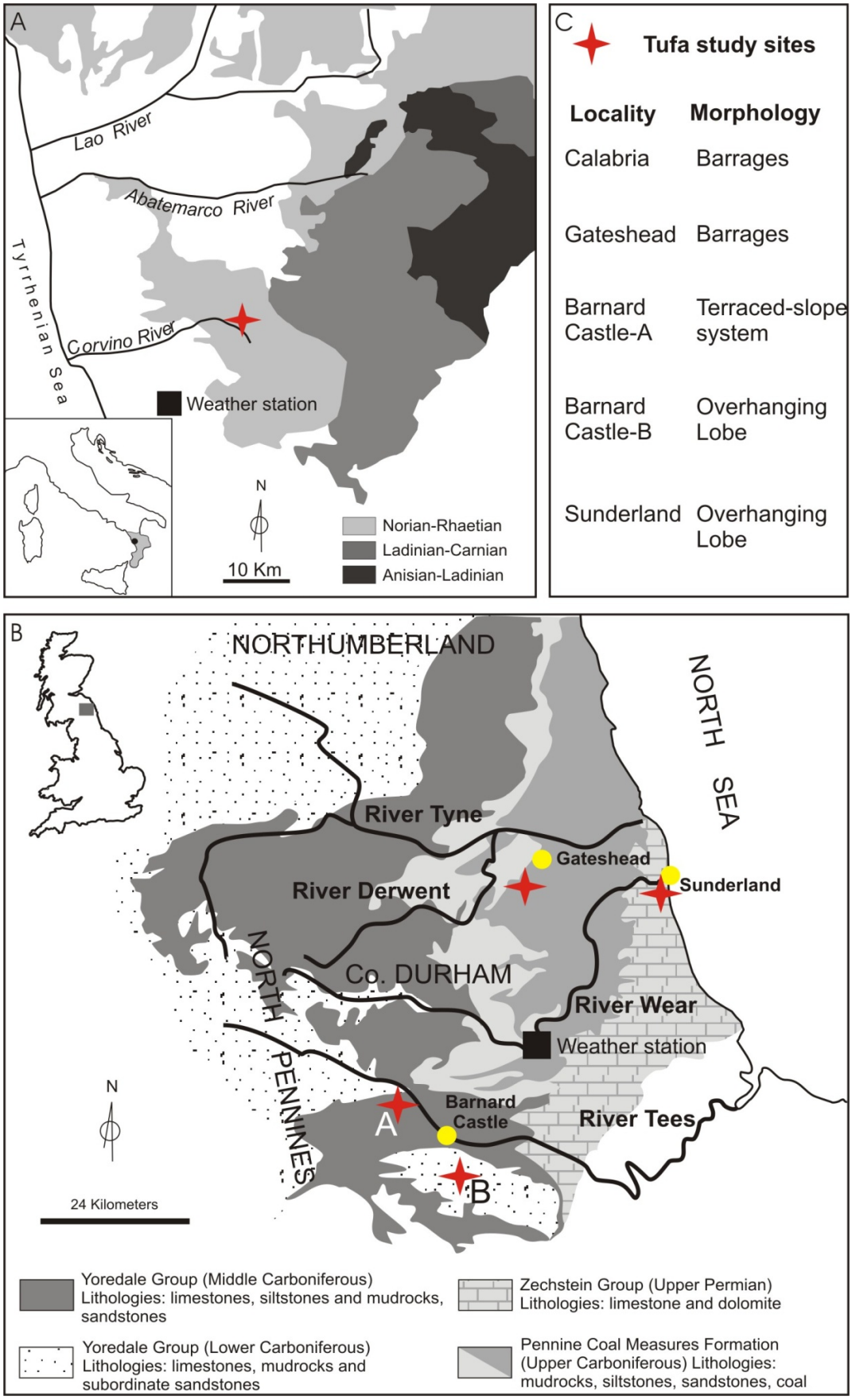

Fig. 2.1. Location of the tufa study sites. A) Simplified geological map of the NW Calabria. B) Geological map of the NE sector of England. C) List of the study sites with related tufa depositional models.

In NE England the climate is generally humid–temperate, with warm wet summers and cool wet winters. Temperature shows both a seasonal and a diurnal variation: January-February are usually the coldest months with mean daily minimum temperatures varying from 0°C to 10°C, whereas July-August are the warmest months with mean daily maximum temperatures varying between 5-20°C (historical series data 1971-2000, metoffice.gov.uk) (Fig. 2.2B). Rainfall is generally well-distributed through the year, with an average annual value of 1500 mm in the higher parts of the Pennines and less than 600 mm along the east coast. The pattern of mean monthly rainfall recorded at the Durham weather station (historical series data 1950 - 2008 metoffice.gov.uk) shows that rainfall is quite constant during the year, becoming more abundant during the autumn/winter interval, even if the maximum values recorded in this weather-station, are in August (Fig. 2.2B).

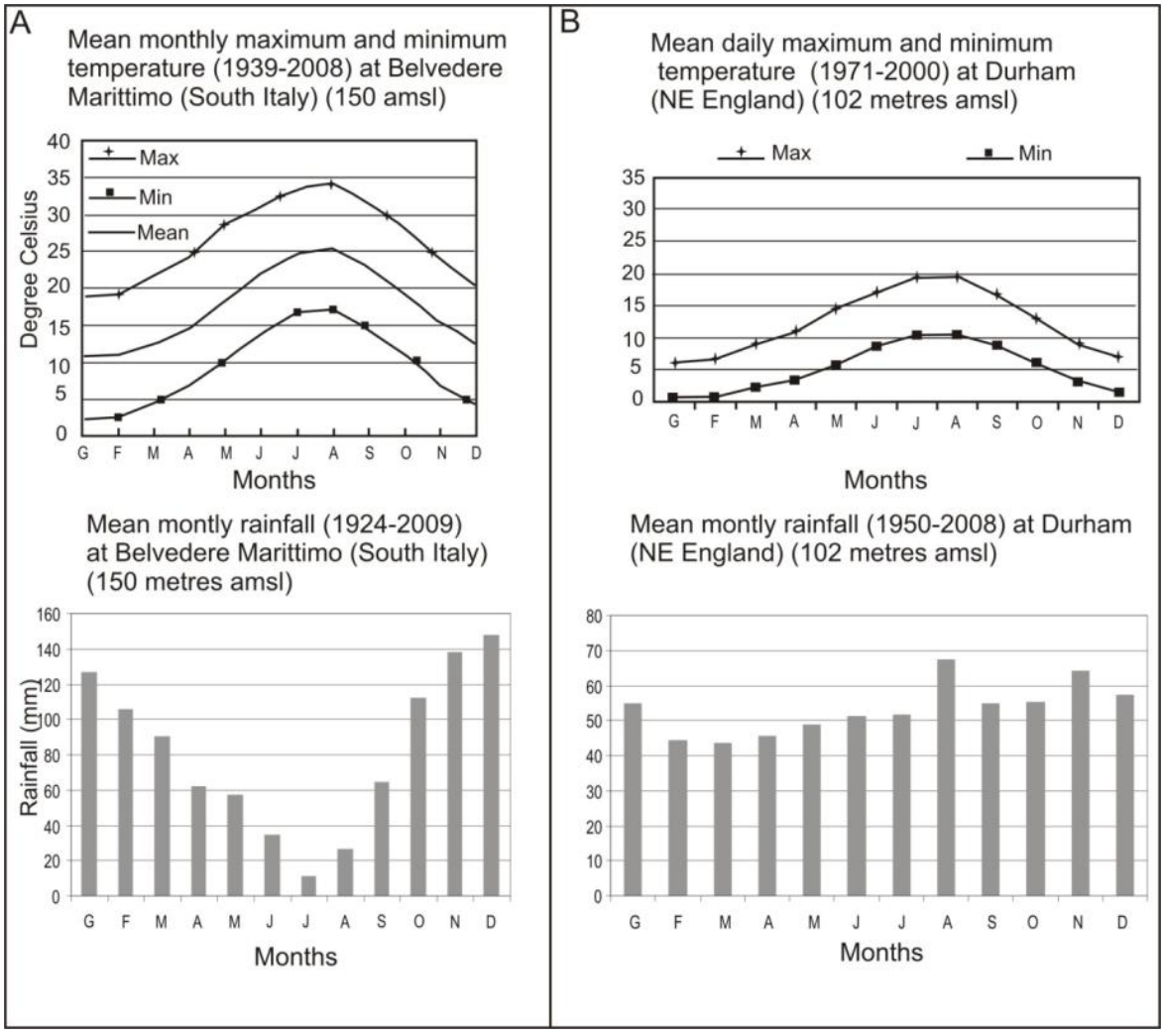

Fig. 2.2. Climatic data recorded near the tufa study sites. A) Belvedere Marittimo weather station (Calabria). B) Durham weather station (NE England).

3. METHODS

In this work, several study methodologies were used, including fieldwork and various laboratory techniques, both for water and rock samples.

❖ *Water analyses*

Temperature, conductivity and pH of water samples were measured in the field both in Calabria and in NE England (Fig. 2.1). In addition, water samples were collected for further laboratory analyses.

Water was filtered through 0.45 μm cellulose acetate membranes and split into two portions: one was stored in polyethylene bottles without further treatment and the other was acidified through addition of HNO_3 and stored in polyethylene bottles. Anions and cations were determined by ionic chromatography and alkalinity by acidimetric titration.

Moreover, in two tufa localities in NE England (Gateshead and Baranrd Castle A- Fig. 2.1B and C), water samples were analyzed by fluorescence spectroscopy, commonly used in the study of dissolved organic matter (DOM) in natural waters.

DOM may originate from a range of sources: some is transported to the hydrological system and is derived from and influenced by the geology, land-use and hydrology of its origin. Some DOM is created in situ through microbial activity which may be an independent source of organic matter or a recycling mechanism for that which is transported to the system. Human activity is also a vast source of DOM much of which is believed to be labile, entering the water system through direct discharge, indirect leaching into groundwater and aerial dispersal (Hudson et al., 2007).

The most commonly studied fluorescent organic components of natural waters include humic substances (subdivided into humic acids, fulvic acids and humins). These are derived from the break-down of plant material by biological and chemical processes in terrestrial and aquatic environments. Amino acids (tryptophan, tyrosine and phenylalaninein) also occur, and are indicative of proteins and peptides (Elkins & Nelson, 2001; Stedmon et al., 2003; Patel-Sorrentino et al., 2004).

As a result of the difficulties associated with definitively identifying individual fluorescent compounds in waters, these groups of fluorophores are commonly named humic-fulvic-like (named C and A) and protein-like, specifically tryptophan (named T) and tyrosine-like (named B). These names relate to their fluorescence which occurs in the same area of optical space as standards of these materials.

Using fluorescence spectroscopy, it is possible to obtain an excitation–emission–matrix (EEM), created by simultaneously scanning excitation and emission wavelengths through a set path-length of aqueous sample. Each fluorophore appears on the EEM as a peak or series of peaks associated

with specific excitation and emission wavelengths (Fig. 3.1). The intensity of the peak can be used as a measure of the concentration of the fluorophore to ppm or ppb levels, depending upon the fluorophore.

In fact recently, it has been demonstrated that using fluorescence it is possible to detect the differences between both anthropogenic and natural DOM sources in rivers impacted by sewerage effluents (Baker, 2001; Baker et al., 2003). Anthropogenic DOM sources, such as farm wastes, sewage treatment outfall or sewerage overflows, are all characterized by high levels of protein-like (tryptophan-like and/or tyrosine-like) fluorescence (Baker, 2001, 2002).

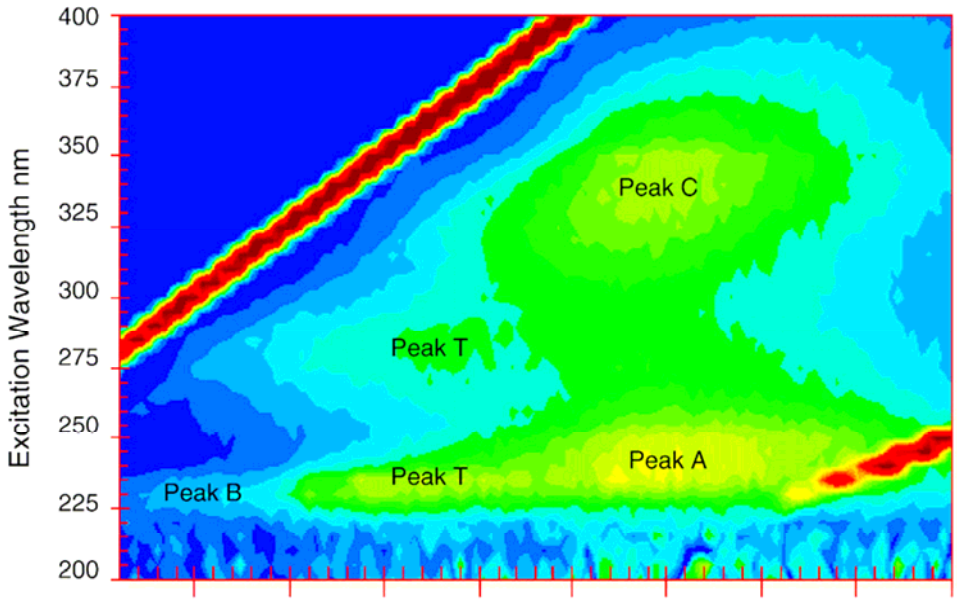

Fig. 3.1. Example EEMs illustrating position of T, C, A and B peaks (Hudson et al., 2007).

❖ *Rock samples*

In order to monitor the growth processes of the carbonate and the precipitation rate of calcite in the tufa-depositing stream located in Calabria (Fig. 2.1A) some natural substrates (dolomite pebbles of the local bedrock), were placed along some barrages. During the period between January 2008 and January 2009, the resulting neo-formed tufa crusts, were collected at seasonal intervals and were compared with the already existing naturally formed deposits.

Similarly, in the tufa-depositing stream located near Gateshead and in the terraced-slope system located near Barnard Castle (A) (Fig. 2.1B), glass slides were used to provide a comparison between the neo-formed crusts developed in the different tufa systems.

To investigate the nano-structures of the tufa neo-precipitates formed in association with organic matter with the Scanning Electron microscope (SEM) a combination of fixation and

dehydration techniques were used to avoid alteration/destruction of the organic tissues and the possible modification of the delicate mineral ultra-structure.

For this purpose, during the fieldwork, tufa samples and the adherent biofilm were fixed by a fixative solution and filtrated water and stored in sterile bottles. The aim was to preserve the samples for their macro and microscopic variations and to make them more resistant to deformation, induced by the successive dehydration events.

Many different sample preparation techniques are well established in the biological literature (Little et al., 1991; Bray et al., 1993). Dehydration techniques are designed to reduce the destructive surface tension forces that occur at the air–water interface during air drying. Ethanol or acetone dehydration alone provides little advantage over air drying (Boyde, 1972), but it is often used to wash out water from a sample before drying with another method. Critical-point drying preserves delicate structures by avoiding the liquid–gas interface altogether (Cohen, 1979).

Fratesi et al. (2004) tested five different dehydration techniques on rock samples and associated biofilm, in order to assess whether the variation was attributable to sample preparation or to intrinsic biofilm heterogeneity. They found that the original morphology of individual bacteria was best preserved by ethanol dehydration with HMDS drying; this is a liquid with low surface tension that evaporates from a sample with minimal distortion.

In this study fresh broken surfaces both of neo-formed tufa crusts and natural samples were treated with formol 40% for the fixation and successively dehydrated in HMDS. This followed the protocol proposed by Fratesi et al. (2004) for high vacuum SEM observations. Several samples were also studied only after fixation in low vacuum ESEM, to distinguish actual structures from artifacts due to the sample preparation processes.

In addition to study at the nano-scale of the relationship between organic matter and mineral formation, samples of both natural and neo-formed tufa deposits were observed by conventional light microscopy for the identification of the petrographic features.

Bulk mineral identification was determined by powder X-ray diffraction (XRD) with a Philips PW1730 diffractometer. Interpretation of detected mineral phases were based on the relative peak intensity from the XRD charts (Hardy & Tucker, 1988). Semi-quantitative analyses of micron-sized spots were performed by an EDAX Genesis 4000 energy - dispersive X ray spectrometer (EDS) during SEM observations.

Moreover, some thin-sections of tufa deposits from Gateshead (Fig 2.1B) were analyzed with an optical microscope equipped with a vacuum chamber and electron gun to examine the cathodoluminescence (CL). Finally, stable oxygen and carbon isotope analyses were measured in different tufa deposits forming in the study sites located in NE England.

4. TUFA ENVIRONMENTAL SYSTEMS

4.1 Barrage systems

Both in northwest Calabria (Italy) and northeast of England (near Gateshead) (Fig. 1A and B), tufa deposits form in moderate-flowing streams, generating a series of barrages and pools (Figs 4.1 and 4.8). The general macro-morphology that characterizes both barrage systems can be compared with the barrage model described by Pedley (1990).

In Calabria, the main sequence of barrages, occurs as a series along the watercourse of the Parmenta stream for a length of 550 m. When the stream meets the main river (Corvino River) flowing in the valley, carbonate precipitation stops (Fig. 4.1A).

In the Parmenta, barrages occur as sinuous to irregular dams usually spanning the channel with a height that may vary from a few centimetres up to several metres as a consequence of the gradient of the stream bed (Figs 4.2-4.5). Each dam is characterized by an upstream ramp, generally steeply inclined (10-30 cm in height), and by an irregular ridge covered in partially calcified leaves and wood fragments (Fig. 4.4). By way of contrast, the downstream ramp, after a smooth surface, passes into tongue-shaped lobes (Figs 4.2 and 4.3). Lobes are normally 20-60 cm in width, although they may reach a metre- in size in the larger dams, where they form waterfalls with a steep slope (Fig. 4.3).

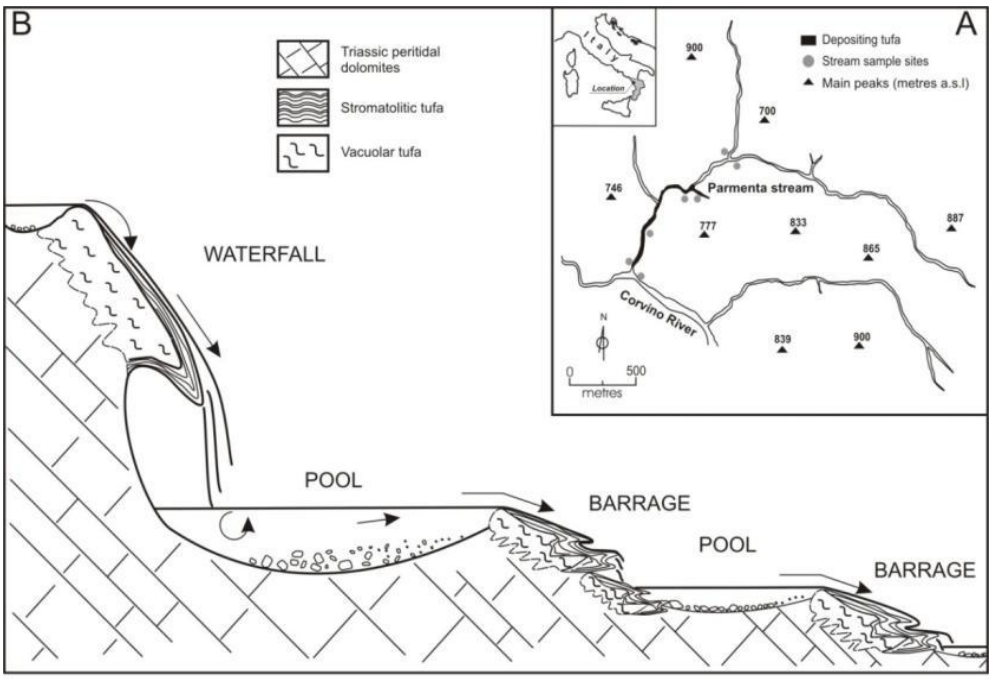

Fig. 4.1. A) Map of the tufa depositing stream along the Corvino Valley showing the distribution of tufa deposits along the stream course. B) Schematic section of the tufa barrage system forming along the Parmenta stream. Section shows the facies distribution in relation to the inclination of the Triassic bedrock. Sketch is not to scale.

Fig. 4.2. Single tufa barrier developing transverse to the Parmenta watercourse. Barrier crest is characterized mainly by calcified leaves with a downstream ramp formed by tongue-shaped lobes.

Fig. 4.3. Large-scale tongue shaped tufa along a waterfall.

Pools vary in length and width from a few decimetres up to 5 metres and water depth ranges from a few centimetres just behind the smallest dams to a few metres on the downstream side of the dam (Figs 4.2 and 4.5). Larger pools are floored by unconsolidated sandy gravel deposits consisting of sub-rounded dolomite pebbles and tufa clasts, rarely covered by a very thin carbonate crust (Fig. 4.4). Small pools also occur within the dam and lobe areas along the front of the barrage, where the river has not developed a sharp break-of-slopes. This type of shallow pool is characterized by the absence of detrital material, and presence of stromatolitic tufa upon the pool floor (Fig. 4.5).

Two main depositional facies form the barrages: stromatolitic tufa and vacuolar tufa (Fig. 4.6). Stromatolitic tufa forms smooth beds on the external surface of the tongue-shaped bodies and on the upper part of the downstream face of the dams. Lamination of stromatolitic tufa is generally even and regular with only gentle doming (Fig. 4.6C). Vacuolar tufa, significantly less in volume, is observable on the upstream surface and along the crests of the dams, where it is usually being covered by stromatolitic tufa (Fig. 4.6A and B). In fact it composes the inner part of the dams, including the core of the tongue-shaped bodies. This facies contains abundant large voids between calcified detrital plant remains with a variable amount of autochthonous bryophytes.

Fig. 4.4. Small-scale barrier mainly formed by calcified to fresh leaves. The barrier rims a shallow pool with detrital pebbles on the bottom.

Fig. 4.5. Series of small-scale tufa barrages rimming shallow pools.

Fig. 4.6. Field view of the tufa depositional facies in the Parmenta system. A) Barrage characterized on the crest by calcified leaves (vacuolar facies) gradually substituted by smooth beds on the downstream ramp. B) Macroscopic view of a piece of a tufa lobe, showing the transition between calcified leaves and smooth deposits, internally characterized by thin laminae (stromatolitic facies). C) Slab surface throughout a sub-fossil stromatolitic tufa.

Different from Calabria, the active barrage system, located near Gateshead (NE England), occurs in an area of Upper Carboniferous Coal Measures, formed by a succession constituted mainly by sandstone and shale (Fig .4.7A). Although there are no limestones in the succession, the occurrence of some calcareous shales, indicated by certain plant species, could be the source of carbonate ions in the stream water, necessary for the tufa calcite precipitation (see Chapter 5).

In this site tufa forms in a small stream, named Thornley Burn, which is a side stream of the Derwent River (Fig.4.7A and B). Both streams are part of the Woodlands Centre, included in the Derwent Walk Country Park, which is the track-bed of the old Derwent Valley Railway.

Tufa develops along the watercourse of the Thornley stream, forming a series of barrages and pools (Fig. 4.8), concentrated in the section between the first foot-bridge and the tunnel, through which the stream passes under the main road towards the Derwent River (Fig. 4.7B and C). In this sector, the distribution of tufa deposits is scattered, forming both single and multiple sequences of barrages and pools, occupying an area of ~ 200m in length. The first barrage occurs around 90m from the first foot-bridge, and many more barrages occur downstream (Fig. 4.7B and C). Along the stream sides there are frequent iron-rich seepages, that seem to be concentrated in the areas where tufa deposits are absents.

The general macro-structure of the barrage, is similar to those forming in Calabria, particularly in their disposition along the watercourse and in the asymmetrical profile of the dam-walls. Dams vary in height from up to 30-50 centimetres to a metre above the stream floor, whit a width ranging from up to 1 metres to 5 metres. The down-stream wall is characterized by a vertical or stepped ramp while the upstream wall passes more gently into the upstream pools (Figs 4.9 and 4.11). The external surface of the down-stream walls is almost entirely colonized by the filamentous green alga *Vaucheria*, that occurs in coalescing micro-scale lobes (Fig. 4.10A and B). These are constituted by partially calcified tufts, varying from up to 5 centimetres to 15 centimetres in length. These produce a light-weight, porous tufa deposit (Fig. 4.10B and C).

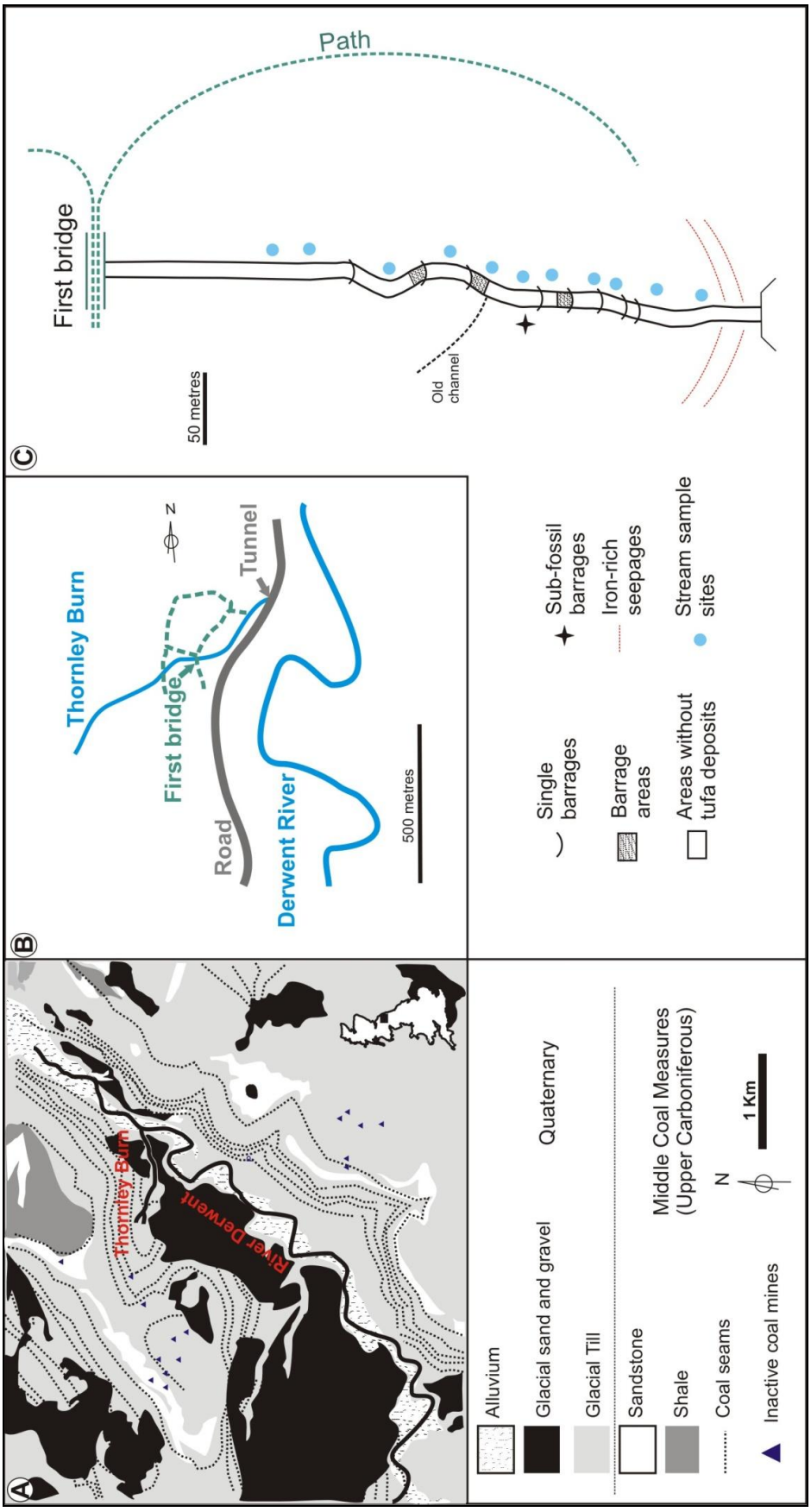

Fig. 4.7. Location of the barrage tufa system in the Derwent valley (NE England). A) Geological map of the area. B) Sketch map of the site. C) Map of the tufa depositing stream, showing the distribution of the deposits along the stream course.

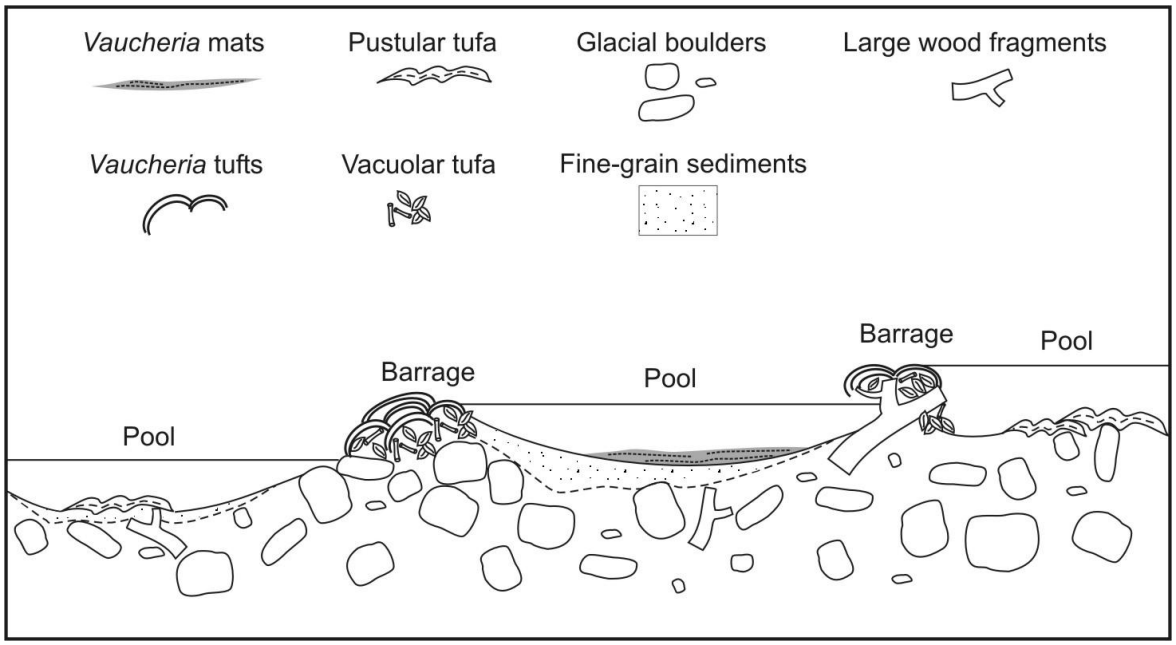

Fig. 4.8. Schematic section of the tufa barrage system forming along the Thornley stream. Section shows the distribution of the three main depositional facies occurring both in the pools and barrages. Sketch is not to scale.

Fig. 4.9. Thornley stream barrage system characterized by a main dam developing transversally to the watercourse, and a secondary dam forming a small-scale pool. The down-stream walls of the dams are made of interconnected micro-scale lobes (*Vaucheria* tufa) whereas in the up-stream wall, tufa deposits occupy the shallower area of the pools.

Fig. 4.10. A) Field view of a barrage downstream wall, on which develops *Vaucheria* green alga. B) Lobes made of encrusted *Vaucheria* tufts, forming light-weight porous deposits. C) Detail of *Vaucheria* filaments entirely calcified.

Pools vary in length from a metre or less to 8-10 metres, with a depth ranging from a few decimetres, in the smaller pools up to a metre in the larger ones. Differing from Calabria, the marginal shallower areas of the pools, as well as the pool-floor, are occupied by tufa deposits together with plant debris and detrital gravel (Figs 4.9, 4.11). Moreover, during the year (spring-autumn), many *Vaucheria* colonies occur on the bottom of the shallower pools, forming extensive uniform mats with incipient calcification (Fig. 4.12).

In this barrage system three main types of tufa deposit are generated: *Vaucheria* tufa, vacuolar tufa and pustular tufa (Figs 4.10 - 4.13). As mentioned above, *Vaucheria* tufa is composed of tufts of calcified filaments (Fig. 4.10B and C), that mainly develop on the down-stream-wall of the barrages (Fig. 4.9) whereas vaucolar deposits, mainly formed by partially calcified leaves and wood fragments, as in Calabria, accumulate on the up-stream side of barrages and on the bottom of pools. Pustular tufa appears to develops only in the quieter, often deeper area of the system, usually in the pools, where water is slower, and also on the upper-stream wall of the barrages (Figs 4.9 and 4.11).

Macroscopically these deposits occur dark in colour and are characterized by an outer edge formed by rounded knobs, each 2-3 mm in diameter, cemented together to form an interconnected pustular structure. The interior part is generally constituted by different calcified plant remains, as leaves and twigs with a vacuolar texture (Fig. 4.13).

Fig. 4.11. Barrage up-stream wall developed pool behind the barrage.

Fig. 4.12. Pool floor colonized by a uniform mat of partially calcified *Vaucheria* filaments.

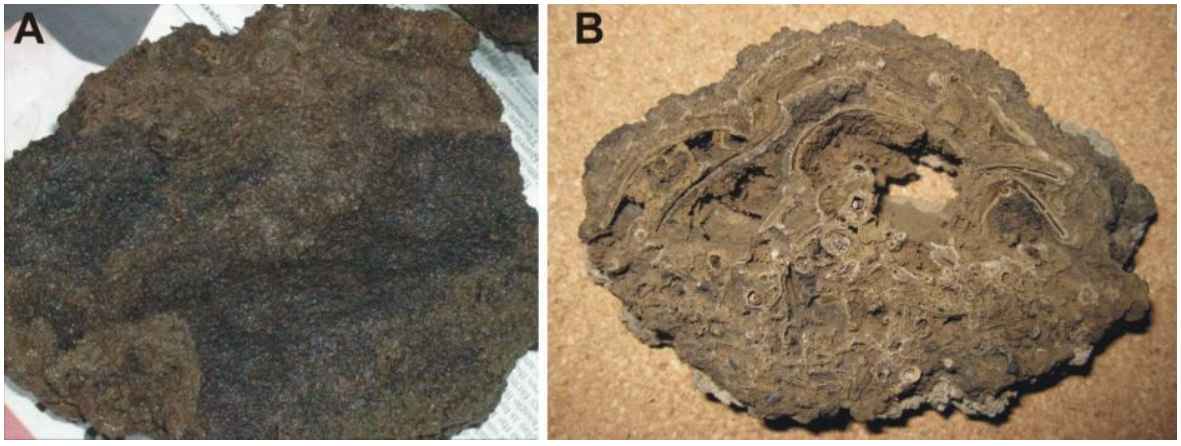

Fig. 4.13. Pustular tufa deposits. A) External surface of a pustular tufa with the typical dark-brown colour. B) Cross section showing the inner part formed by encrusted twigs and leaves (vacuolar tufa), overlain by the current growth surface, with a more massive structure.

4.2 Terraced slope system

In the Teesdale area, near Barnard Castle (A), tufa is forming along a sector of the valley-side of the River Tees (Fig 2.1B and C). Locally here, a tiny stream draining agricultural land runs over a 30-metre high scarp, which is constituted of sub-horizontal sandstone beds, belonging to the Middle Carboniferous (Fig. 2.1B). Water emerges in the upper part of the slope, and descending down towards the river in a small stream-let, creates a series of natural steps (Fig. 4.14). In the upper part of the slope where the gradient is stepper and the water flux is faster, tufa occurs as sub-vertical 5-10 cm thick, near-continuous carbonate crusts characterized by an undulating external surface (Fig. 4.15A). Near source points, crusts develop directly overlapping the external surfaces of rock exposures or soil, whereas descending few decimeters along the slope, crusts cover scattered plant remains, mainly leaves, twigs and pine cones and also detrital grains, mostly sandstone clasts (Fig. 4.15B and C).

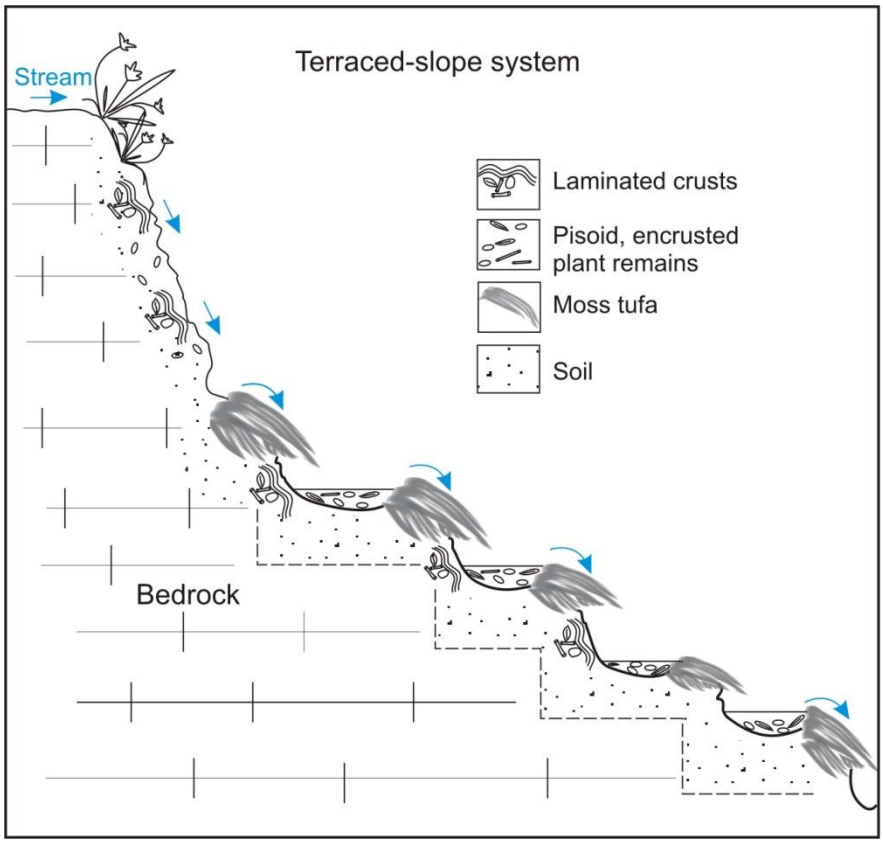

Fig. 4.14. Schematic section of the terraced-slope system forming along a sector of the valley-side of the River Tees. Section shows the facies distribution in relation to the inclination of the bedrock. Sketch is not to scale.

Fig. 4.15. Field view of tufa deposits forming in Barnard Castle (A). A) Carbonate crusts forming on the top of the slope characterized by an undulating external surface. B) Plant remains cemented by carbonate crusts. C) Sandstone pebble covered by a thin tufa crust.

Descending towards the River Tees, the dip of the slope reduces to 25-30° and tufa deposition creates a series of almost interconnected steps, similar in their external morphologies to rimmed pools.

Pools are only a few decimeters across and few centimeters depth; are regularly interrupted by sinuous rims (corresponding to the edge of the pool), occupied in their frontal area by partially

calcified mosses and liverworts (Fig. 4.16A). Encrustation of these macrophytes gives to the tufa deposits a vacuolar texture (Fig. 4.16B).

Toward the drop wall of the pool, encrusted mosses are gradually substituted by carbonate crusts, similar to those that form along the top of the slope (Fig. 4.17). These crusts are often connected to the pools, in which pisoids and partially calcified plant remains accumulate (Fig. 4.17).

Pisoids range from rods to sub-spherical forms, up to several cm long or a cm or more in diameter (Fig. 4.18). The external surface is a smooth dull surface, occasionally green in colour, whereas the nucleus may be constituted by plant fragment, tufa intraclast or rock fragments.

Fig. 4.16. A) Down slope side of the pool characterized by a rim of partially calcified mosses and liverworts. B) Cross section through tufa deposit forming on the edge of the pool showing encrusted mosses.

Fig. 4.17. Drop wall side of the pool characterized by an undulose carbonate crust, whereas on the pool-floor pisoids and plant remains accumulate.

Fig. 4.18. Detail of pisoids occurring in different size and shape, varying from rod to sub-spherical.

4.3 Tufa overhanging lobes

In Sunderland and near Barnard Castle (B), in the vicinity of some springs, tufa deposits develop in the form of overhanging lobes (Fig. 2.1B and C). Their macro-morphology is quite similar and they are forming substantial prograding deposits, characterized by a convex profile (Figs.4.19 and 4.22).

In Sunderland a tufa lobe is located behind the building of the Marina Activity Centre, where it was discovered for the first time in 1992, during the reconstruction of the dock. In a corner of this building, tufa develops on a retaining wall on which it forms a suspended lobe (Fig. 4.19A). In order to preserve and stabilize this structure, engineers have used different supports to avoids the collapse of the deposit including the channeling of the water (Fig. 4.19B). Spring-water drains Permian limestones, that crop out in a small buried valley, filled by glacial-fluvial sands. During the engineering work, the water was diverted away from the site. Subsequently a valve located upstream of the site now controls the water flow to the tufa lobe. In addition, at the base of the tufa deposit, a pool was constructed to which some pipes drain any excess water (Fenwick & McLean, 1996).

Externally the tufa lobe consists of a mass, ~3 metres wide and 4-5 metres high, composed of a vacuolar deposit made of calcified macrophytes and plant debris (Figs.4.19). In the lower part of the lobe and on the wall beneath it, a series of well-developed stalactites have formed (Fig.4.20), mainly made of calcified roots. On the top of the reinforced concrete base, where water drops constantly, the precipitation of calcite has created sub-spherical coated grains resembling the "cave pearls", common in caves (Fig.4.21).

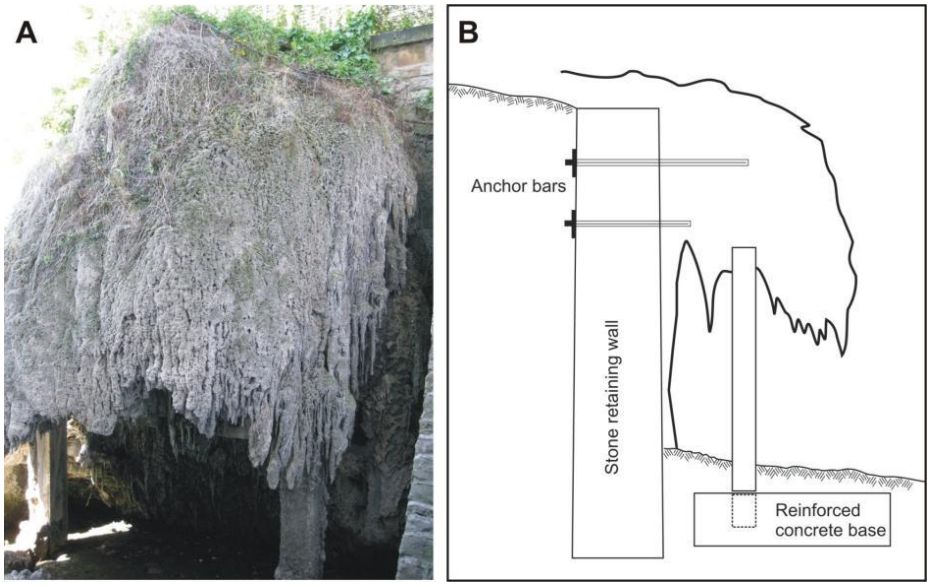

Fig. 4.19. Tufa lobe located in the Marina Activity Centre of Sunderland. A) Tufa deposit develops on a retaining wall forming an overhanging lobe. B) Cross-section of the retaining wall and tufa deposit showing the anchorage and pre-cast concrete frame. (Based on a sketch reproduced in Fenwick & McLean, 1996).

Fig. 4.20. Internal part of the tufa lobe where carbonate precipitation has generate stalactites.

Fig. 4.21. Top of the reinforced concrete base on which occur sub-spherical “cave pearls”.

In the vicinity of the town of Barnard Castle (B in Fig. 1B), a tufa deposit occurs in the vicinity of a spring located on a ~3 meters high slope. As in Sunderland, the deposit develops in the form of overhanging lobe (Fig.4.22A). The deposit is composed mostly of calcified mosses and *Vaucheria* (Fig.4.22B) that develop across the external surface of the deposit, and produce, as in the others localities, a vacuolar tufa (Fig.4.22C).

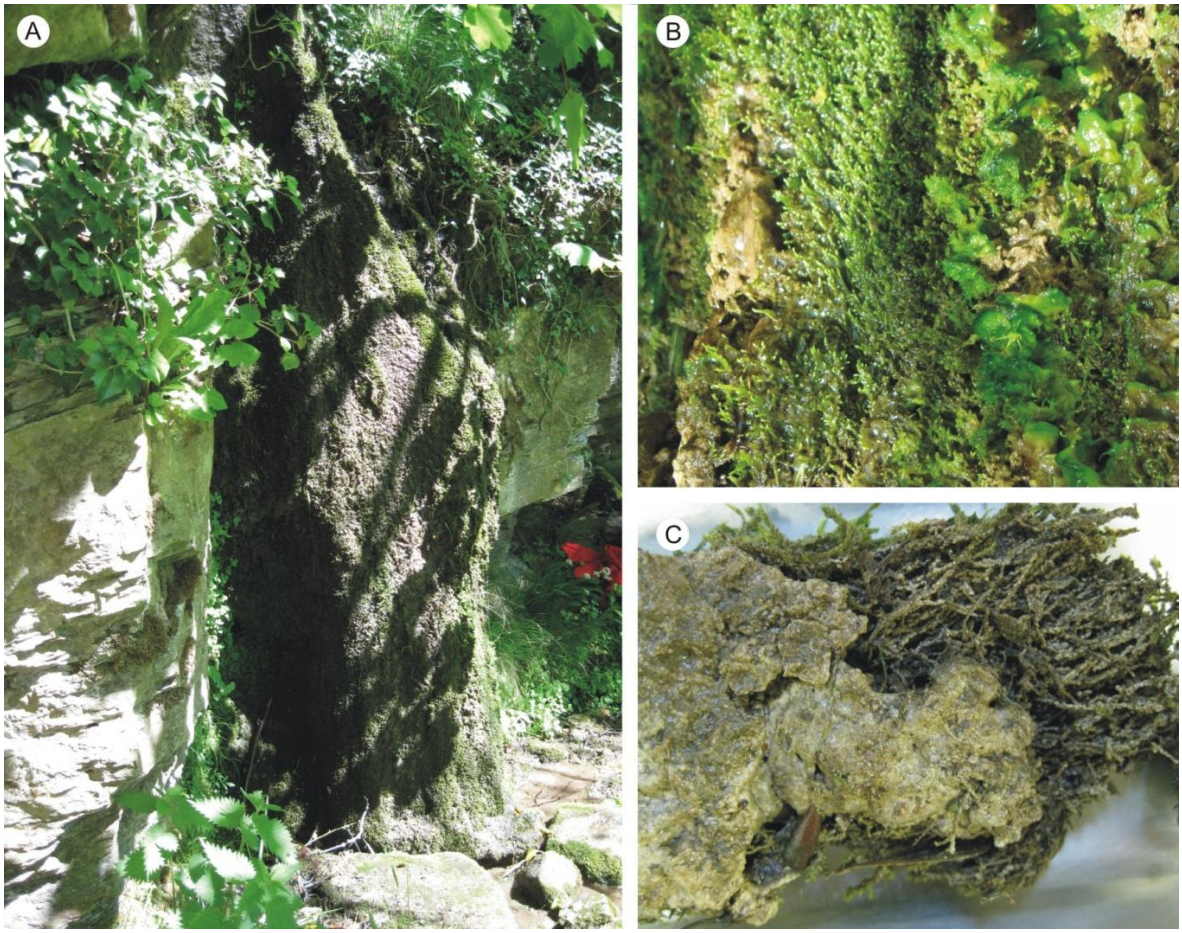

Fig. 4.22. A) Field view of tufa lobe forming near Barnard Castle. B) Detail of the external surface of tufa lobe showing partially calcified mosses (left) and Vaucheria tufts (right). C) Cross-section through tufa lobe characterized by calcified mosses.

5 WATER CHEMISTRY

Different parameters of the stream-water were measured in the field both in the barrage systems in Calabria and near Gateshead (Fig. 2.1) whereas cation and anion contents were determined by ionic chromatography and alkalinity by acidimetric titration (see Chapter 3). In addition, in the English barrage system and in the terraced-slope system (Fig. 2.1), water samples were analyzed by fluorescence spectroscopy to characterize the dissolved organic matter (DOM) present in the water.

In Calabria water parameters and chemical analyses have been measured both in the Parmenta stream and Corvino River (Fig. 4.1A). In general, both streams are characterized by a similar chemical composition.

Water analyses show that both streams are characterized by a Ca-HCO_3 chemical composition with variation in salinity of 8-12 meq/L (Fig. 5.1). In the Parmenta Ca^{2+} and Mg^{2+} are present with a mean concentration of 59 and 27.2 ppm respectively whereas anions show mean concentrations of 305.1 ppm (HCO_3^-) and 34.3 ppm (SO_4^{2-}). In the Corvino Ca^{2+} and Mg^{2+} are present with a mean concentration of 41.3 and 20.1 ppm respectively whereas the main anions show concentrations of 236 ppm (HCO_3^-) and 10.1 ppm (SO_4^{2-}) (Table 5.1).

Cations such as Na and K are also present in the Parmenta with mean concentrations of 4.6 ppm (Na) and 0.4 ppm (K) whereas in the Corvino they show concentration of 3.8 ppm (Na) and 0.2 ppm (K). Sr is present only in the Parmenta water with a maximum concentration of 5.4 ppm. Other anions present with minor concentration in both streams are Cl with mean concentration of 8.1 ppm and 7.1 ppm in the Parmenta and Corvino respectively, whereas SiO_2 and NO_3 show values of 3.4 ppm (SiO_2) and 6.9 ppm (NO_3) in the Parmenta and in the Corvino with concentration of 2.2 ppm (SiO_2) and 1.7 ppm (NO_3). (Table 5.1).

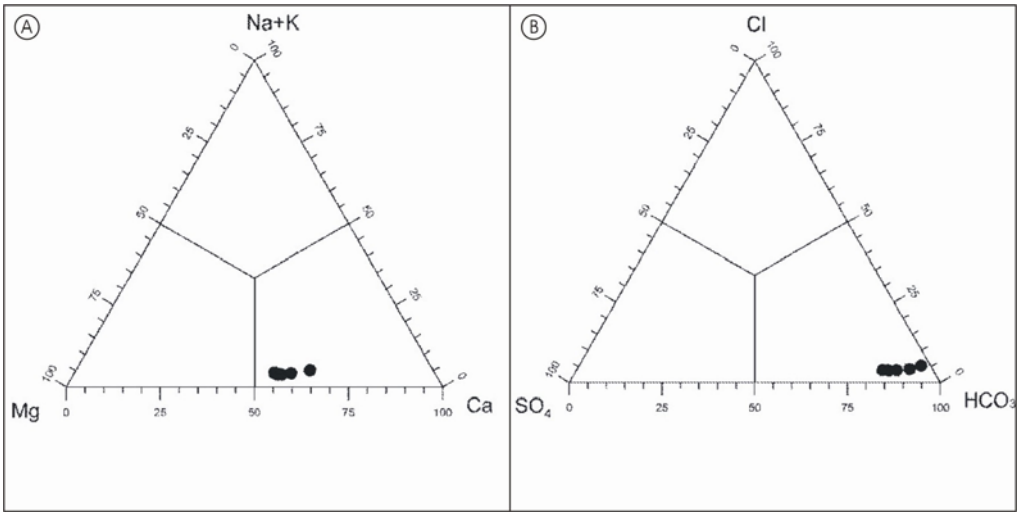

Fig. 5.1. Triangular diagrams of (Na+K)-Ca-Mg (A) and Cl-SO_4^--HCO_3^- (B) for the Parmenta and Corvino waters, reported in equivalent units.

	Ca	Mg	Na	K	SO_4	Cl	SiO_2	NO_3	HCO_3	Sr
Corvino	41,3	20,1	3,8	0,2	10,1	7,1	2,2	1,7	236,0	
Parmenta	59,0	27,2	4,6	0,4	34,3	8,1	3,4	6,9	305,1	3,17

Table 5.1. Chemical composition of the Corvino and Parmenta waters. Values are reported in ppm.

In both streams, water temperature shows a positive correlation with the variation of air temperature recorded during the monitoring year, with one difference: during the winter water temperature reaches values of ~8°C in both streams while in the summer, water temperature shows values of ~13°C in the Corvino and ~17°C in the Parmenta. The range of pH values in the Parmenta is 8.2 in winter and 8.4 in summer, while in the Corvino it is ~8.06 and ~8.2 respectively (Table 5.2).

The saturation index (SI) shows that both streams are oversaturated with respect to $CaCO_3$ (SI>0). In the Parmenta SI is ~0.75 during the winter and ~0.89 during the summer, whereas in the Corvino river SI values are ~0.35 and 0.42 respectively (Fig. 5.2).

Samples	pH	Water T (°C)	Air T (°C)
C1	8,06	8,6	12
C2	8,30	10	15
C3	8,23	13	20
C4	8,64	9,1	18
P1	8,24	6,8	12
P2	8,33	12	15
P3	8,47	17	20
P4	8,03	8,4	18

Table 5.2. Chemical data of the Corvino (C1-C3) and Parmenta (P1-P3) waters. WT=water temperature, AT= air temperature.

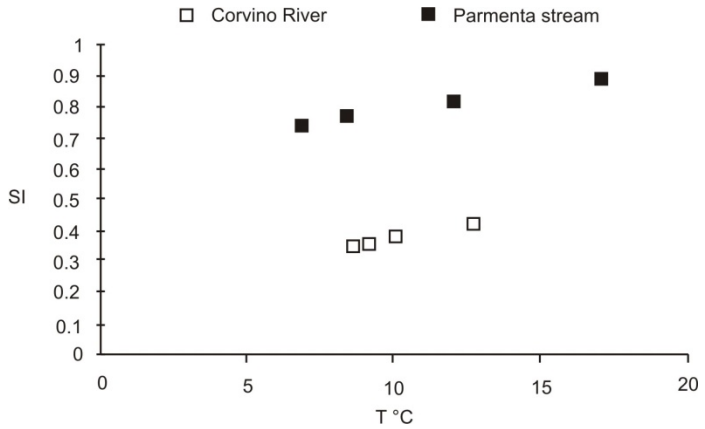

Fig. 5.2 Correlation plot of the saturation index (SI) versus temperature, calculated for the Parmenta stream and Corvino River waters in the interval 2008-2009.

In Thornley Burn (Fig. 4.7C) sampling along the stream shows that the chemical composition of the water is very similar along its watercourse (Fig 5.3 and Table 5.3). Plotting the values of the main cations and anions in the triangular diagrams, water chemistry shows a Ca-SO_4^{2-} composition (Fig 5.3). In fact the main cations present are Ca^{2+} with a mean concentration of 154 ppm and Mg with a mean value of 56 ppm whereas SO_4^- is present with a mean concentration of 361 ppm while the HCO_3^- shows a mean concentration of 327 ppm. Moreover, other cations present are Na with a mean value of 33 ppm and K with a mean concentration of 9,7 ppm; the anions as Cl and NO_3^- show mean concentration of 55 ppm and 1.3 ppm respectively (Table 5.3).

pH values range between 7.03 and 7.89 in the interval April-September while in October values range between 8.01 and 8.3, and conductivity varies between 1119 and 1473 µS cm^{-1} in the interval May-October (Table 5.4).

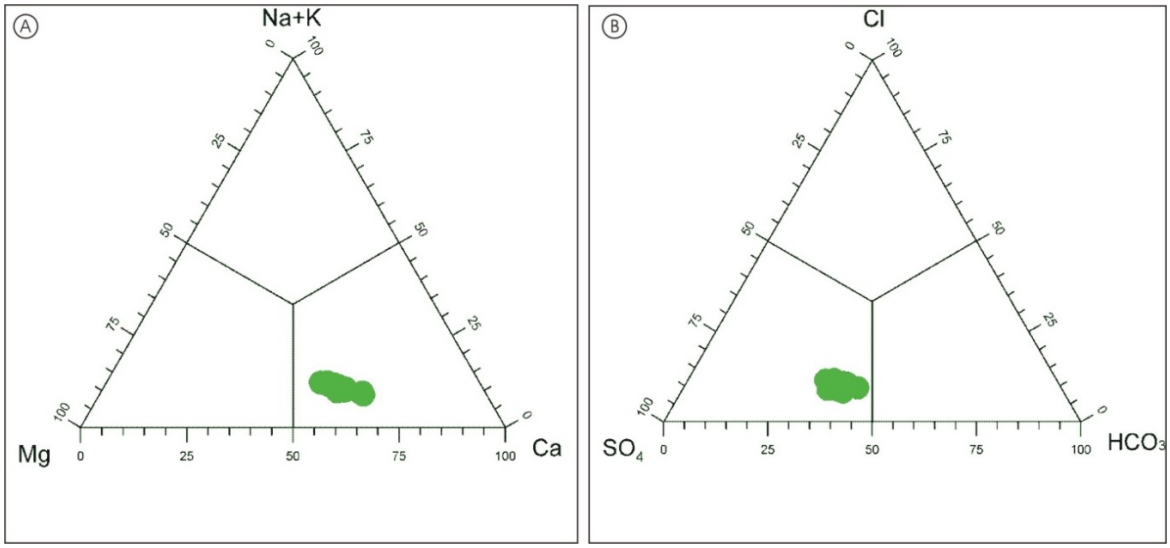

Fig. 5.3. Triangular diagrams of (Na+K)-Ca-Mg (A) and Cl-SO_4^--HCO_3^- (B) based on the Thornley Burn water concentrations, reported in equivalent units.

In the tufa system located near Barnard Castle (Fig. 2.1B), the main cations present in the water samples are: Ca with a mean concentration of 40.5 ppm, Na 9.5 ppm, Mg 7.8 ppm and K 1.8 ppm in Barnard Castle A, and Ca 31.2 ppm, Na 15.4 ppm, Mg 12.8 ppm and K 2.1 ppm in Barnard Castle B (Fig. 5.4).

Water chemical parameters measured in Barnard Castle A are reported in Table 5.5. Here pH varies over the study period from 7.08 to 8.39, whereas conductivity varies between 416 to 624 µS/cm.

Code	Sampling point	Sampling period	Ca	Mg	Na	K	SO4	Cl	HCO3	NO3	F
M1	first bridge	May 2009	179,3	68,1	30	10,4	412,4	59	450	1,6	0,1
M2	below first bridge		141	51,2	25,3	8,8	348,1	48,5	300	1,3	0
M3	6th dam pool		130	50,8	27,1	9,6	332,2	52,2	300	1,4	0
M4	6th dam		148,3	57	29,1	10,1	363,4	56,7	300	1,5	0
M5	6th dam pool		129,2	53,9	29	10,1	346,7	56,4	300	1,5	0
M6	5th dam		139,2	56,8	28,4	9,7	378,6	55,8	300	1,5	0
M7	4th dam pool		152,2	43,9	21,7	7,6	347,9	41,6	300	1	0
M8	4th dam		140	52,2	27,5	9,4	348,5	53,6	300	1,4	0
M9	3rd dam pool		151,8	52,8	25,3	8,5	373,5	49,1	300	1,3	0
M10	2nd dam pool		152	52,3	27,3	9,0	361,7	52,9	350	1,3	0
M11	2nd dam		137,7	39,1	20,3	6,9	329,6	39,1	230	1	0
M12	2nd pool bottom		143	40,5	19,5	6,4	321,1	37,4	300	1	0
M13	2nd pool bottom		163,5	59,7	30,1	10	393,7	58,6	350	1,6	0,1
M14	stream near tunnel		105,8	46,9	24	7,9	302,6	46,6	230	1,3	0
M15	1st dam		121,3	54,6	27,9	9,7	339,5	54	280	1,4	0,3
TB 1	first bridge	November 2009	197,4	67,2	76,1	10,5	381	93,3	450	2,9	0,2
TB 2	pool		212,2	75,6	49,6	11,7	443,1	60,8	400	0,7	0,1
TB 3	dam		208,5	79,8	83,2	11,3	463,2	99,5	400	0,5	0,1
TB 4	towards tunnel		143,8	52,6	33,4	10	304,5	54,7	400	1,2	0,1
TB 5	dam		160,7	59,9	28,3	11,7	342,9	43,1	350	0,6	0,1
TB 6	pool		158,2	61,2	25,9	11,5	347,4	42,8	300	0,6	0,1
T 13	dam		167,2	61,4	30,4	12,4	357,3	46,5	300	1,4	0,1

Table 5.3. Chemical composition of the Thornley Burn waters. Values are reported in ppm.

April 2009			June 2009			September 2009			October 2009			
Sample	pH	Cond	Sample	pH	Cond	Sample	pH	Cond	Sample	pH	Cond	
			Th1(tunnel)	7.35	1299	D31 (dam)	7.57	1390	Tw6 (dam)	8.04	1422	
D1	7.03	900	Th2	7.43	1398	D31 (pool)	7.05	1393	Tw7 (pool)	8.00	1435	
D2	7.03	930	Th3	7,63	1389	D30 (pool)	7.53	1385	Tw8 (dam)	8.04	1420	
D3	7.04	960	Th4	7,05	1415				Tw9 (pool)	8.00	1445	
			Th5	7,6	1367				Tw10 (dam)	8.03	1423	
May 2009			Th6	7,8	1379	**October 2009**			Tw11 (pool)	8.02	1448	
Sample	pH	Cond	Th7	7,86	1361	Sample	pH	Cond	Tw12 (dam)	8.04	1420	
D5 (dam)	7.06	1345	Th8	7,81	1356	TB1	7,65	1317	Tw13 (pool)	8.04	1415	
D6 (dam)	7.06	1310	Th9	7,84	1358	TB2	7,65	1360	Tw14 (dam)	8.03	1437	
D7 (dam)	7.05	1323	Th10	7,87	1380	TB3	7,89	1406	Tw15 (pool)	8.01	1449	
D8 (dam)	7.04	1351	Th11	7,89	1410	TB4	7,71	1256	Tw16 (dam)	8.04	1423	
D9 (side stream)	7.05	1119	Th13	7,86	1396	TB5	7,9	1416	Tw17 (first bridge)	8.00	1440	
D10 (pool)	7.05	1134	Th14	7,7	1410	TB6	7,92	1375	Tw18 (first bridge)	8.36	1410	
D11 (side stream)	7.02	1665	Th15	7,59	1425	Tw1 (tunnel)	8.01	1405	Tw19 (second bridge)	8.18	1470	
D11 (iron-rich seepage)	7.15	1466	Th16	7,3	1441	Tw2	8.02	1419	Tw20 (second bridge)	7.53	1473	***Notes***
D12 (iron-rich seepage)	7.01	1581				Tw3	8.07	1383	D1	7.73	349	*Derwent river*
D13 (dam)	7.04	1336				Tw4	8.03	1431	D2	7.53	662	*Derwent river*
D14 (dam)	7.03	1324				Tw5 (pool)	8.06	1415	D3	7.75	667	*Derwent river*

Table 5.4. Chemical data of the Thornley Burn water. Conducibility (Cond.) is expressed in µS/cm.

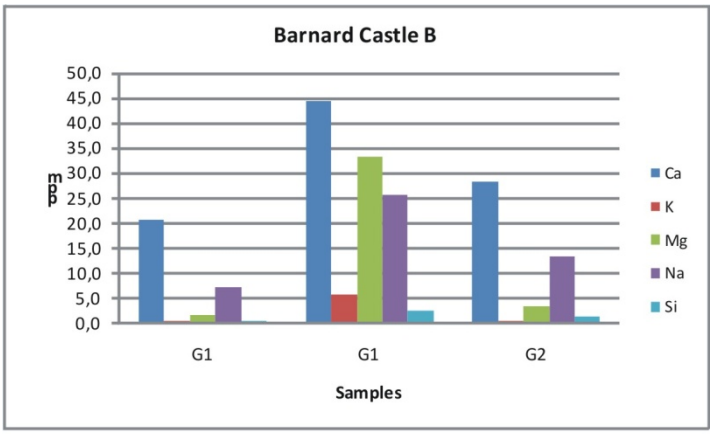

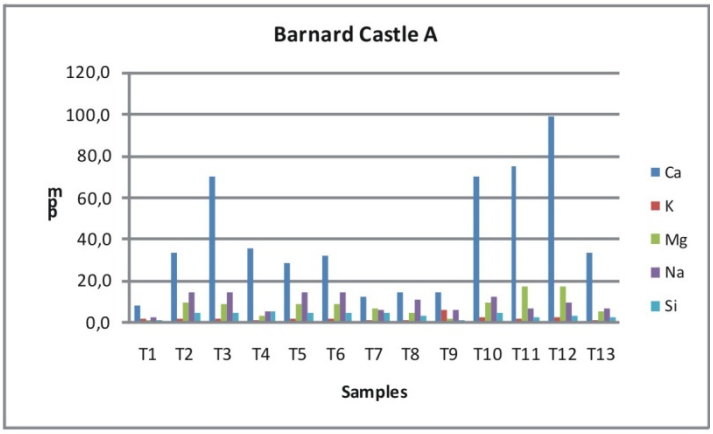

	October 2008			October 2009	
Sample	**pH**	**Cond**	**Sample**	**pH**	**Cond**
T1	6.07	100	R1	7.08	144
T2	7.08	624	R2	7.07	177
T3	8.15	590	R3	7,86	529
T4	8.18	580	R4	7,95	541
T5	8.24	587	R5	7,89	586
T6	8.28	590	R6	8.04	517
T7	8.39	439	R7	8.05	527
T8	8.42	413	R8	8	540
T9	8.33	93	R9	8.02	566
			R10	8.13	583
Notes			R11	8.12	602
T1	River Tees		R12	8.05	598
T2	River Tees		R13	8.36	608
R1	River Tees		R14	7.48	643
R2	River Tees		R15	8.22	410
R3	side-stream				
R14	side-stream				

Fig. 5.4. Diagrams of the main cations present in Barnard Castle A and B. Table of the chemical data of water samples in Barnard Castle A.

Concerning the fluorescence analyses, performed for water samples collected in Thornley Burn (Fig. 4.7C) and in Barnard Castle A (Fig. 2.1B), the typical EEMs obtained are shown in Fig. 5.5. The EEMs matrix shows that in all samples the fluorescence centres of tryptophan-like (T) and tyrosine-like material (B), taken as tracers of sewage effluents in natural waters (Baker et al., 2003), are absent.

The EEMs matrix for water samples from the Derwent River and River Tees are different (Fig. 5.6). Here the intensities of peaks T and B, especially for the Derwent River (Fig. 5.6 top) are higher in comparison with the tufa-depositing stream water.

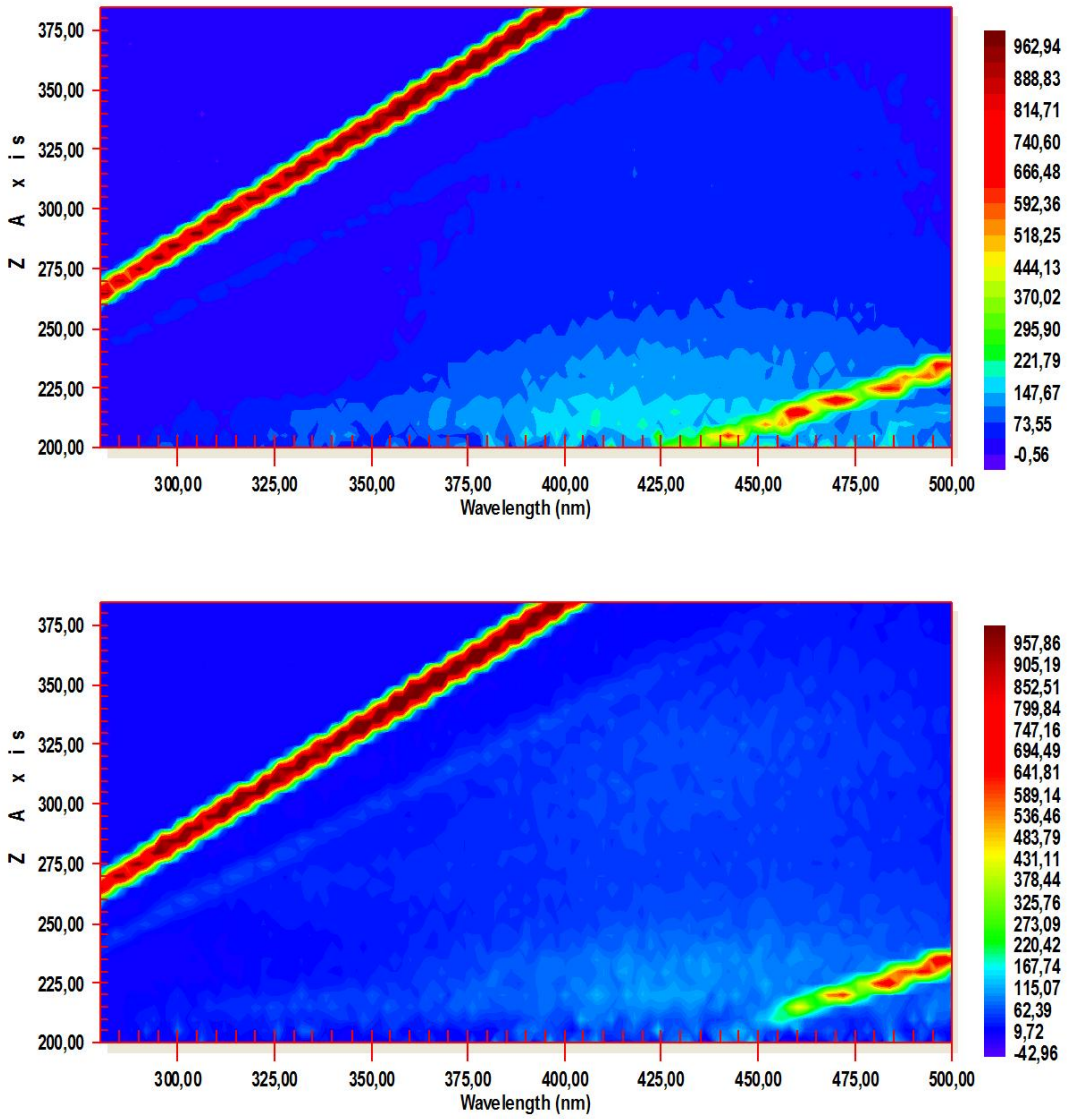

Fig. 5.5. Typical fluorescence EEMs observed in this study. Top: EEMs matrix generated by water samples from Thornley Burn; bottom: EEMs matrix generated by water samples on drained slope in Barnard Castle (A).

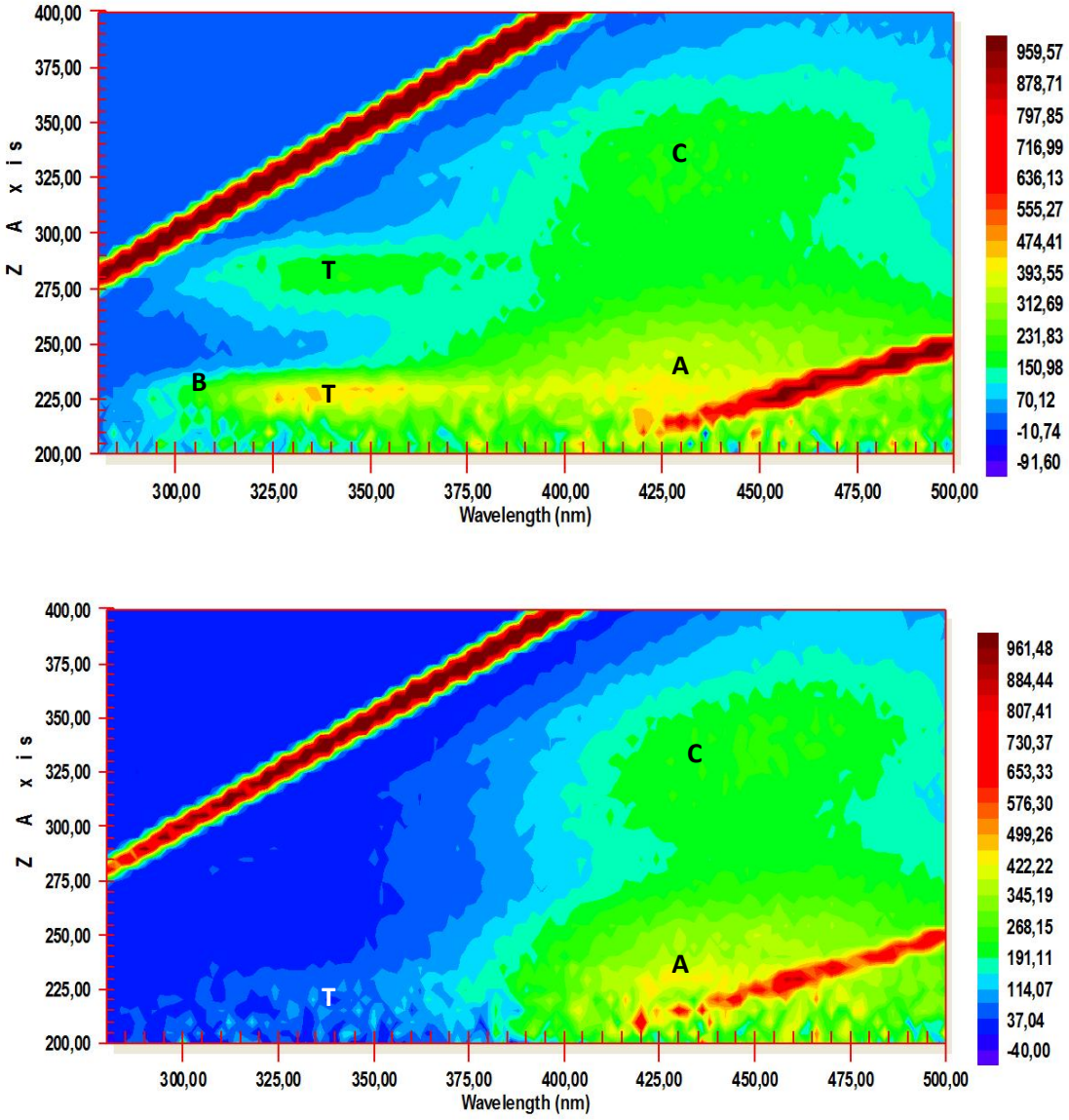

Fig. 5.6. Top - EEMs matrix generated by water samples from the Derwent River: bottom - EEMs matrix generated by water samples on Tees river.

6. TUFA DEPOSITIONAL FACIES

6.1 Mineralogy and geochemistry

Mineralogical and chemical investigations were performed on all tufa samples. In particular, XRD analyses were carried out on all facies, excluding samples collected in Barnard Castle B (Fig. 2.1), where tufa facies from both barrage systems and the terraced- slope system were investigated by dispersive X ray spectrometer (EDS) for chemical semi-quantitative analyses. Finally, stable isotope analyses were performed on rock samples collected from the various tufa depositional systems located in the NE England.

X-ray diffraction analyses of bulk samples reveal that the main mineral phase is calcite (Fig. 6.1). The position of the d_{104} peaks detected in the different depositional facies, range between 29.4 2θ and 29.6 2θ; this is comparable with the d_{104} value of 29.4 2θ reported in the X-ray diffraction pattern of standard calcite (Hardy & Tucker, 1988). Moreover, XRD analysis shows that samples contain low amounts of quartz and some dolomite was found in the deposits of the Parmenta system (Figs 6.1, 6.2).

EDX electron microprobe analyses performed on tufa samples collected in the three studied sites confirm that the main mineral phase forming tufa deposits is calcite with a few mole % Mg. The Mg content is similar in both the Parmenta barrage system (stromatolitic and vacuolar facies) and in the terraced- slope system (moss tufa, crusts and pisoids), varying respectively from 0.9 to 3.9 mole % and from 0.4 to 2.5 mole % whereas minor elements such as Sr and S range from 0.5 to 1.2 mole % Sr, detected only in the barrage tufa deposits whereas S content is less than 1 mole % (Table 6.1). Quartz and dolomite represent allochthonous detrital minerals incorporated into the tufa deposits (Fig. 6.2).

In tufa samples collected in the Thornley barrage system, and in particular in the pustular facies, although XRD confirms that calcite is the principal crystalline phase (Fig. 6.1), petrographic observations (see below) and EDX analyses, reveal the occurrence of distinct areas or layers characterized by amorphous crystalline phases of variable composition, alternating with low-Mg calcite (1.3-3.5 mole %) (Fig. 6.3).

Principal elements that constitute these amorphous crystalline phases are: Mn with a mean content of ~38 mole %, Si with ~20 mole %, Ca with ~17 mole %, Al with ~13 mole %, Mg with ~5 mole % and Fe with ~4 mole %. The elements Na, K and Cl are present with a mean value of ~2 mole % whereas S and Ti show a mean content of ~1 mole % (Table 6.2). Under the SEM, the corresponding crystal morphologies forming these areas, vary from poorly-ordered structures to better defined crystalline phases. In the first case, they form a sort of network that covers and/or forms sub-spherical aggregates of ~1-5 μm in size occupying cavities or occurring packed on the

external surface of probable filamentous bacteria. The well-ordered crystalline structures occur as platy crystals (Fig. 6.4).

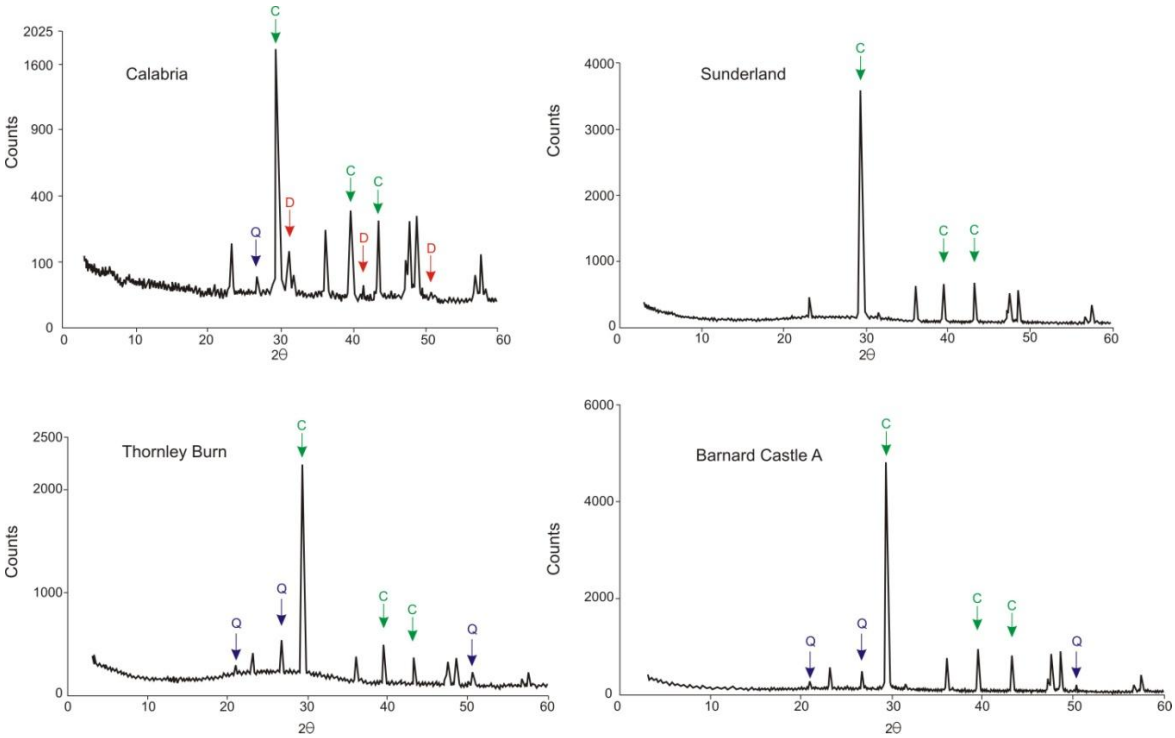

Fig. 6.1. X-ray diffraction charts of tufa samples collected in the different study sites. Mineral phases are indicated by the three main peaks detected for calcite (C), quartz (Q) and dolomite (D).

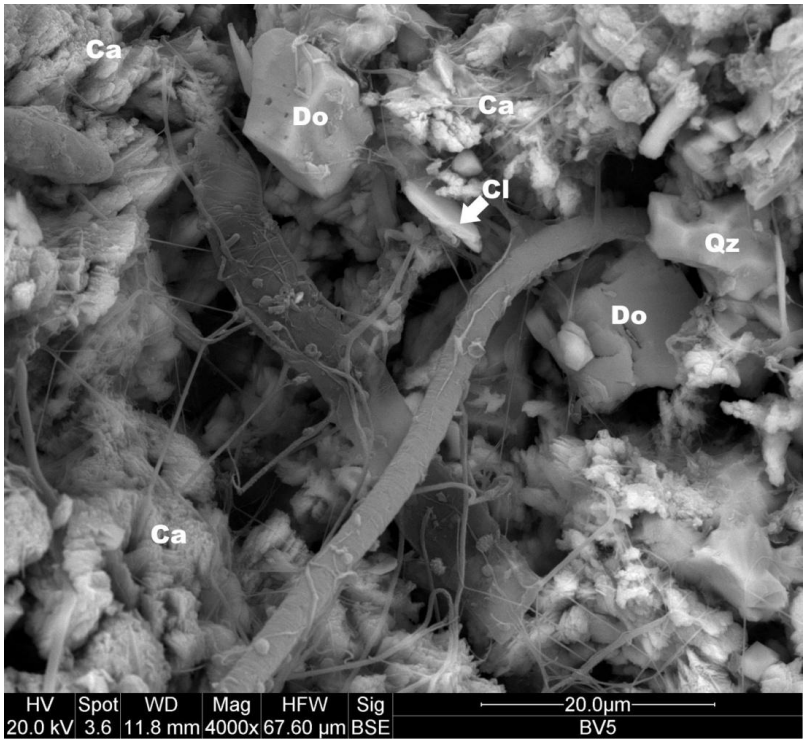

Fig. 6.2. Detrital dolomite (Do), quartz (Qz) and clay (Cl) in calcite (Ca) tufa deposits.

SAMPLE Ⓐ	Mg	Al	Si	Sr	S	Ca	Fe
BV-001	2,2			1,1	0,4	95,6	0,76
BV-002	2,8			0,9	0,7	95,6	
BV-003	1,9			1,0	0,6	96,6	
BV-004	2,3			1,1	0,8	95,8	
BV-005	2,3			1,0	0,7	96,0	
BV-006	3,9			1,2	0,5	94,4	
BV-007	2,2			0,8	0,5	96,5	
BV-008	2,1			1,0	0,6	96,4	
BV-009	2,9	1,0	1,7	0,7	0,4	93,4	
BV-010	2,3	0,6	0,7	0,6	0,4	95,5	
BV-011	2,9			0,9	0,5	95,6	
BV-012	2,1			1,1	0,6	96,2	
BV-013	2,1			0,8	0,2	96,9	
BV5_009	3,2			0,5		96,3	
BV5_010	3,2			0,6		96,2	
BV5_011	2,5			0,6		96,9	
BV5_012	1,5			0,6		97,9	
BV5_013	2,1			0,7		97,3	
BV5_014	2,3			0,8		97,0	
BV5_015	0,0			0,6		98,4	
BV5_016	0,1			0,8		97,1	
BV5_017	0,1			0,8		97,9	
BV5_018	0,9			0,7		98,4	
BV5_019	1,9			0,6		97,5	
BV5_020	2,4			0,8		96,8	
BV5_021	2,1			0,7		97,3	
BV5_022	1,8			0,7		97,5	
BV5_023	1,0			0,6		98,3	
BV5_024	1,4			0,7		97,9	

SAMPLE Ⓑ	Mg	Al	Si	S	Cl	Ca	Fe
UK1p-001	1,8	3,3	4,6	0,6	0,2	88,7	0,74
UK1p-002	1,1					99,4	
UK1p-004	1,4					98,6	
UK1p-005	1,5					98,5	
UK1p-006	1,8	1,4	2,7	0,6		93,6	
UK1p-007	1,8	1,3	1,3			95,7	
UK1p-008	1,6	1,9	2,8	0,6		93,1	
Ukt-001	2,5					97,5	
Ukt-002	1,8	2,7	3,0	0,6		91,9	
Ukt-003	1,9	1,2	1,1	0,7		95,1	
Ukt-004	1,3	1,2	1,1			96,4	
Ukt-005	0,4	0,9	4,6			94,0	
Ukt-006	0,5	1,0	1,7			96,7	

Table 6.1. Spot-size EDX analyses performed during SEM observations on representative samples from the Calabrian barrage system (A) and terraced- slope system (B). Values are reported in mole %.

SAMPLE	Na	Mg	Al	Si	S	Cl	K	Ca	Ti	Mn	Fe
derwF_001	0,75	2,88	13,36	44,92			4,33	22,07	0,67	4,74	6,28
derwF_002	2,52	8,12	9,3	27,04			1,46	12,91	0,28	34,26	4,09
derwF_003	1,83	7,79	14,06	18,49			1,07	14,82	0,44	38	3,49
derwF_004	1,43	6,82	16,69	26			1,64	13,44	0,57	27,42	5,98
derwF_005	1,72	6,65	16,68	27,88			1,75	12,37	0,41	26,65	5,9
TH-01		3,59	21,89	30,27	0,97	2,05	2,35	7,98		25,59	5,32
TH-02		6,12	7,49	6,45	0,95	1,67		26,08		48,44	2,81
TH-03		3,61	12,41	16,32	1,23	2,67	1,15	44,39		11,74	6,47
TH-04		2,95	24,94	38,55	0,64		3,17	17,63		5,45	6,68
TH-06		5,87	15,64	21,14		1,35	2,16	8,91		41,29	3,63
TH-07		4,99	15,53	21,67		1,86	1,46	29,94		20,96	3,59
TH-10		6,3	16,14	18,37	1,44	3,09	1,4	12,42		34,23	6,61
TH-11		6	8,05	16,08	1,16	1,69	0,75	18,95		43,21	4,1
TH-12		6,02	9,73	11,93	0,95	1,45	1,68	21,7		43,05	3,49
TH-13		5,25	11,53	21	0,63	1,27	1,73	17,74		37,42	3,43
Th004		1,56	34,85	52,87			2,84	5,43	0,53		1,92
Th005		8	3,46	7,38		4,29		13,21		61,74	1,91
Th012	1,65	4,48	2,21	2,94	1,1	0,55	0,3	15,23		69,41	2,08
Th015		3,52	3,89	6,3	0,92	0,49	0,8	27,67		56,39	
th6	3,95	5,29	10,39	12,58	0,74		1,51	10.05	1,11	50,76	3,62
th8	2,8	4,87	1,84	2,05	0,64			11,61		74,05	2,19

Table 6.2. Spot-size EDX analyses performed during SEM observations of the areas formed by amorphous crystalline phases. Values are reported in mole %.

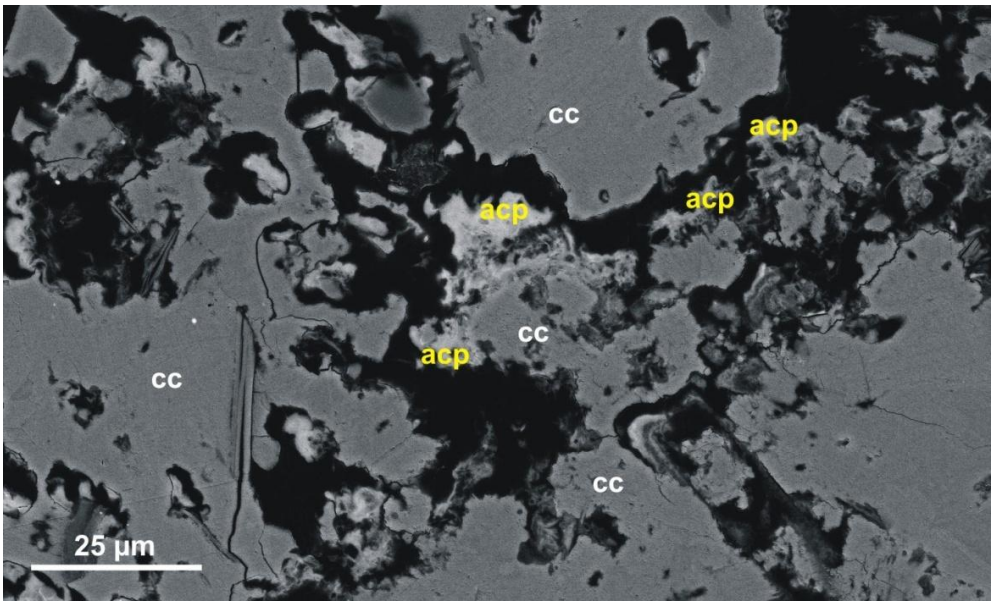

Fig 6.3. Backscattered electron image of pustular tufa facies showing the distribution of Mn-rich amorphous crystalline phases (acp), alternating with calcite crystals (cc).

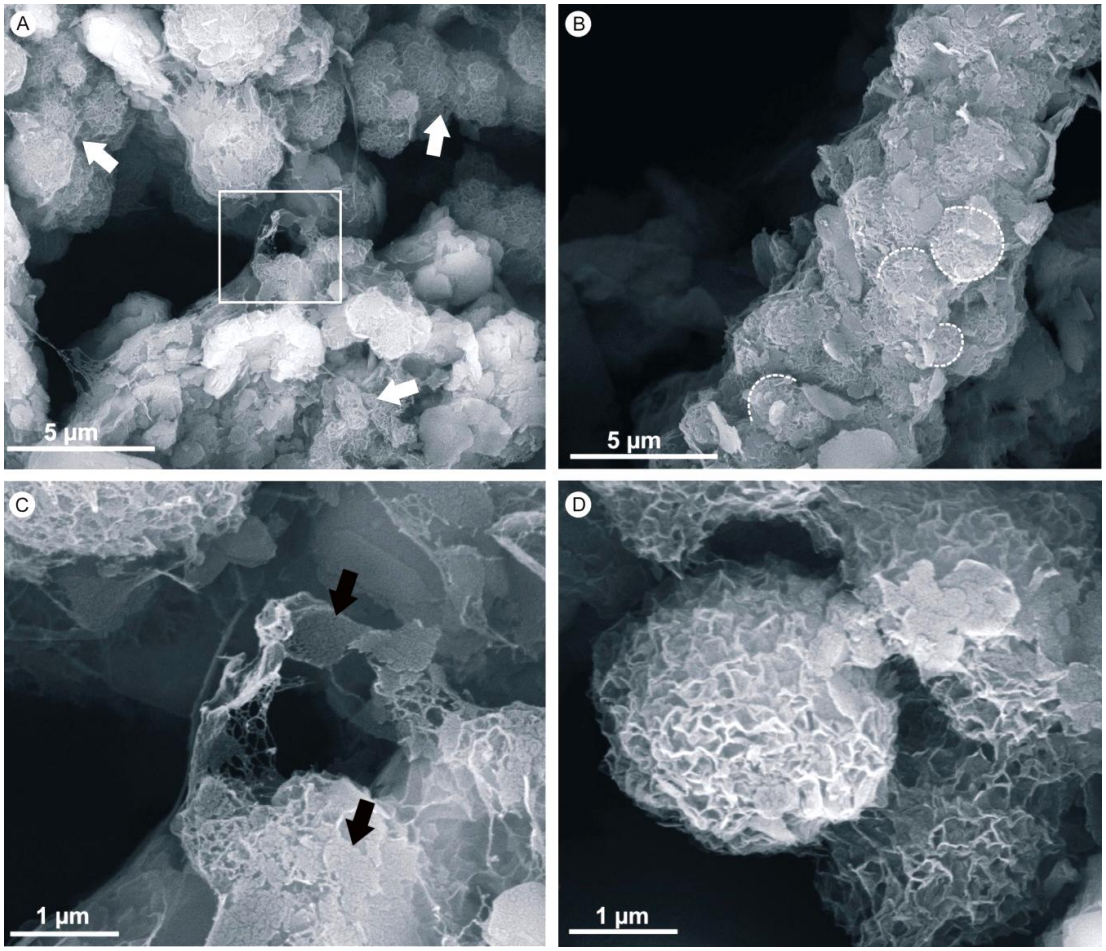

Fig. 6.4. SEM images of the crystal morphologies forming Mn-rich layers in pustular tufa facies. A) Sub-spherical forms (white arrows) covered by networks of poorly-ordered crystalline structures. B) Aggregation of sub-spherical forms on the external surface of probable filamentous bacteria. C) Detail of A. Association of poorly-ordered structures being gradually substituted by more definite crystalline phase, occurring as platy crystals (black arrows). D) Sub-spherical forms covered by poorly- ordered crystalline structures.

Other than these amorphous crystalline phases, there are also pyrite crystals that commonly occur with a framboidal texture, produced by the aggregation of densely packed micron-sized crystals (Fig. 6.5A); they were occasionally observed with well-defined prismatic crystals of calcium phosphate composition (Figs 6.5B and C).

Spot-size EDX elemental analyses across calcite to Mn- rich layers reveal that the carbonate phase has an enrichment of different minor elements, including S, Mn and Fe (Figs 6.6, 6.7 and Table 6.3). In particular, the Mn content is higher in the areas formed by amorphous crystalline phases (Fig. 6.7A and B), with a mean concentration of 40 mole % (Fig. 6.3 and Table 6.2), and reduces gradually to less than 1 mole % in calcite crystals (Fig. 6.7C and D). Moreover, the Mn-enrichment in calcite is evidenced also by cathodoluminescence (Fig. 6.8).

Stable isotope data ($\delta^{18}O$ and $\delta^{13}C$) of tufa samples are reported in Fig. 6.9. The $\delta^{18}O$ composition ranges from -5.4 to -6.6, and these are in the range of typical tufa deposits (Andrews & Brasier, 2005; Andrews, 2006). The $\delta^{13}C$ composition shows values between -5.4 and -14.1‰ in all tufa facies (laminated crusts, moss tufa, pisoids) forming in the drained-slope system and in cave pearls, and these are also comparable with data reported in the literature (Andrews and Brasier, 2005; Andrews, 2006) however, the tufa deposits that occur in the barrage tufa system of Thornley show positive carbon values of 2.9-3.8‰, recorded in the different depositional facies (pustular-vacuolar-*Vaucheria* tufa). This is very unusual.

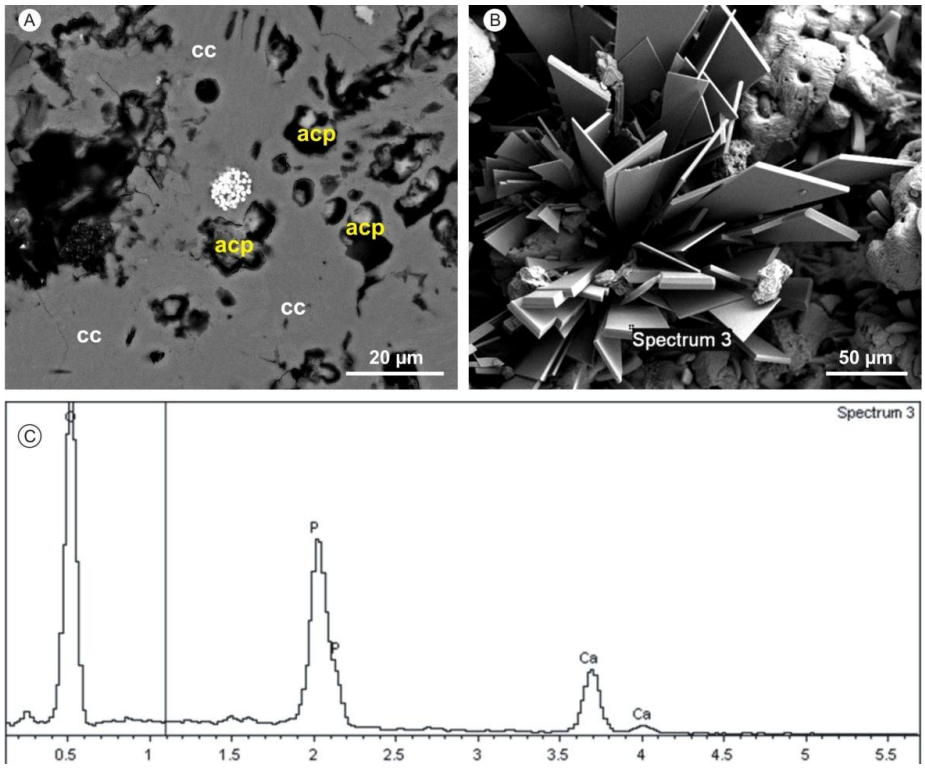

Fig 6.5. A) Framboidal pyrite associated with calcite (cc) and Mn- amorphous crystalline phase (acp). B) Well defined apatite crystals forming in pustular tufa. C) EDX spectrum produced by the point marked in B, showing Ca and P related peaks.

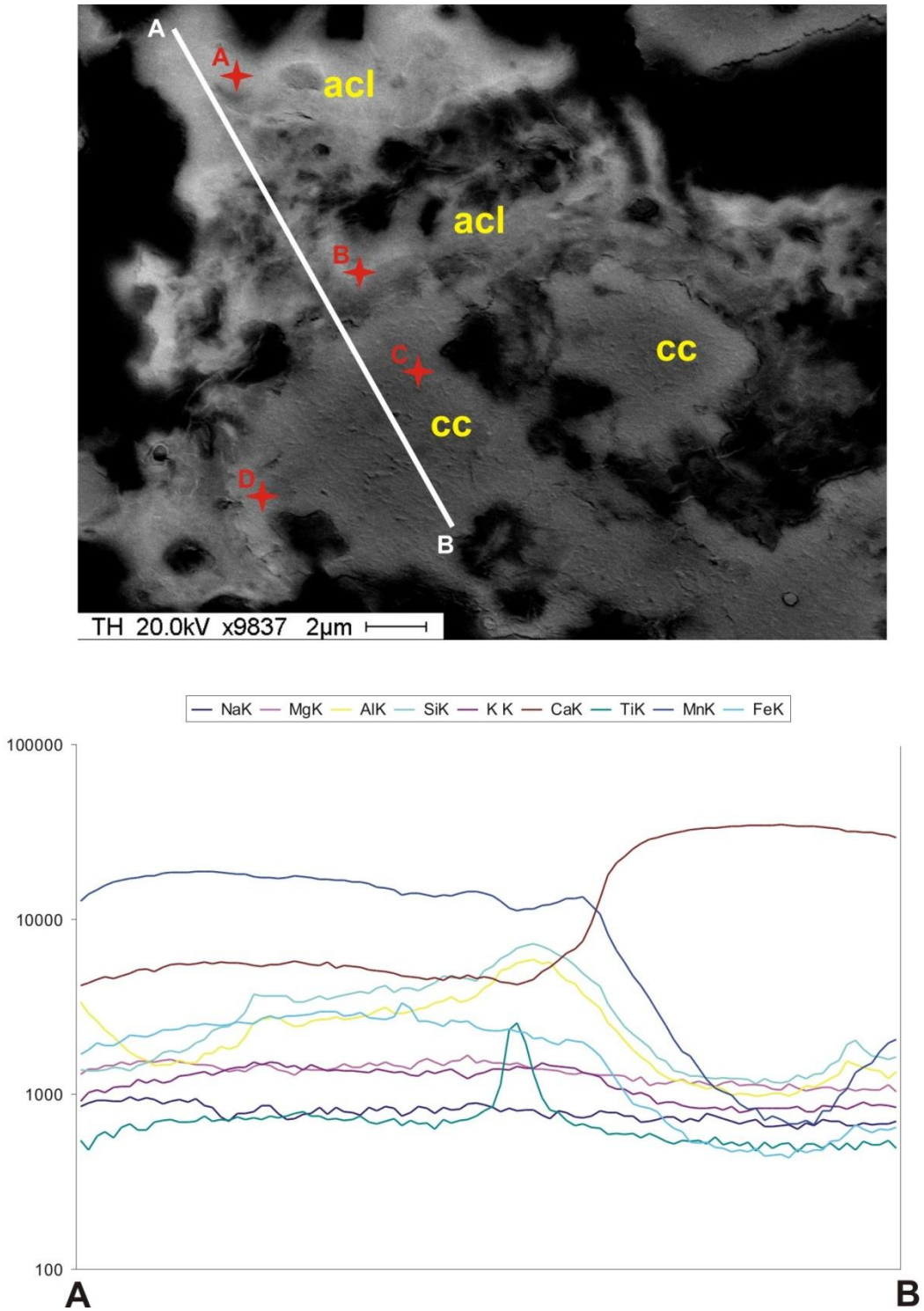

Fig 6.6. Upper image shows the sites of size-spot analyses (marked with letters from A to D) performed along the mapping-line (transect A-B) across calcite layers (cc) alternating with Mn- amorphous crystalline layers (acl). Lower image shows element distributions recorded along the line A-B.

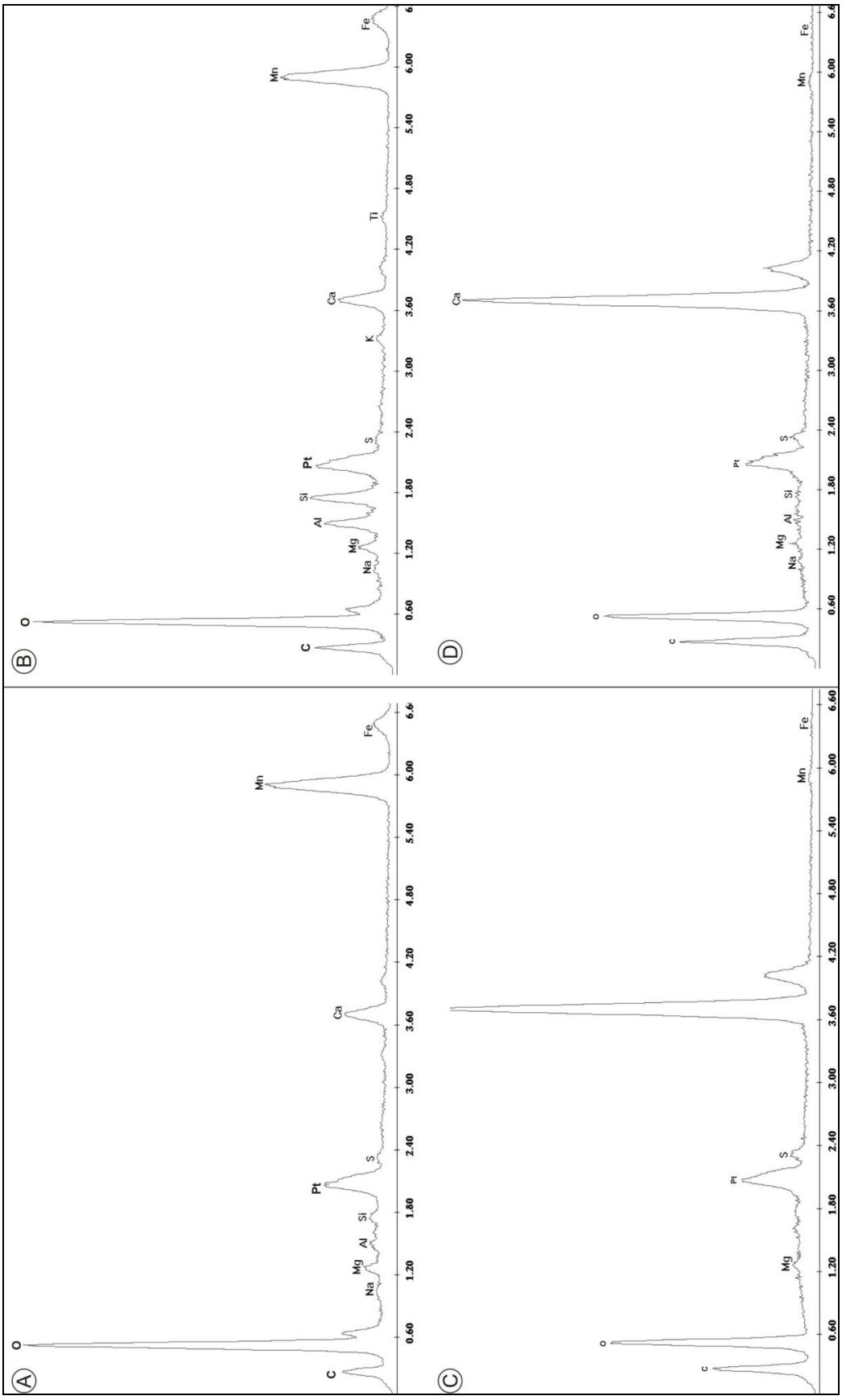

Fig 6.7. EDX spectra produced by spot-size analyses performed along the line A-B across Mn- amorphous crystalline layers (spectra A and B) alternated with calcite layers (spectra C and D)

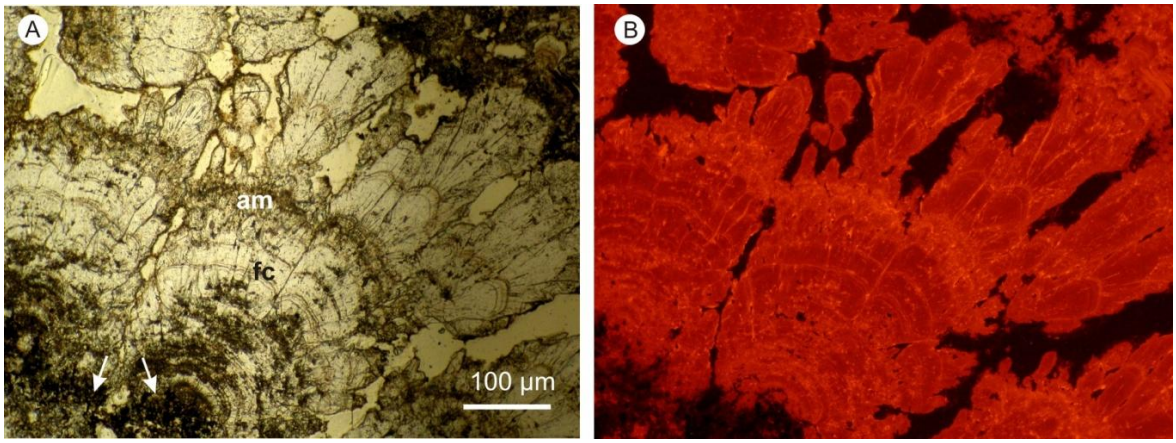

Fig 6.8. Cathodoluminescence images of calcite crystals in pustular tufa facies. A) and B) Fibrous calcite (fc) alternating with aphanitic microspar layers (am) and Mn-rich layers (white arrow).

SAMPLE	Na	Mg	Al	Sr	Si	S	K	Ca	Mn	Fe
Th001		2,4						97,6		
Th002		2,1	3,9		4,2	2,1	0,6	86,1		1,0
Th005	1,1	1,6	2,8		3,8	1,1		86,8	1,8	0,9
Th006		1,5	0,5		0,5	1,8		95,2	0,4	0,2
Th007	0,9	2,3				1,6		95,3		
Th008		1,8				1,5		95,5	1,1	
Th009	2,8	3,5	1,7	1,1		2,4		87,5	0,5	0,5
Th010	0,9	1,3	0,3	0,5		1,9		94,7	0,2	0,3
Th011		2,3		0,4		1,8		95,1	0,2	0,2

SAMPLE	Mg	Al	Si	S	Ca	Mn	Fe
Th013	1,6	0,4	0,7	2,1	93,7	0,3	
Th014	1,7	0,8	1,1	1,6	94,8		
Th015	2,2		0,7	1,8	95,3		
th1	2,2			2,1	94,9	0,7	0,4
th2	2,3			1,8	95,2	0,5	0,3
th3	2,1			1,8	95,2	0,6	0,3
th4	1,7			2,0	95,1	0,6	0,6
th5	1,7			2,1	93,9	1,7	0,6
DERW-001	2,8				97,2		

Table 6.3. Spot-size EDX analyses performed during SEM observations on representative sample of pustular tufa deposits, forming in the barrage system of Thornley stream. Values are reported in mole %.

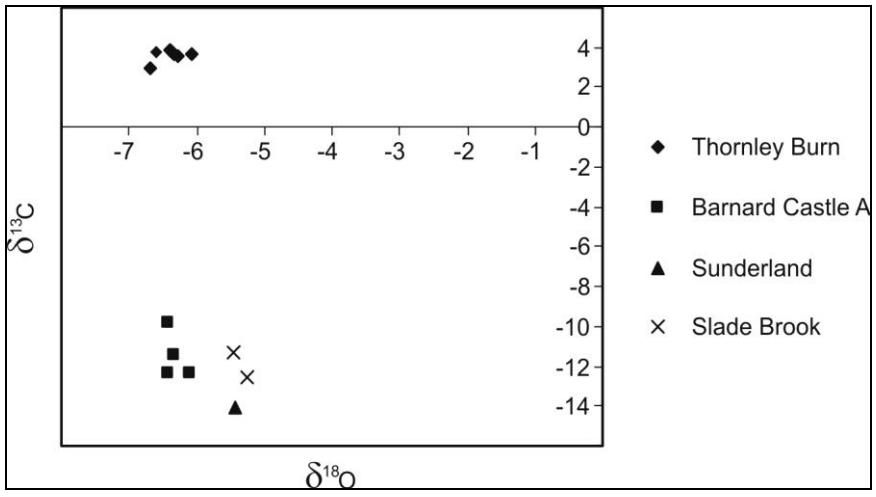

Fig 6.9. Stable isotope composition ($\delta^{18}O$ and $\delta^{13}C$) of tufa deposits, forming in different depositional settings.

6.2 Petrography and mineral fabrics

Thin-section observations show that the most common petrographic components of the studied tufa deposits are: micrite (anhedral mostly opaque crystals < 4 μm), microspar (subhedral to euhedral clear crystals between 5 and 15 μm) and spar or pseudospar (euhedral clear crystals > 15 μm). These, singly or associated, give rise to several mineral fabrics (Figs 6.10- 6.11).

Micrite and microspar are often associated with four types of fabric: peloidal to aphanitic, laminar and dendrolitic (Fig. 6.10).

The peloidal fabric consists of anhedral brown micrite crystals that constitute aggregates of 20-30 μm in size with sub-rounded to irregular shape (Fig. 6.10A and D). Commonly these micritic aggregates are surrounded by an isopachous rim of microspar (Fig. 6.11B). The peloidal fabric locally passes to a more homogeneous texture (aphanitic micritic fabric) (Figs 6.10A-B and 6.11D). Microspar can become much more abundant, producing a sort of aphanitic microspar fabric (Fig. 6.10A).

Laminar fabric mainly consists of the same brown micrite organized into thin, even to crinkly laminae, 8-10 μm thick, forming layers up to ~ 40 μm, alternating with microsparitic laminae of similar thickness (Fig. 6.10A and C).

Dendrolitic fabric originates from the encrustation of filamentous, in some cases branching, organic material, mainly represented by filamentous cyanobacteria. Filaments are often mineralized by micrite and/or microsparite, but even by sparitic calcite crystals (Fig. 6.10E).

Sparry calcite can occur in layers composed of isolated to coalescent fan-shaped crystals or fibrous calcite, that can form botryoids of 100-150 μm in size or continuous crusts ~100-200 μm thick (Fig. 6.11). Sparry crusts develop mainly on organic substrates (leaves and mosses) or line empty cavities (Fig. 6.11A and D). Crusts commonly form multi-layer structures alternating with thin laminae of brown micrite, generating a laminar fabric (Fig. 6.10B). Isolated botryoids and spherulites are widely found in association with all described fabrics (Fig. 6.11 A and B).

Fig. 6.10. Micrite-microspar mineral fabrics in neoformed tufa deposits. A) Layers of aphanitic (a), laminar (l) and peloidal (p) micrite-microspar fabrics. B) Detail of aphanitic (a) and laminar (l) micrite associated with sparry crusts (sp). C) Close-up view of laminar micrite. D) Peloidal micrite formed by sub-rounded to irregularly shaped aggregates. E) Dendrolitic fabric (dashed line) formed by mineralized cyanobacterial filaments, visible in transverse and longitudinal sections (white arrows), creating layers with branched microstructures. Filaments are mineralized by micrite (m), microspar (ms) and spar (s). Plane polarized light.

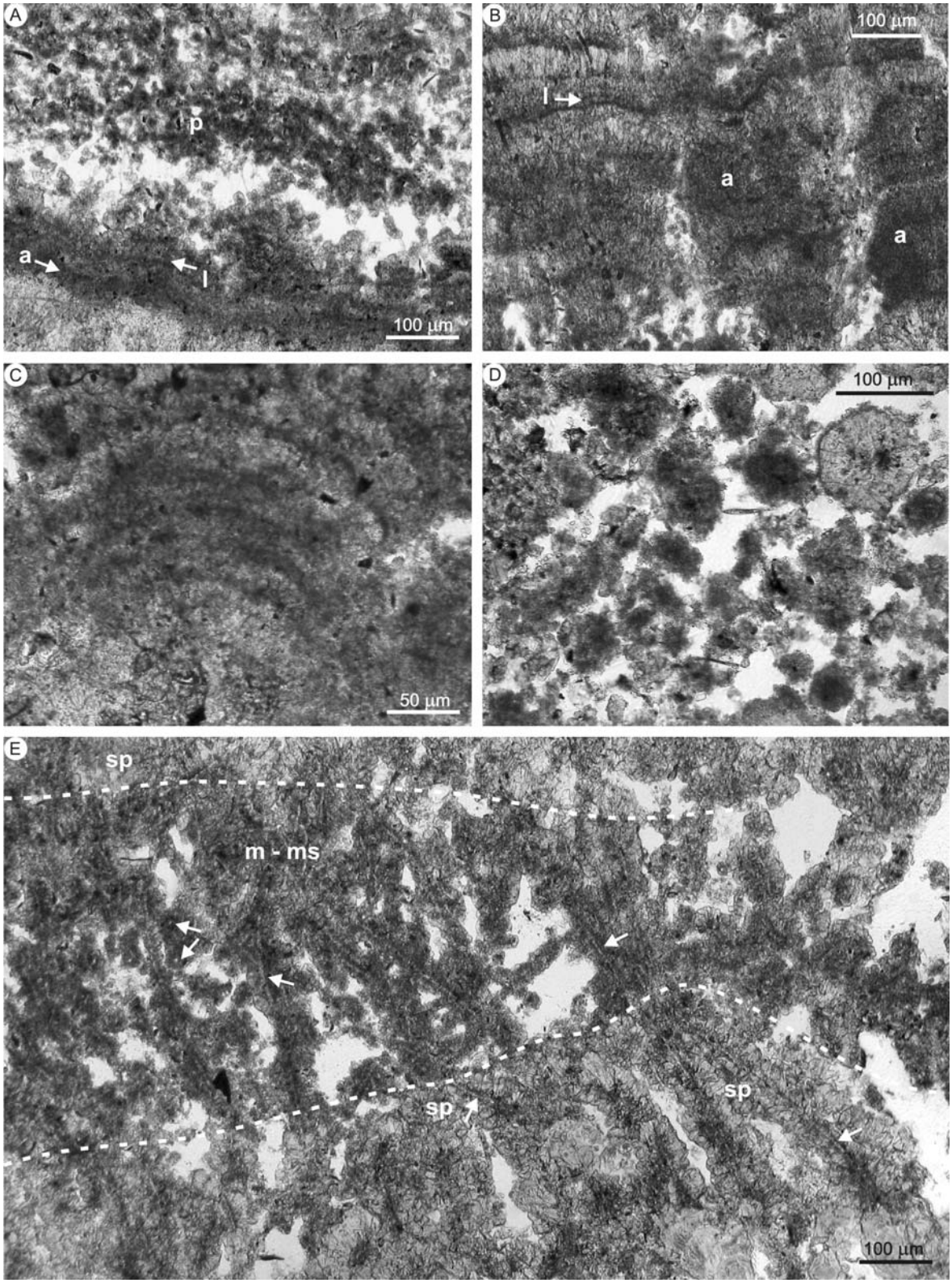
A
p
a
l
100 µm
B
100 µm
l
a
a
C
50 µm
D
100 µm
E
sp
m - ms
sp
sp
100 µm

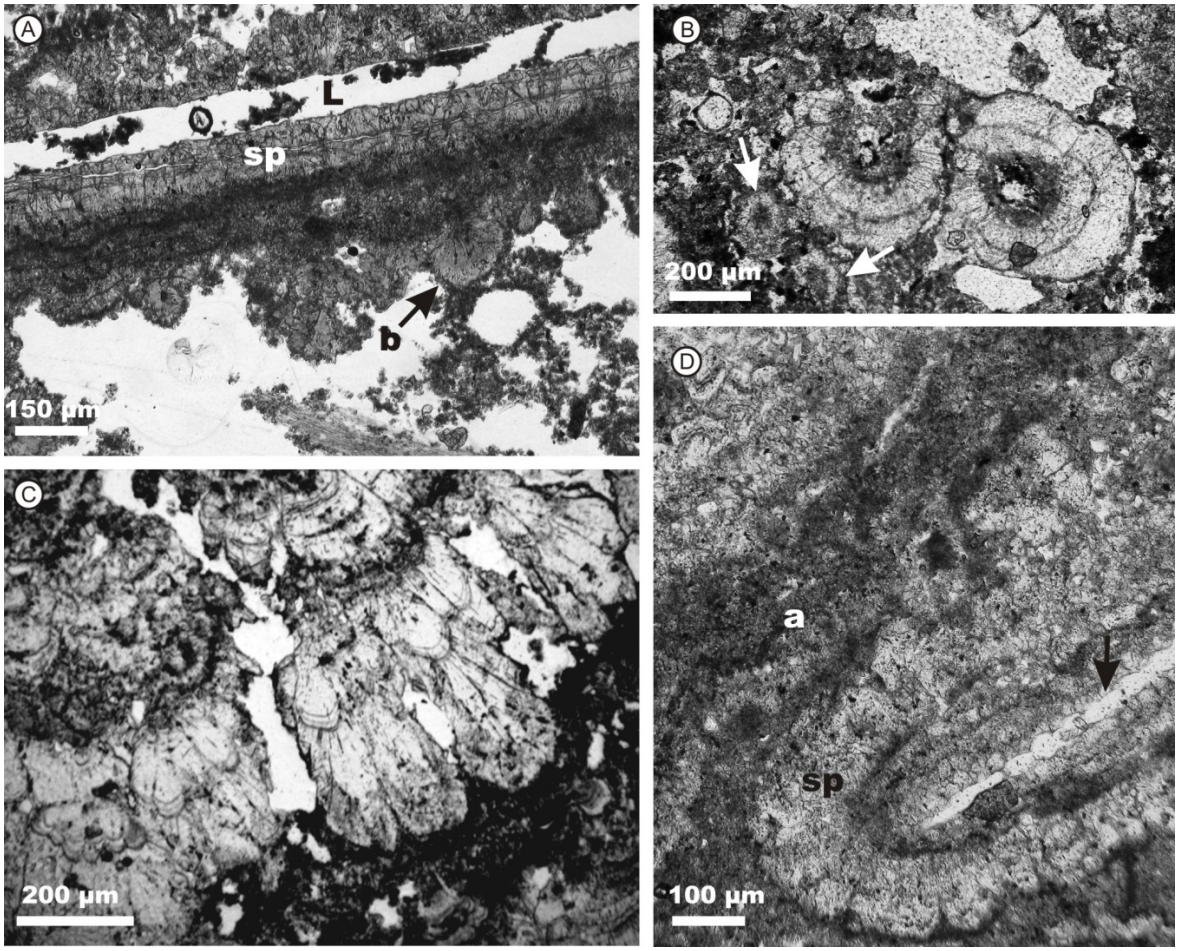

Fig. 6.11. Sparry mineral fabrics in tufa facies. A) Association of an isopachous sparry crust (sp) that covers a degraded leaf (L), followed by a micritic layer and then by isolated botryoids (b). B) Spherulitic-sparry crystals that developed on micritic nuclei, associated with rimmed peloids (white arrows). C) Sparry crust formed by fibrous calcite crystals. D) Sparry layer (sp) developing on a leaf mould (black arrow) alternating with aphanitic micrite (a). In all pictures white areas are porosity. Plane polarized light.

6.3 Fabric occurrence in tufa depositional facies

Independently of the macro-texture the studied tufa deposits can be divided into two basic types: laminated (i.e. stromatolitic tufa and crusts) and vacuolar texture (i.e. moss tufa, *Vaucheria* tufa). Petrographic observations reveal that all petrographic components and their associated fabrics are present in almost all depositional facies (Figs 6.12-6.15). For example, laminae in stromatolitic tufa, which are 1-2 mm in thickness, can originate by the alternation of three main types of layer: micritic, dendrolitic and sparitic layers (Fig 6.12A). Dendrolitic laminae, up to 1-1.5 mm thick, contain mineralized upward-growing cyanobacterial filaments, a few microns in diameter, forming bush-like fans or tufts (Figs 6.11E and 6.12A). Micritic layers generally are characterized by an aphanitic-peloidal fabric (Fig. 6.10A), whereas sparitic layers are present mainly as crusts (Figs 6.11A,C,D and 6.12A). Laminae of stromatolitic tufa are also characterized by the presence of empty tubes, sub-spherical-lenticular in section, probably created by larvae of arthropods (Fig 6.12A). Some detrital layers are also present, characterized mostly by encrusted mineral or rock clasts.

Similarly, dendrolitic layers, aphanitic micrite/microspar and sparry crusts are also common in laminated crusts (Fig. 6.12B). As in the stromatolite tufa, dendrolitic layers are created by mineralized upward-branching cyanobacterial filaments, that may alternate with multi-layered micro-structures formed by laminar brown micrite and aphanitic micrite-microspar. Moreover, layers of peloidal micrite are also present, alternating with both dendrolitic and aphanitic microspar laminae.

Multi-layered micro-structures are also well developed in coated grains, as pisoids and “cave pearls” (Fig. 6.12). In fact these deposits are generally characterized by a concentric lamination created by alternating layers with different micritic-microsparitic fabrics (Fig. 6.13A and B).

In pisoids, laminae are formed of micrite layers with an homogeneous to laminar fabric, varying from ~ 20 to 150 μm in thickness, alternating with aphanitic microspar of similar thickness, both commonly forming a dense lamination around a nucleus of plant fragments, detrital tufa or rock fragments (Figs 6.13A and B). In cave pearls laminae occur as thin layers, 10-20 μm in thickness, created by the alternation of brown-dark laminar micrite and microspar, locally interrupted by fan-shaped sparitic crystals (Fig. 6.13C and D). Differing from pisoids, the nucleus can consist of sparitic crystals of 120-180 μm in size or fibrous calcite crystals of ~50 μm in size (Fig. 6.13E), often rimming sub-spherical moulds, ~20 μm in diameter, of probable filamentous bacteria (Fig. 6.13F).

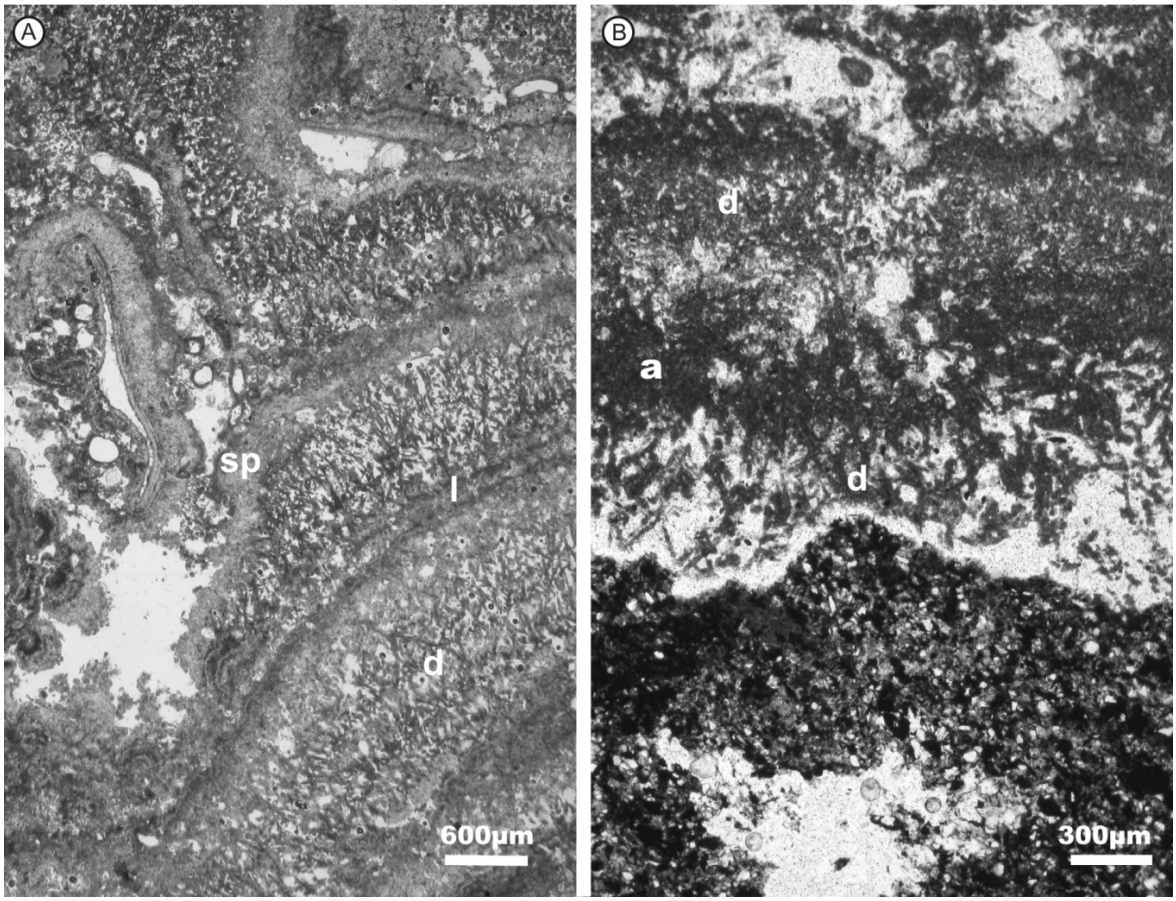

Fig. 6.12. Fabric associations in stromatolitic and laminated tufa crusts. A) Alternating layers of dendrolitic (d), laminar (l) and sparitic crust (sp) fabrics; sub-circular openings probably created by arthropod larvae (left area in the picture). B) Dendrolitic layers (d) alternating with aphanitic micrite (a), developing on a sandstone clast.

Fig. 6.13. Common fabric associations in coated carbonate grains. A) Pisoids, different sizes and shapes, characterized by concentric lamination formed of micritic-microsparitic layers. Commonly these multi-layered micro-structures develop on plant remains and detrital grains. B) Alternation of laminar micrite and aphanitic microspar forming the cortex of pisoids. C) Cross-section through a "cave pearl" characterized by a nucleus surrounded by a laminated cortex. D) Detail of the cortex showing the alternation of laminar dark micrite and laminar light microspar. In some cases, multi-layers are interrupted by sparitic crystals (sp). E) Cross-polar image showing sparitic fan-shaped crystals, characterized by undulose extinction. F) Sparry crystals occurring in the nucleus. Crystals are commonly overgrown by bacterial filaments (black arrows).

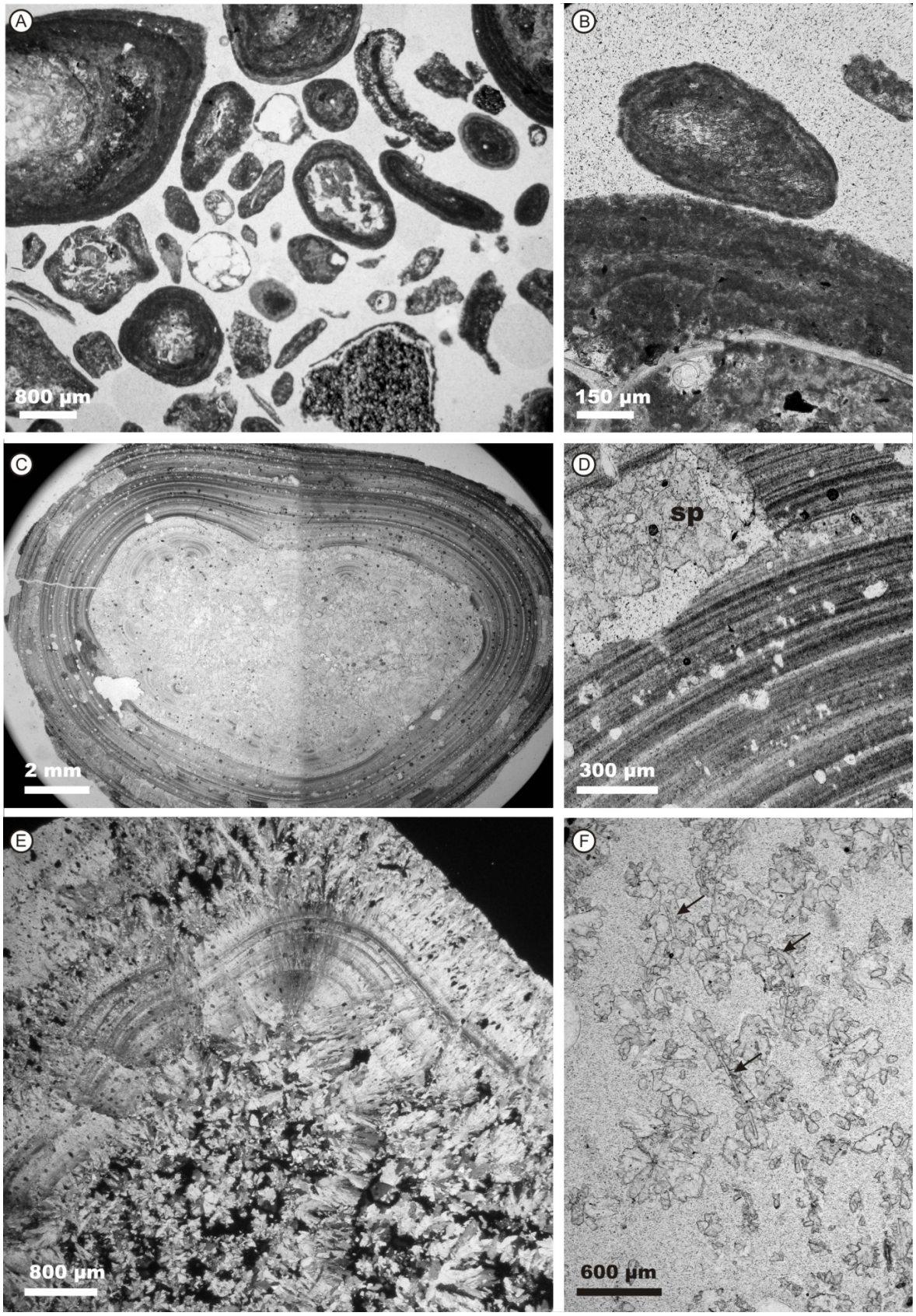
A
800 µm
B
150 µm
C
2 mm
D
sp
300 µm
E
800 µm
F
600 µm

Vacuolar tufa is formed of thin carbonate crusts (only few millimetres thick) around three main types of organic support: detrital plant remains (leaves and twigs), autochthonous Xanthophycae algae, belonging to the genus *Vaucheria*, and by bryophytes, including mosses and liverworts. The complex morphology of these organic supports together with their poor preservation, favour the formation of large cavities, often empty or filled by detrital particles, that give a porous macro-texture to the deposit.

Sub-millimetre-thick carbonate crusts forming around leaves, twigs and mosses, commonly consist of continuous sparry crusts of 50-100 μm in thickness, alternating with aphanitic or peloidal micrite (Fig. 6.14A, B, D).

Coarse calcite developing around *Vaucheria* filaments is characterized by microsparitic crystals occurring with an aphanitic fabric (Fig 6.14C) or by fibrous calcite crystals up to ~100 μm in size, that commonly develop around empty filaments.

Pustular tufa forming in the Thornley stream (NE England) is characterized by an outer edge formed by sub-millimetric rounded knobs, crudely laminated in hand specimen, that usually develop on encrusted plant remains (vacuolar tufa). Here the common petrographic components and related fabrics are: fibrous calcite crystals, aphanitic microspar and/or locally peloidal micrite, alternating with Mn-rich layers (as reported in Section 6.1) (Fig. 6.15A and C). These layers, that only occur in this type of deposit, are formed of sub-spherical forms (~5 μm in diameter), mainly arranged in layers of 20-40 μm in thickness (Fig. 6.15B), and tufts of probable filamentous bacteria, varying in length between 50-100 μm (Fig. 6.15D).

Fig. 6.14. Fabric associations in vacuolar facies. A) Moss tufa characterized by large cavities (marked with the letter C and dashed line), to produce a vacuolar fabric. Cavities may be empty or filled by detrital grains, and are lined by sparitic crusts (sp) with aphanitic-peloidal micrite (ap). B) Moss stems (M) encrusted by sparry crusts (sp) and peloidal micrite (p). C) Transverse and longitudinal sections of empty *Vaucheria* filaments encrusted by aphanitic microspar or forming rims around the filaments. Between microsparitic crystals pinnate diatoms (d) abound. D) Association of botryoids (b), fibrous calcite crystals (fc) and aphanitic microspar (a), developing on degraded leaf (L) and gastropod shell.

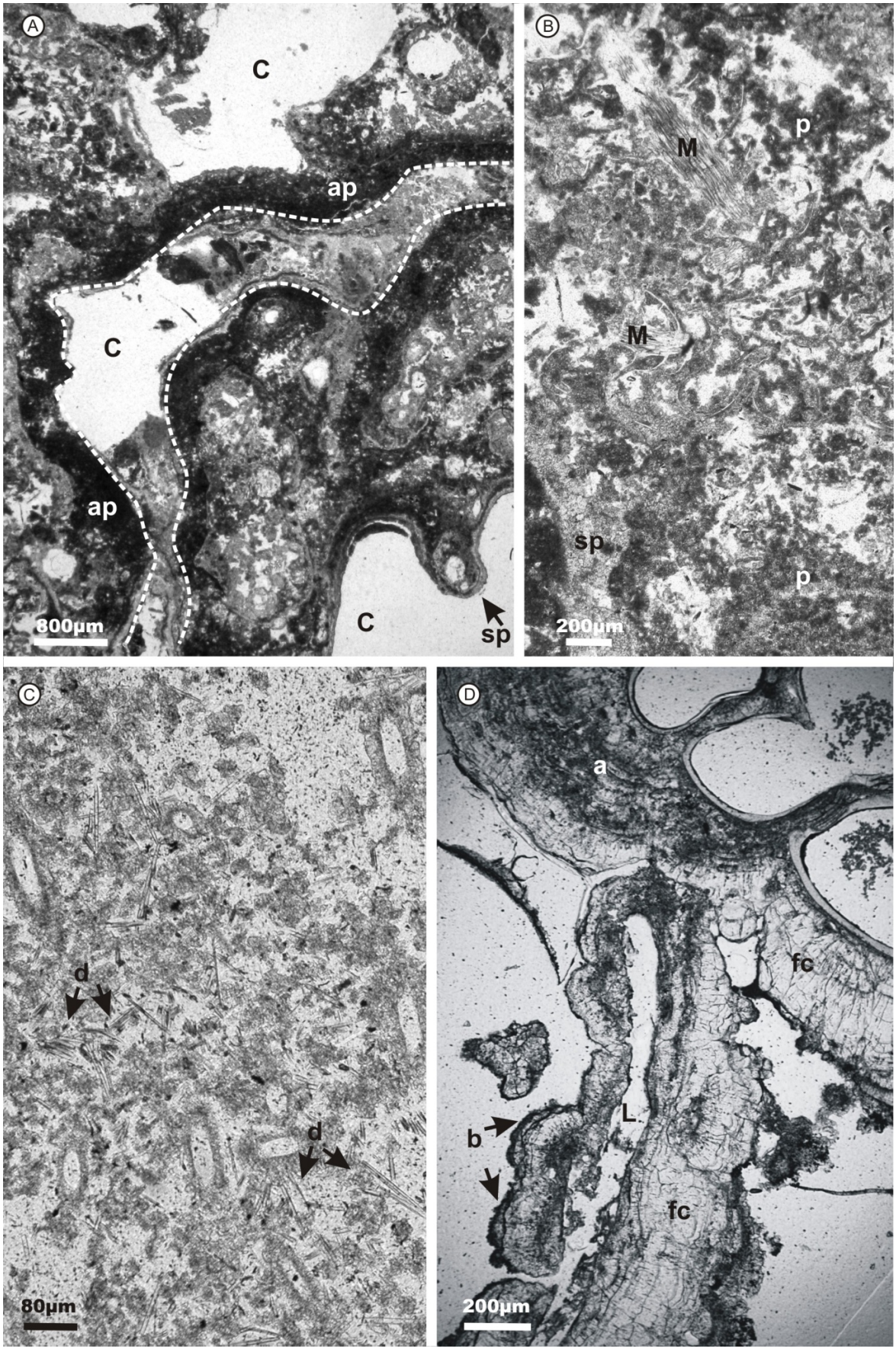
A
C
ap
C
ap
C
sp
800μm
B
M
p
M
sp
p
200μm
C
d
d
80μm
D
a
fc
L
b
fc
200μm

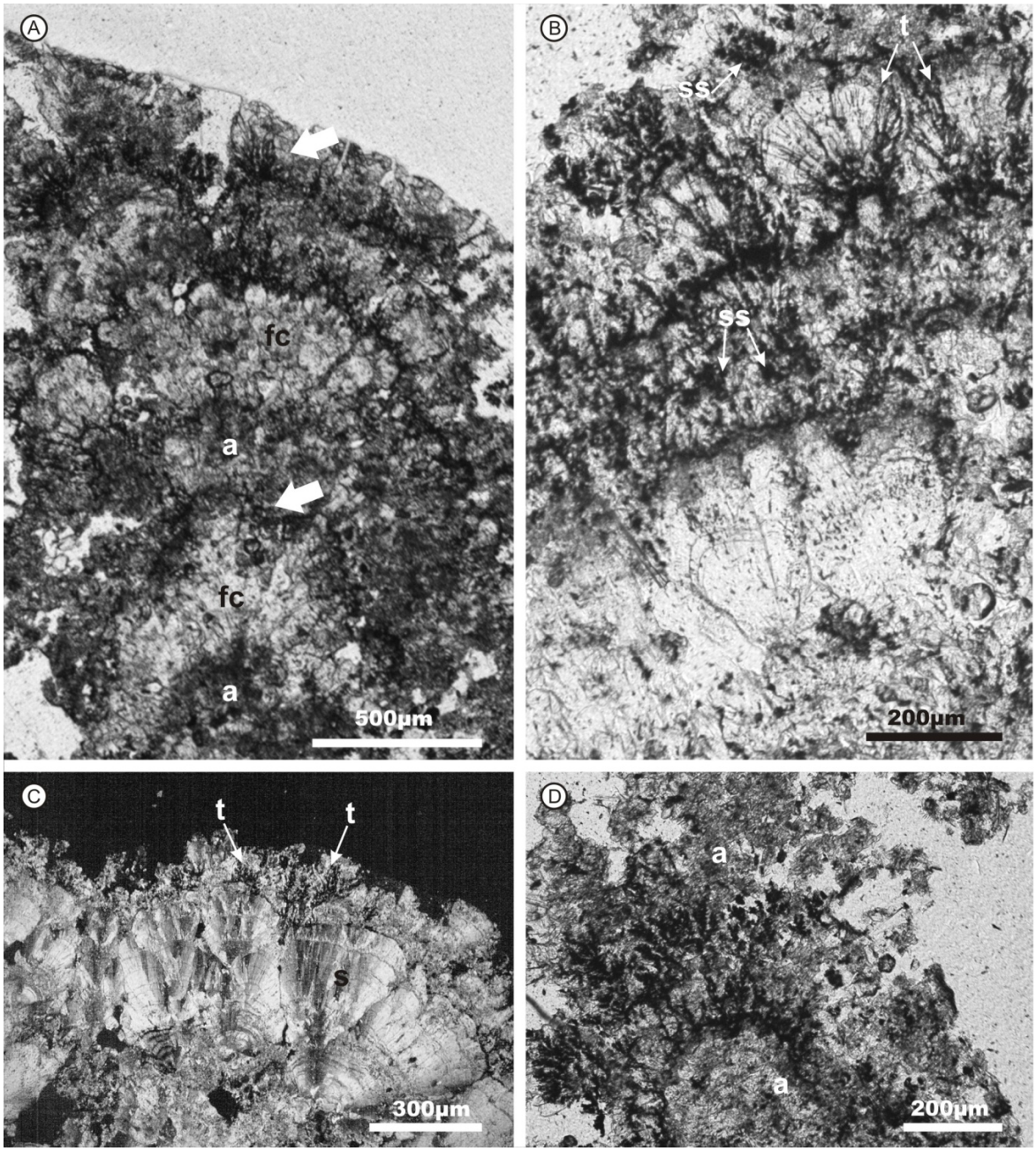

Fig. 6.15. Sparitic and microsparitic fabrics associated with Mn-rich layers, in pustular tufa. A) Alternation of aphanitic microspar (a), fibrous sparry crystals (fc) and Mn-rich layers (white arrows). B) Detail of A. Mn-rich layers are characterized by two micro-structures: sub-spherical forms (ss) and tufts of probable filamentous bacteria (t), overgrown by fibrous calcite fans. C) Cross-polar image showing the alternation of sparry crystals (s) and Mn-rich layers, formed by sparse bacterial tufts (t). D) Aphanitic microspar (a) associated with branching Mn-rich bacterial filaments.

7. FACTORS CONTROLLING TUFA DEPOSITIONAL SYSTEMS: DISCUSSION

7.1 Tufa environments and facies associations

Five sites of actively-forming tufa located in northern Calabria and in north-east England have been studied for this project and three main tufa depositional environments have been distinguished: the barrage tufa system, terraced-slope tufa system and overhanging-lobe tufa system (Fig. 2.1).

❖ *Barrage tufa*

Barrage tufa systems commonly develop in fluvial environments and two end-members have been described in the literature: the barrage model and the braided model (Pedley, 1990). These are separated mainly on the basis of the morphological features of the deposits, the gradient of the watercourse, and the petrographic facies (Ford & Pedley, 1996; Carthew et al., 2003; Glover & Robertson, 2003; Ordóñez et al., 2005).

The barrage tufa systems studied here show close similarities with the general barrage model described in Pedley (1990) and Ford & Pedley (1996), with sinuous to irregular natural dams alternating with shallow pools (Figs 4.1 and 4.8).

In the Parmenta system, the downstream wall is characterized by tongue-shaped lobes, variable in their dimensions and angle of dip. The variation of lobe-size depends on the substrate morphology which, in this area, is constituted by peritidal dolomite beds, creating natural barrages, slopes and pools, through their steep westward dip, transverse to the stream flow.

In the Thornley system, the down-stream wall of the barrages is characterized by a vertical to stepped ramp, whereas the upstream side passes more gently into a pool. Here, the external surface of the down-stream walls is composed of coalescing micro-scale lobes, formed by partially calcified *Vaucheria* tufts (Fig. 4.10). The occurrence of the yellow-green filamentous alga *Vaucheria* is common in other barrage systems (e.g. Pentecost & Viles, 1994; Pentecost et al., 2000; Golubic et al., 2008; Gradziński, 2010). This genus frequently occurs in freshwater, marine and terrestrial habitats, forming greenish mats or pads, covering various substrates (Schagerl & Kerschbaumer, 2009). Most of the *Vaucheria* species seem to have their optimum growth at times of lower temperatures; the major development is reported in the cold season. Their growth forms on the other hand seem to be related to the flow velocity (Schagerl & Kerschbaumer, 2009). In fact, there is a sort of relationship between the colony form (mat or pad) and water flux, in the studied tufa barrage systems: widespread pads develop on the downstream wall of barrages where the water energy is faster, whereas greenish mats occur within the pools, where the water flow is usually slower. The development of the barrages and associated pools in low-gradient areas, constituted by gravels of Quaternary tills, is favoured by the accumulation of detrital material, such as large branches of trees, resulting from floods events.

The style of the Parmenta and Thornley tufa barrage systems is comparable with those reported by Viles et al. (2007) from fossil and active fluvial tufa systems in Namibia formed under an arid climate, but they are somewhat different from those in Ruidera Park in Spain, formed under a semi-arid Mediterranean climate (Pedley, 2009). This confirms the idea that a major control on barrage morphology is the nature of the substrate (Viles et al., 2007) rather than that of the climatic regime (Pedley et al., 1996; Pedley & Rogerson, 2010).

In the barrage model of the Mediterranean-Northern European area, dams are reported to be composed almost exclusively of phytoherm framestones (Pedley, 1990; Pedley 2009), whereas phytoherm boundstone (stromatolitic), phytoherm framestone and phytoclastic facies compose the dams in an Australian system (Carthew et al., 2006). The Calabrian barrages are composed of vacuolar tufa deposits covered by stromatolitic crusts, similar to the Australian ones, but they have downstream tongue-shaped lobes as described from a Japanese system (Kano & Fujii, 2000). In fact, vacuolar tufa, being composed of both calcified detrital plant remains and autochthonous bryophytes, corresponds to a mixture of phytoclastic and framestone tufa sensu Pedley (1990), whereas stromatolitic tufa corresponds to the phytoherm boundstone tufa. In the same way, the English barrages are composed of vacuolar tufa (calcified detrital plant remains, i.e.phytoclastic tufa sensu Pedley, 1990) and *Vaucheria* tufa. According to Pentecost & Viles (1994), *Vaucheria* tufa is classified as microbial tufa whereas using Pedley's scheme, it would correspond to a phytoherm framestone.

In the same barrage model of Pedley (1990; 2009), dams create quiet water-bodies and pools in which lithoclastic, phytoclastic, microdetrital and cyanolith tufa deposits usually form, together with stromatolitic deposits in the marginal areas of the pools. The Parmenta stream pools contain mainly unconsolidated sandy gravel of dolomite clasts, only partially coated by a thin carbonate crust, and rarely encrusted mosses (phytoherm framestone). The absence of autochthonous tufa deposits in the pools and of coated grains (i.e. cyanolith or oncoidal tufa), could be a result of the hydraulic regime of the Parmenta stream, which for most of the year sees intense flood events that rework the gravel, so preventing the development of a stable biofilm on the grains (see discussion Part II).

On the other hand, the marginal shallower areas of the pools, as well as the pool-floor of the Thornley barrage system, are occupied by tufa deposits together with plant debris and detrital gravels. Deposits forming in these quieter and deeper areas of the system are characterized by an outer edge formed by rounded knobs, a few millimeter in diameter, cemented together to form an interconnected pustular structure; the inner part usually has a vacuolar texture, formed by calcified plant remains. Moreover, during the spring-autumn interval, on the floor of the shallower pools, extensive uniform mats of *Vaucheria* colonies abound. Although these colonies occur with incipient calcification, they do occur within the pustular tufa, as scattered calcified empty tubes.

These could be explained by the occasional high-energy destructive hydraulic regime of the stream, and the consequent diverse growth-style of the green alga *Vaucheria* (see earlier section).

❖ *Terraced-slope tufa system*

In the terraced-slope system examined here, three types of deposits are formed: laminated carbonate crusts (phytoherm boundstone sensu Pedley, 1990), moss tufa (phytoherm framestone sensu Pedley, 1990) and pisoids (Fig. 4.14). Three factors appear to control the formation and distribution along the slope of such tufa deposits: variation in the inclination of the slope; morphology of the slope profile, and presence of detrital material (plants fragments and rock clasts). Slope profile is generally characterized by a high-angle wall in the upper part that prevents the formation of pools but does facilitate crust formation on the exposed surfaces of sandstone beds. Pisoids may begin to form here around plant remains and rock clasts. In the middle-lower part of the slope, the gradient decreases and a staircase-like profile develops, partly a result of the sub-horizontally dipping sandstone beds, and this allows the formation of small pools. These pools are characterized by a steep back wall (encrusted by a laminated crust) and by a downstream rim, made of partially calcified mosses. Pisoids accumulate and grow within the pools to several cm in diameter.

A step-like morphology is common in other active tufa systems (Evans, 1990; Violante et al., 1994; Ford & Pedley, 1996; Kano & Fujii, 2000; Pedley, 2009), as well as in active and fossil hot-springs where travertine is being precipitated (Julia, 1983; Chafetz & Folk, 1984; Pentecost, 1990; Guo & Riding, 1998). In hilly country and typically on steep valley sides, Ford & Pedley (1996) reported the perched springline model as a common tufa environment. This system is composed of proximal deposits developed close to and below resurgence points, that consist of lobate or fan-shaped mounds in plan-view, formed of calcified mosses, and distal deposits forming on the lower valley slopes, that are composed of intraclast and detrital tufa (Pedley, 1990).

Guo & Riding (1998), working on the lithofacies of a late Pleistocene travertine system, defined the slope depositional system as characterized by three main depositional facies: terrace slope facies, smooth slope facies and waterfall facies. The terrace slope facies consists of vertical to overhanging terrace walls, sub-horizontal terrace pools, and raised intervening terrace rims. The convex outer, upper face of the terrace walls consists of downward thinning wedges of crust, whereas the lower face is usually overhanging. The dominant facies are laminated crystalline crusts. Terrace pools are filled by different lithotypes, including pisoids, and form extensive flat areas on low-angle slopes; they may also develop many narrow terraces on steeper surfaces. Smooth slope facies consist of non-terraced travertine sheets that are composed of decimetre-thick laminated crystalline crusts.

A terrace tufa morphology described by Kano & Fujii (2000) consists of a series of stair-like terraces, 30-70 cm in height and 20-100 cm in width, characterized by a raised rim around the edge and a slightly depressed plane to the back. Their external morphology is similar to rimstone pools forming in caves.

❖ *Overhanging-lobe tufa system*

Two active overhanging tufa lobe systems have been studied, forming in the vicinity of localized springs in Sunderland and Barnard Castle B (Fig 2.1). They are characterized by a convex profile and by a fan shape in plan, as the precipitation begins from the emergence point and progrades downstream along the wall. A difference exists between the two deposits: in the Sunderland lobe a cave has formed underneath the lobe between the front of the lobe itself and the floor at the base of the wall, whereas in the Barnard Castle (B) system, the front of the lobe is directly connected with the base of the slope. This difference is probably due to the different height of the wall on which tufa deposit is forming, that is of ~ 8 metres in Sunderland and ~ 3 metres in Barnard Castle B.

In the literature these types of tufa deposit are ascribed to the cascade model (Pedley, 1990; Ford & Pedley, 1996; Pentecost, 2005; Pedley, 2009), and they differ substantially from the barrage system in the absence of any upstream pools (Pedley, 1990; Chafetz et al., 1994).

7.2 Water chemistry

Analyses of stream water reveal that the chemical composition of the tufa-depositing streams belong to the calcium-bicarbonate (Parmenta stream) and calcium-bicarbonate-sulphate (Thornley stream) systems, characterized by average Ca^{2+} concentrations of 59 ppm and 153 ppm, respectively (Tables 5.1 and 5.3). Both values are comparable with those reported in elsewhere in western Europe (Pentecost, 2005). Although Parmenta water is similar to that of other karstwater-streams (Pentecost, 2005 and references), few Ca-HCO_3-SO_4^{2-} stream waters depositing tufa have been reported (Pentecost, 2005; Arp et al., 2010). In effect, the difference in the concentration of these anions is low; during the studied period mean values of ~ 300 ppm HCO_3 and 360 ppm SO_4^{2-} respectively were recorded.

In the Parmenta stream, values of the Saturation Index (SI) measured in the interval January 2008-January 2009, show that water is oversaturated with respect to $CaCO_3$ (SI>0), varying from ~0.75 during the winter to ~0.89 during the summer (Fig. 5.2). The main river flowing into the valley (the Corvino River) has a similar water chemistry and is oversaturated with respect of calcite (SI values of 0.35- 0.42), but tufa is not being precipitated there.

This condition can be explained by the constant SI < 0.5 recorded in the Corvino River. In effect, it seems that the saturation index of water in respect of calcite has to be > 8-10 fold for spontaneous precipitation (Kempe & Kazmierczak, 1990; Mertz-Preiß & Riding, 1999; Arp et al., 2001b).

Although it has not been possible to calculate the saturation state of the Thornley stream water, the active precipitation of calcite forming the tufa is evidence for an oversaturated state. From a comparison of four tufa-depositing streams (both calcium-bicarbonate and calcium-bicarbonate-sulphate) in Germany, Arp et al. (2010) observed that the highest values of SI are distinctive of calcium-bicarbonate-sulphate stream-waters. The Thornley stream-water has a similar chemical composition; this suggests that a very high saturation level does not depend on the initial Ca^{2+} to alkalinity ratio, but on the contribution of foreign ions such as Mg^{2+} and SO_4^{2-}, that inhibit calcite precipitation (Arp et al., 2010 and references).

Although, the supersaturation of the water with respect of calcite is an essential environmental condition for tufa formation, it has recently been observed that no spontaneous precipitation occurs on biofilm-free natural substrates, even under highly supersaturated conditions (Bissett et al., 2008; Shiraishi et al., 2008a, 2008b; Arp et al., 2010) (see discussion Part II).

7.3 Geochemistry

Modern tufa is commonly composed of low-Mg calcite with a small amount of magnesium <4 mole %, and a fairly low level of strontium <200 ppm (wt) (Pentecost, 2005 and references therein; Pentecost & Zhang, 2008). Despite the variability of the studied tufa environments, including water chemistry, climatic conditions, and different lithology of the catchment areas, all the deposits are composed of low Mg-calcite (Mg 1.0 - 3.5 mole %), except those from Thornley barrage, in which the calcite is also enriched in S, Mn and Fe. In general, the 80-90% by volume of all the samples is calcite and the rest is detrital material.

Calcite in Parmenta tufa has a typical mean tufa Mg value, even though the catchment area is composed of stoichiometric dolomites. Moreover, although the Mg/Ca ratio is almost constant in the water during the year (Mg/Ca ~0.9), the Mg content in the calcite varies over a wide range, indicating some other, probably a climatic control on its partition. It is well known that temperature strongly influences the Mg content of calcite rather than saturation or precipitation rate (Tucker & Wright, 1990). This suggests that the seasonal variation in water temperature of the Parmenta stream (8°-17°) controls the recorded Mg values. At the same site, strontium is quite high (Sr 0.5 - 0.8 mole %) in comparison with other known, unaltered tufa deposits. The stream water contains ~4 ppm (wt) of Sr^{2+} and this varies little during the year. The partition coefficient of strontium in calcite, in contrast with magnesium, is significantly altered by the Sr/Ca ratio of water, the

precipitation rate and the presence of other cations (Tucker & Wright, 1990). The Parmenta drains Norian dolomites that have a Sr content 90-120 ppm (wt) and Carnian-Norian deposits which contain sulphate evaporites (Mastandrea et al., 2006); these could have influenced the chemical composition of the stream water.

Minor elements in the calcite of the Thornley tufa are present with the following ranges (all mole %): Mg 1.3 - 3.5, Mn 0.2 – 1.8, Fe 0.2 – 1, S 1.1 – 2.4 (Table 6.3); these fall into the typical range of many known tufas (Pentecost, 2005). Enrichment of Mn/Fe in calcite crystals is also confirmed by CL observations, since the luminescence properties of natural carbonates are determined largely by the incorporation of Mn^{2+} and Fe^{2+}, of which the first is the most prominent activator element and the latter the most important quencher element. During the precipitation of calcite, the incorporation of such foreign cations depends on the physicochemical conditions of the aqueous solution. In the case of Mn and Fe, the Eh–pH conditions strongly affect the presence of the divalent cations of these elements in the solution. In particular, suboxic to anoxic conditions are required for the incorporation of Mn^{2+} and Fe^{2+}, as these cations are easily oxidized. In the case of the studied tufa deposits forming in a fluvial environment, which is a very shallow stream in the Dervent Valley, the only possible poorly oxygenated sub-environment could be found along the bottom of stagnant pools, where a hyporheic zone containing anoxic and hypoxic pockets associated with irregularities in the stream floor or local deposits of organic matter, could exist (Boulton et al., 1998). This model can explain the Mn and Fe enrichment in the tufa deposits of Thornley since only the pustular tufa forming in the quite water pools, contains these elements.

At a micro-scale, it has been observed that calcite in the pools does not present a uniform pattern in these minor elements, but a detectable enrichment in Mn and Fe starts few microns before the occurrence of the Mn-rich layers (see below) (Fig. 6.6). This indicates that the environmental changes that lead to the precipitation of these Mn-rich non-carbonate phases, inhibit calcite formation during the equilibrium, but favour Mn and Fe incorporation into the calcite itself in a transitional phase.

Finally, the presence of sulphate in the calcite of Thornley would be related to the presence of SO_4^{2-} anions in the water. This probably derives from organic matter degradation in the soil and/or pyrite oxidation within the coal measure beds, as in the catchment area, there is a lack of sulphate evaporites.

Stable isotope analyses ($\delta^{18}O$ and $\delta^{13}C$) performed on the samples collected in different tufa depositional environments of NE England (Fig. 6.9) reveal that the $\delta^{18}O$ composition is between -5.4 and -6.6‰. This falls within the range of typical tufa deposits (e.g. Andrews and Brasier, 2005; Andrews, 2006). In the same way, the $\delta^{13}C$ composition of -9.8 to -14.1‰ for the Tees, Sunderland and Slade Brook (SW England) samples, is also comparable with those reported in the literature (Andrews and Brasier, 2005; Andrews, 2006). However the tufa deposits of the Thornley barrage

system are quite different; they show positive carbon values between +2.9 and +3.8‰, recorded in all depositional facies, both in fast and slow flow conditions.

From experimental work, positive isotope data of $\delta^{13}C$ have been obtained in the presence of methanogenic bacteria utilizing CO_2 and H_2 as the energy source (Schidlowski, 2000). Normalized to atmospheric CO_2 as the feeder substance, the fractionations reported by Fuchs et al. (1979) give a range between -41 and +6‰ for the bulk biomass synthesized. Spiro & Pentecost (1991) found that the $\delta^{13}C$ of cyanobacterial calcite in a hardwater creek in Yorkshire is on average 3‰ heavier than the stream-average noontime $\delta^{13}C$ of total DIC. Moreover, the cyanobacterial calcite was more than 2‰ heavier than biologically unaffected "travertine" on bryophytes; this difference in $\delta^{13}C$ was interpreted as an effect of photosynthesis. Nevertheless, cyanobacterial photosynthesis also has a unique effect in producing positive $\delta^{13}C$ values; this could be considered a limiting cause for the studied tufa deposits, because the presence of a major group of microorganisms (e.g. prokaryotes, eukaryotic algae), involved in calcite precipitation (see discussion Part II). Andrews et al. (1997) basing on positive $\delta^{13}C$ values, measured in mussel shell aragonite and associated microbial carbonates, found that a micro-environmental photosynthetic effect is only evident at sites where water flushing rates are low. This explanation is less plausible in the Thornley case, since depositional facies form in both fast flowing water and stagnant pools and all show positive $\delta^{13}C$ values.

❖ *Mn precipitates in the Thornley barrage system*

Light microscopic observations and SEM-EDX spot-size analyses performed on tufa deposits forming in the Thornley barrage system revealed the occurrence of distinct layers of Mn-rich precipitates with minor elements: Si, Ca, Al, Mg, Fe, alternating with calcite (Figs 6.6 and 6.15). Crystal nano-morphologies of these precipitates vary from poorly-ordered amorphous structures, forming a sort of network, to better-defined platy-shaped crystalline phases. Poorly-ordered phases form sub-spherical aggregates with a uniform dimension of ~1-5 μm, that can be related to some mineralized bacterial forms, since these aggregates have always been seen associated with similar living microorganisms forming the biofilm covering the tufa deposit. This interpretation could suggest that these mineral phases are biominerals, with some microbial processes inducing their formation.

A microbial contribution to the solid phase partitioning of metals in sediments comprises a continuum of sorption and precipitation reactions (Ferris, 2000). Sorption reactions tend to predominate over precipitation where metals are undersaturated with respect to their least soluble compound; the opposite occurs when pore-water concentration of dissolved metals exceeds equilibrium constraints on mineral solubility. Both types tend to be sensitive to pH and/or redox potential, while their overall progress is commonly sustained by microorganisms (Buffle, 1990;

Stumm & Morgan, 1996). Microbial contribution to metal sorption-precipitation can be passive or active (Ferris, 2000). In the first case microbial cells (living or dead) behave as solid phase sorbents of dissolved metals while metabolic activities of some microorganisms bring about metal precipitation indirectly through production of organic ligands, e.g. sulphide, phosphate, dissolved organic carbon or directly through enzyme mediated changes in the redox stage, e.g. oxidation of reduced iron and manganese (Bachofen, 1994).

In oxic environments below pH 8.0, the dominant manganese ion in solution is Mn^{2+} (Stumm & Morgan, 1996) and this can be transformed through oxidation to Mn^{4+} by various processes to produce a variety of Mn oxide minerals (Nealson, 1983). Douglas et al. (2007) studying modern polymineralic microbilates (Mn hydroxide/calcite/gypsum) forming in a spring pool in Death Valley National Park (California), observed that metabolic activities of microorganisms occurring within the black biofilm associated with these deposits, generate manganese oxyhydroxides and calcite, while gypsum is an abiogenic product. Concerning the origin of these Mn amorphous phases, these authors observed that although the pool-water contains a high concentration of Mn, Mn oxyhydroxides did not spontaneously precipitate in the water column, but they were only found on surfaces of spherical microbial cells. The mineral nanostructures of these Mn precipitates are quite similar to those found in the Thornley calcite tufa deposits.

Mn-rich precipitates found in tufa deposits also contain minor elements including Si, Ca, Al, Mg and Fe. The presence of these elements could indicate a possible derivation from some biogenic clay-like phases, commonly forming within biofilms in lakes and rivers (Konhauser, 2007). Independently of the chemical composition of the waters from which they were sampled, it has been observed that these clay-like phases occur with the following similar properties (Konhauser, 2007): amorphous to poorly ordered structures, grains size < 1 μm, attached in a tangential orientation around lightly encrusted cells whereas those on heavily encrusted cells have a more random orientation, and finally a composition dominated by iron, silicon and aluminium in variable amounts. Although in this study Mn is more abundant than Fe, it is possible to suppose that this enrichment is due to the minor Mn oxidation in comparison with Fe, favouring a major concentration in oxic waters and sediment/soil pore waters.

7.4 Origin of petrographic facies

The petrographic components of neo-formed tufa deposits found in the various tufa environments are: micrite, microspar and the less abundant spar, give rise to the peloidal, aphanitic, laminar and dendrolitic fabrics (Figs 6.10 and 6.11). All fabrics occur in the macro-laminae that form the structure of stromatolitic tufa, as well as in the phytohermal framestones and phytoclastic deposits of vacuolar tufa (Figs 6.13-6.15). Despite the apparent uniformity seen here, a great variability in the occurrence of the different petrographic components and fabrics is described in the literature. According to Pedley (1992) framestones are mainly composed of fringes of bladed calcite spar, usually alternating with laminae of opaque micrite, but they may also be formed of just micritic layers (clotted or grumose). Jassen et al. (1999) reported stromatolitic boundstones composed of three types of laminae: 1) bushes of upward-branching cyanobacterial filaments encrusted by micrite, 2) porous micritic laminae, and 3) more or less continuous laminae of columnar sparry calcite fans. Arp et al. (2001a) recognized alternating layers of porous (dendrolitic) microsparite and dense micrite in stromatoltic tufa, whereas in their bryophytic tufa only euhedral sparry crystals occurred. Turner and Jones (2005) also observed sparry blocky calcite in bryophytic tufa.

The presence of variable types of components and fabric is also known in allochthonous tufa (or clastic tufa deposits, sensu Ford & Pedley, 1996). In fact, Pedley (1992) indicated that phytoclastic and intraclastic deposits are characterized by micrite laminae composed of dense micrite clots (20-200 μm) surrounded by spar fringes (= peloidal fabric) and less commonly by only micrite peloids formed around random-sized detrital nuclei. Also phytoclastic tufa from Belgium is composed of micritic and columnar sparry calcite crystals (Jassen et al., 1999).

Considering that many authors do not differentiate between spar and microspar, it is evident that autochthonous tufa (both phytohermal framestones and boundstones) as well as allochthonous tufa, can be formed by all types of calcite petrographic components, organized in variable fabrics.

In the studied tufa systems the non-preferential distribution of petrographic components in single depositional facies and fabrics could indicate that the origin of the different crystalline habits of calcite is not dependent on the substrate (i.e. plant remains, bacteria, etc.), nor on where the mineral precipitates (i.e. barrier, pool, etc.) and consequentially not on the energy of the water flux. Petrographic fabrics on the other hand do essentially show a preferential distribution of one or more mineral components. Commonly they are organized into layers with a more or less well-developed cyclicity that has the best expression in the stromatolitic lamination. In this sense, it is particularly significant that the same cyanobacterial filaments are mineralized by cyclic differentiated layers of micrite, microspar and sparry calcite, each of which reflects diverse seasonal conditions (Fig. 6.10E). Even phytoclasts, pisoids and phytoherm framestone are encrusted by a stratiform mineral structure due to the sequence of different seasonal conditions

(Figs 6.13 and 6.14). Pedley (1992) already recognized in freshwater phytoherm reefs (barriers) the presence of a general organization of all petrographic fabrics into isopachous fringes, a sort of layering, independent from the components and facies (phytoclastic or framestone).

Apart from the crystal habit determined by the (seasonal) saturation state of water (see discussion Part II), what controls the origin of the different fabrics seems to be the substrate on which the minerals precipitate. If an even and regular surface forms the substrate for the development of the mineral component, a continuous layer will be created to give an aphanitic crust or laminar fabric, depending on whether the precipitate is of one or more mineral components.

Peloidal fabric is formed where several sites of precipitation are spaced and randomly distributed, giving the opportunity for scattered mineral precipitation around detrital organic micro-fragments.

Dendrolitic fabric forms exclusively when the bush-like cyanobacterial filaments are mineralized, as the filaments themselves then form the substrate for the precipitation of the mineral. In this case it is easily observed that it is the substrate that determines the fabric, since all mineral components can generate this particular structure (Fig. 6.10E).

PART II

NEO-PRECIPITATED MINERALS AND ASSOCIATED BIOFILM COMPONENTS

INTRODUCTION

Several mechanisms of mineral precipitation have been proposed to explain tufa formation, and these vary from a purely abiotic to a purely biotic explanation. The abiotic physico-chemical control on mineral precipitation is driven by CO_2 degassing from water that leads to passive calcification of organic and inorganic substrates (Kano et al., 2003; Kawai et al., 2006). The intermediate positions see a mix of abiotic and biotic processes (Mertz-Preiß & Riding, 1999; Ford & Pedley, 1996; Arp. et al., 2001a; 2010), in some cases with the suggestion of a prominent, but not exclusive, role played by the tufa-associated biofilm (Pedley et al., 2009; Pedley & Rogerson, 2010; Rogerson et al., 2008; 2010). Cyanobacterial take-up of CO_2 should be the most common process involved in biologically-induced mineral precipitation, since these microbes are generally abundant, although recently much evidence has been put forward for a prominent role of the EPS produced in the biofilm (Turner & Jones, 2005; Pedley et al., 2009). Stromatolitic tufa deposits have been considered a type of microbialite (e.g. Bissett et al., 2008; Shiraishi et al., 2008a), since cyanobacterial photosynthesis is a basic mechanism by which mineral precipitation can take place.

Microbial communities in mats and biofilms can produce mineral deposits (microbialites) through several processes of organomineralization, including metabolic microbial activities and passive mineralization of organic matter (Dupraz et al., 2009). These micro-ecosystems have been well studied in the marine domain, but calcifying freshwater biofilms, always associated with active tufa deposits, essentially remain unknown. Investigations of freshwater tufa systems are mainly based on the measurement of biochemical parameters (CO_2, DIC, pH etc.), both in the macro-environment and at the micro-scale along the interface of the biofilm-deposit. Furthermore, the study of the mineral components (fossil and recent precipitates) is often limited to the traditional thin-section, petrographic approach, and it is only recently with the use of high-powered SEMs that the positive association with the biological components can be confirmed.

The petrographic components, micrite, microspar and spar, are the dominant constituents of tufa. Their interpretation in terms of genesis is often inherited from studies of marine facies. A strict biological driving-force has often been suggested for the origin of the micro-scale early-stage precipitates (micrite), but the early precipitated sparry calcite in tufa is commonly considered an inorganic product, that is a cement, although it commonly occurs in close association with the biotic micrite in thin alternating layers.

SEM studies of tufa deposits (natural or produced in the laboratory) are often deficient in their descriptions of the physical and biological structure of the biofilm. The identification of the actual location of the earliest stage of mineral formation in the region of the biofilm is also poorly known. Using advanced SEM techniques, Turner & Jones (2005) demonstrated an intimate association between organic substances and nm-sized dendritic calcite fibres in some sites of calcification associated with EPS. Recently, Pedley et al. (2009) suggested that where living cyanobacterial

sheath substrates are available there is rapid localized development of long-crystallite dendrite triads, and that where there is a diverse living biofilm with abundant EPS both micro-peloid aggregates of nm-sized spherulites and short-crystallite dendrite triads form. It is likely that the ultra-structures of minerals can be used for discriminating their origin in terms of a biotic versus abiotic origin. Several authors have already used such an approach in the study of modern marine and fossil microbialites. They found a basic common mineral ultrastructure (composed of a nm-sized nanospherical or nanoglobular texture), in all microbial-organic matter-mediated precipitates (Perri & Tucker, 2007; Bontognali et al., 2008; Sánchez-Román et al., 2008; Spadafora et al., 2010).

This part of the thesis illustrates the results of some field experiments performed in both barrage tufa systems (Parmenta and Thornley) and in the terraced-slope tufa system of Barnard Castle (Fig. 2.1). The experiment consisted in the observation with different microscopic techniques (SEM-ESEM-optical microscope), of neo-precipitated tufa deposits formed on natural and artificial substrates (rock pebbles, glass slides) and compared also with the already existing naturally-formed deposits. In particular, in the Parmenta barrage system, tufa neo-formed crusts have been collected at seasonal intervals during a monitoring period of 12 months (January 2008-January 2009). Fresh tufa samples and adherent biofilms were treated with a combination of fixation and dehydration techniques for scanning electron microscope (SEM) examinations. Moreover, untreated samples were also observed under low-vacuum ESEM for comparison. Details of sample preparation techniques were described in Chapter 3.

The neo-formed crusts formed on artificial substrates in the two tufa systems were collected at irregular intervals during the observation period (October 2008-November 2009). In this case, fresh tufa samples and the associated biofilm were preserved with a fixative solution to avoid alteration of the organic components, whereas for SEM examinations of their mineral nano-structures, untreated samples were used. Although the results obtained during these last two field experiments are preliminary in terms of the applied methodologies, they allowed a useful comparison with the Parmenta case study. This has given useful support for the description and interpretation of the mineral nano-structures commonly found in such biologically induced deposits. In any case, further detailed studies are required to elucidate the contribution of intrinsic environmental and biological factors in these tufa systems.

As a result of this multidisciplinary and multi-scale approach, it has been possible to obtain a detailed description of the morphological and biological structure of the biofilm and its ultra-structure. It has also been possible to identify the sites of early mineral nucleation within the interface between organic matter and mineral components. The results obtained have demonstrated a substantial uniformity of nano-structures of the microbial-organic matter-mediated precipitates, formed in all different tufa depositional systems.

8. BIOTA

In all studied sites the external surface of the tufa deposits is ubiquitously covered by a thin microbial biofilms (Fig.8.1). In the Parmenta barrage system, the biofilm occurs as a yellowish uniform sheen with scattered greenish-brown patches covering all depositional surfaces, including the shallow internal cavities within the vacuolar tufa (Fig. 8.1A and D). Along the rimmed pools but mainly on the upper surfaces of the lobes, the biofilm reaches a few millimetres in thickness and varies in colour developing a sort of stratification, as the basal yellowish layer extends underneath the greenish-brown patches. These greenish-brown areas appear as mm-scale localized sub-circular spots, which in places coalesce to cover dm-scale portions of the surface (Fig. 8.1A).

SEM, ESEM and light microscope observations of fresh and dehydrated samples allowed characterization of the micro-organisms present on the basis of their morphological features. The biofilm is composed by an oligotipic community of micro-organisms which shows only small seasonal variations in the relative abundance of species. The biofilm displays a heterogeneous framework built by epilithic and endolithic forms composed mainly of filamentous cyanobacteria, green algae, unicellular prokaryotes, Actinobacteria and fungi (Fig. 8.2).

Three filamentous cyanobacterial morphotypes have been distinguished on the basis of their cell shapes and dimensions of the filaments (EPS sheath and trichome). A first morphotype occurs in motile filaments typically arranged in upright tufts which macroscopically correspond to the brownish mm-size patches. Trichomes are isodiametric with cells ~4 μm in diameter (Fig. 8.2C) and 4.5-5 μm long, terminating with a cone-shaped apical cell. Trichomes are also covered by a thin adherent sheath, less than 0.1 μm in thickness, where the cell morphology can be distinguished. A second morphotype displays cylindrical cells, ~4 μm in diameter, protected by a ~1 μm-thick external sheath (Fig. 8.2D). This EPS tubular structure often appears empty (using a light microscope), since it is much longer than the trichome itself that hides the cell partitions. The external surface of the sheath appears uniform, with a characteristic nervate structure. A third morphotype is distinguishable by its small trichome diameter of 0.7-1 μm. It is characterized by isodiametric cells and occurs locally in solitary filaments (Fig. 8.2E). On the basis of dimensional features and microstructural characters (i.e. calyptra, heterocystis, EPS, branching), all cyanobacterial morphotypes are Oscillatoriales. Moreover, morphotypes 1 and 2 belong to the genus *Phormidium* or *Phormidium* (*Lyngbya*) and type 3 to Oscillatoria, although the precise taxonomy is sometimes controversial (Arp et al. 2001a; Marquardt & Palinska, 2007; Merz-Preiß & Riding 1999; Pentecost, 2005).

Many sub-micron morphotypes of single-cell prokaryotes occur as rods, spirilla and subordinately cocci (Fig. 8.2F), sometimes enclosed in EPS sheets. As they lack any chlorophyll pigment, which is fluorescent under UV light, and because of their shape and dimensions, most of these bacteria could be referred to as heterotrophic species. Bacteria with a more complex

morphology also commonly occur in the biofilm. They appear with very fine (<1 μm) septate branched filaments departing from a mycelium, that appears like a solid or network-like nucleate sheet (Fig. 8.2G). Filaments can also have terminal chains of spores. From their general morphological features, these forms probably belong to the Family Streptomycetaceae (Hazel & Wilkinson, 2003). In addition, fungal hyphae have been occasionally seen under the SEM. Pennate diatoms (raphid and araphid) are also an important component of the microbial community forming the biofilm (Fig. 8.2E), whereas *Oocardium* has rarely been seen (Fig. 8.2H)**.** Mosses (mainly *Cratoneuron*) are also scattered within the biofilm and they locally form large cushions (Fig. 8.1A)**.** Finally, arthropod larvae colonize the external surface of deposits leaving mm-scale elongate cavities (Fig. 8.1B). Results of periodic sampling show that the biofilm community does not vary significantly in terms of components, but during the spring-summer time diatoms and cyanobacteria seem to be more abundant in comparison with the autumn-winter period.

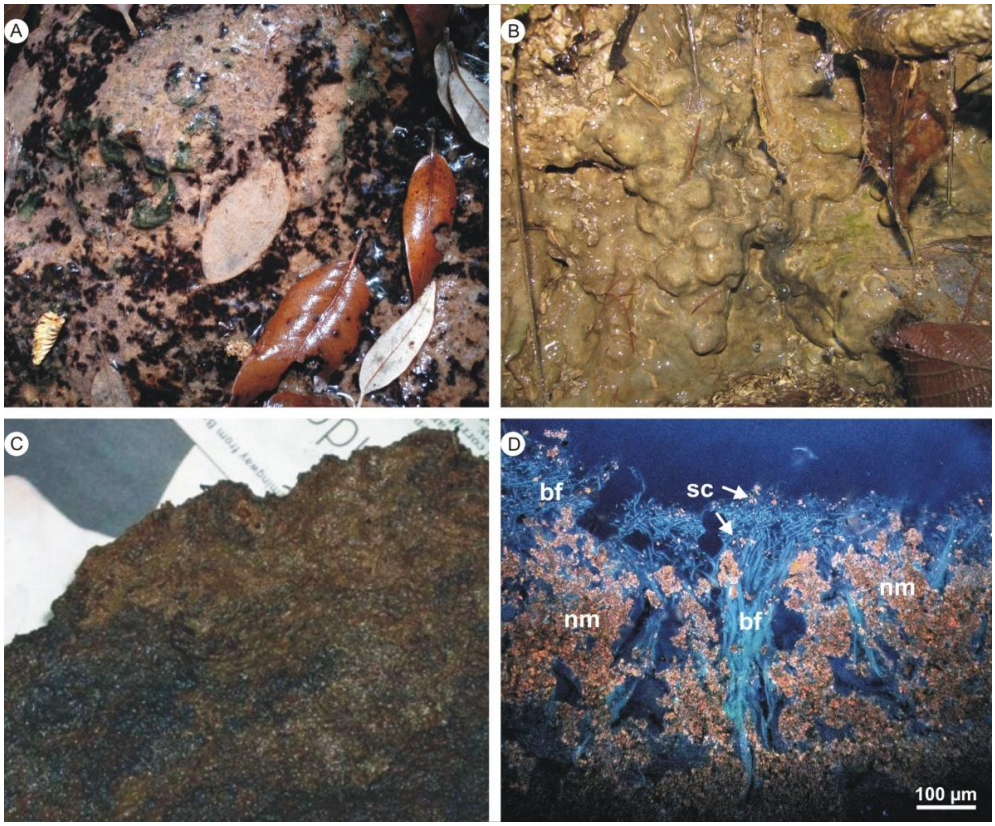

Fig. 8.1. Microbial biofilms associated with tufa deposits. A) Macroscopic view of the biofilm covering the external surface of tufa deposits forming in the Parmenta barrage system. Biofilm appears as a yellowish uniform sheen with local green-brownish patches of sub-circular shape, which may coalesce to cover wider areas. B) Blue-green biofilm covering the external surface of the drop-wall side of pools in the terraced-slope system. White tubes represent trace of arthropods larvae. C) Macroscopic view of dark-brown biofilm developing on the external surface of pustular tufa, formed in pools of the Thornley barrage system. D) Vertical section through the top of the external surface of a growing tufa deposit showing the broad biofilm distribution (bf) in relation to the neo-formed minerals (nm). Photosynthetic organisms (cyanobacteria and diatoms) are florescent under UV light. Calcite is seen under visible-light with crossed polars. Note some suspended crystals within cyanobacterial tufts (sc).

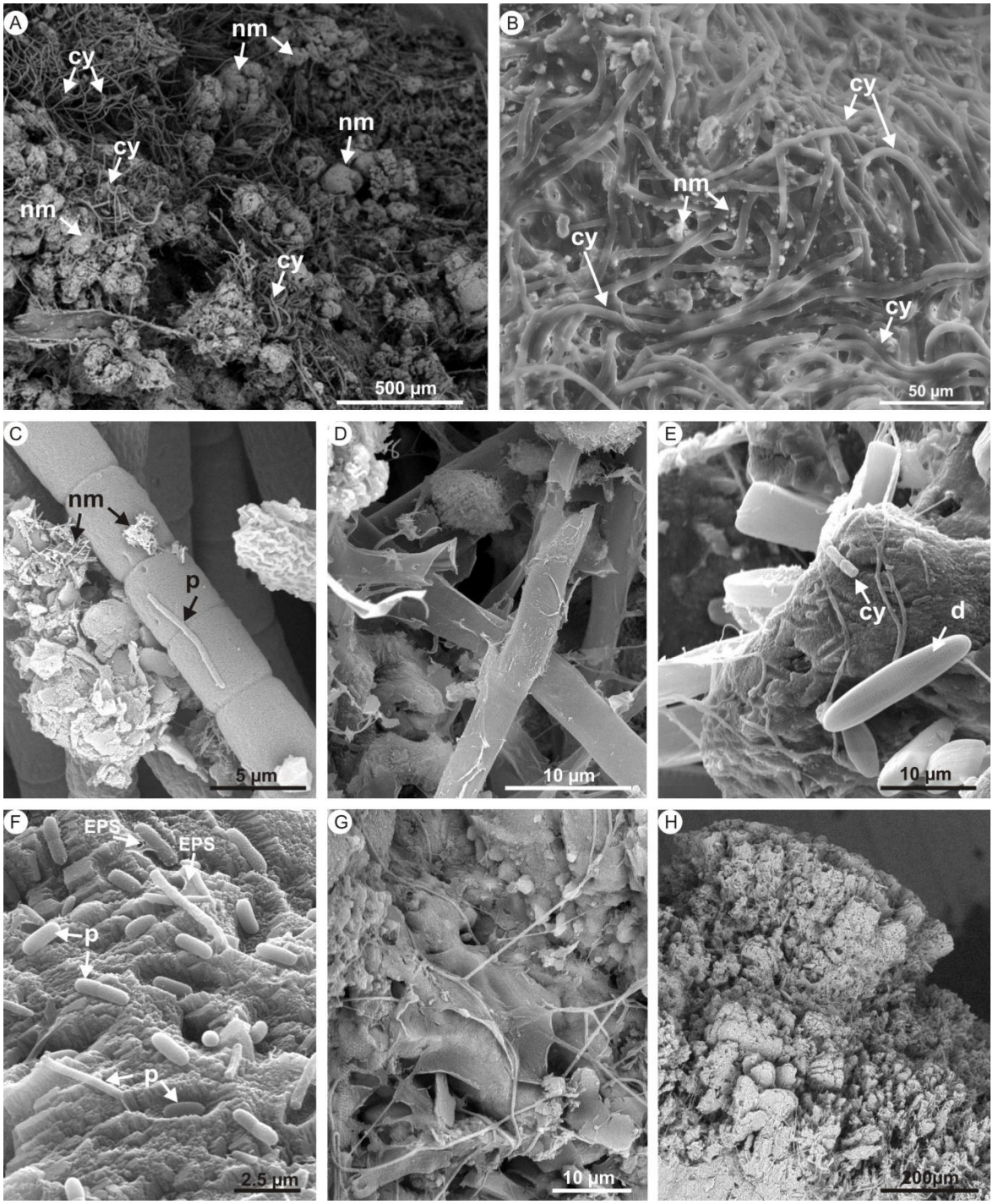

Fig. 8.2. Microbial communities in Parmenta tufa deposits. SEM (A) and ESEM (B) view of the growing tufa surface colonized by the biofilm. Cavities present between neo-formed minerals (nm) are occupied by cyanobacterial tufts (cy). Compare with Fig. 8.1D. C) Isodiametric cells characterizing trichome of cyanobacteria morphotype 1; note a single-cell prokaryote (p) and neo-formed mineral (nm). D) Cyanobacteria morphotype 2 characterized by a thick sheath covering the internal trichome. E) Pennate diatoms (d) and a cyanobacterial filament of morphotype 3 (cy). F) Colony of single-cell prokaryotes (p) occurring as rods and cocci, with some EPS material, on the calcite neo-formed surface. G) Actinomycetes-like bacteria characterized by branched terminations connected to a uniform central area representing a mycelium stage. H) Oocardium colony characterized by branched calcified tubes partially occupied by cells.

9. THE BIOFILM STRUCTURE

With regard to the relationship between the microbial community and neo-formed tufa, SEM observations on samples collected during the monitoring year show that the biofilm always develops on an irregular surface made of micro-columns of neo-precipitated calcite separated by interstitial channels with inner cavities (Fig. 9.1A and B). Micro-columns usually are characterized by a mushroom or pinnacle morphology that can vary in size from 50 to 150 µm. A similar morphological configuration of the neo-formed precipitates associated with the biofilm was observed in the other field experiments (Fig. 9.1C and D).

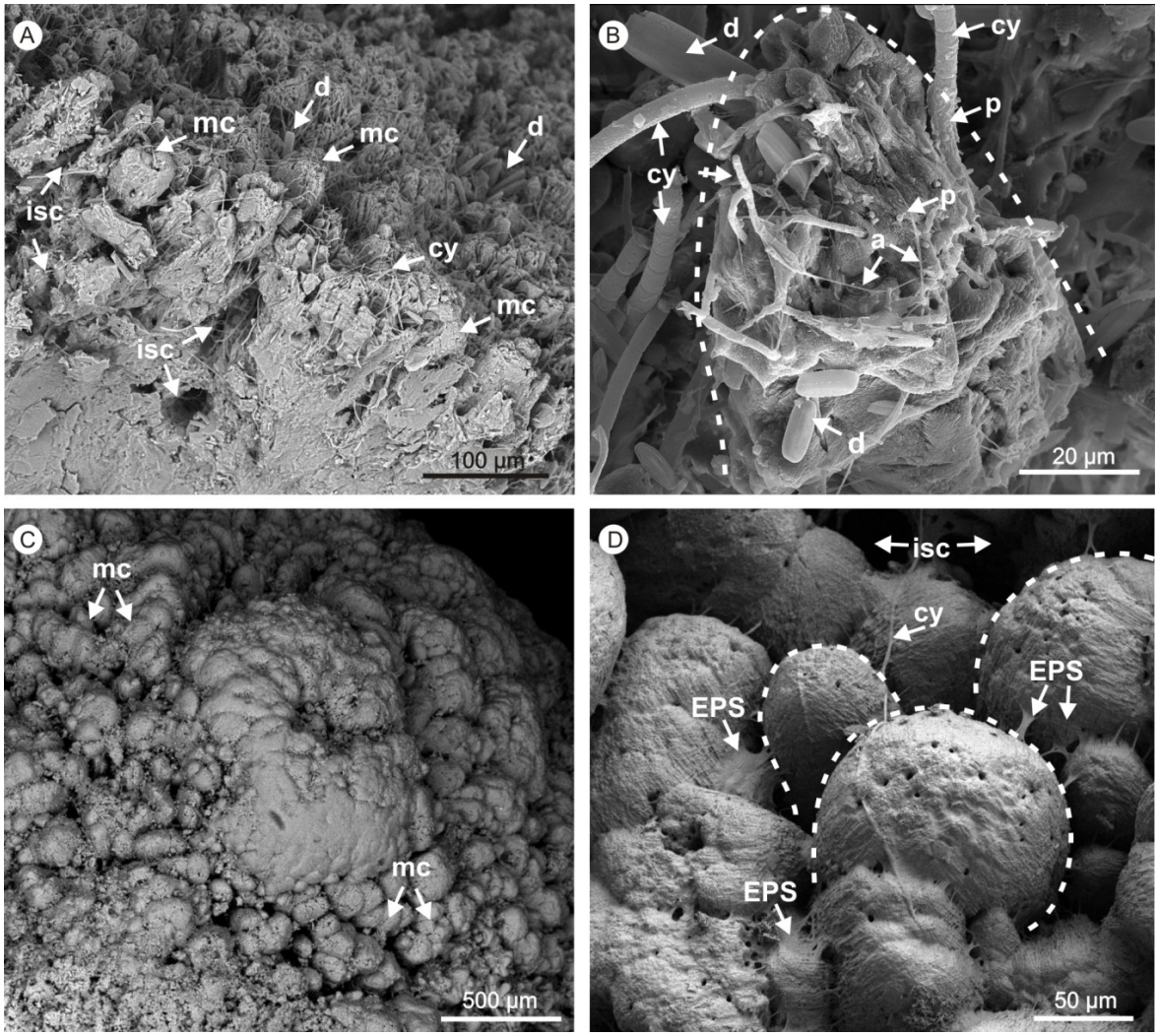

Fig. 9.1. Features of the active deposition zone (ADZ). A) Transverse view of a section of the micro-columnar structure forming the ADZ. Pinnacle-shaped micro-columns (mc), interstitial spaces and inner cavities (isc) can be distinguished, as well as the biofilm with cyanobacteria (cy) and diatoms (d). (B) Close-up view of the main biofilm components on a micro-column (dashed line): Unicellular prokaryotes (p), diatoms (d), cyanobacteria (cy), actinobacteria (a). C) Top view of the of the growing tufa surface in Thornley barrage system, characterized by micro-columns of neo-precipitated calcite (mc). Note the similarity with A and B. D) Close-up view of micro-columns (dashed lines) showed in C. Micro-columns, forming inner cavities (isc), are connected by EPS sheets and cyanobacterial filaments (cy).

The distribution of the micro-organisms forming the biofilm in relation to the micro-columns appears as follows. Cyanobacteria are mainly arranged in colonies of upright tufts that rim columns and interstitial spaces. They also occupy restricted areas, generally originating from an inter-column space (Figs 8.2A and 9.2). Macroscopically tufts correspond with the greenish-brown patches, whereas the yellowish areas of the biofilm are composed of green algae, Actinobacteria, unicellular prokaryotes, and sporadic cyanobacterial filaments (Fig. 8.1A).

Diatoms live preferentially on the top of the columns, often arranged in groups of a few individuals, but sometimes also occupying cavities themselves.

Actinobacteria form a sort of covering network (when in the mycelium stage), especially within the interstitial spaces and deep cavities of the micro-columns. They are attached to the mineral substrate, as well as to cyanobacteria, diatoms and other organic tissues (such as leaves and mosses). Branches departing from mycelia develop aerial filaments that can join columns through bridging structures. These filaments demonstrate an adhesive behaviour through trapping allochthonous particles and adherence on organic substrates.

Single-cell prokaryotes are widespread. They occupy the external surface of the micro-columns, including cryptic cavities, and they can colonize any organic substrates, including degrading ones.

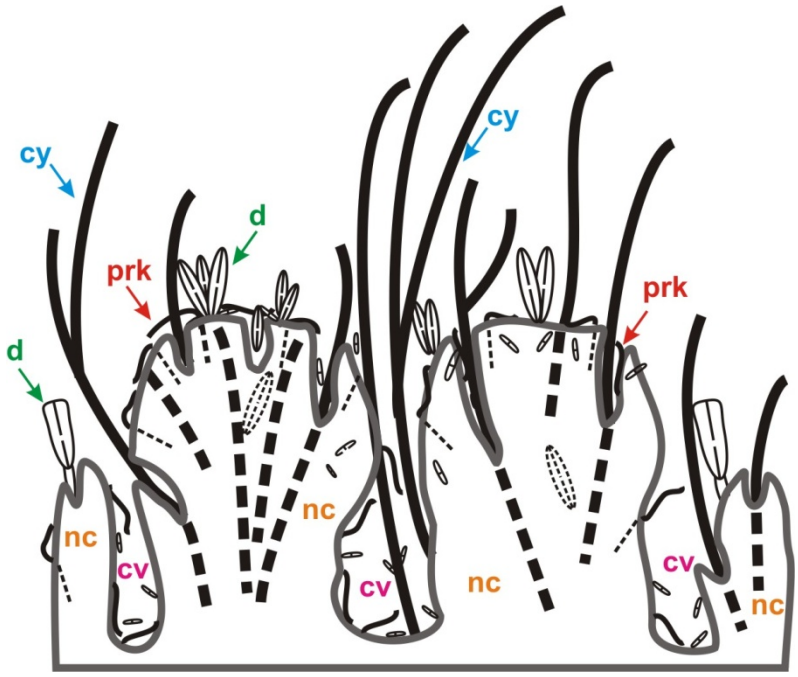

Fig. 9.2. Scheme representing the distribution of the main biofilm components in relation to neo-formed micro-columns. Cyanobacteria (cy) and diatoms (d) occupy the inter-column space and cavities (cv). Diatoms are also common on the top of the neo-formed surface (nc) whereas Actinobacteria and single-cell prokaryotes (prk) are widespread in all domains of the growth surface of the deposit.

9.1 Nano-scale features of neo-precipitates in the active depositional zone

As precipitation can take place in all sub-domains of the biofilm, this space is called the 'active depositional zone' (ADZ) (Figs 9.1, 9.2). Irrespective of the type of organic substrate on which precipitation occurs, neo-formed calcite originates in the upper part of the micro-columns and pinnacles, and in the interspaces between them, directly on the free fluid-solid interface and within cavities (Fig. 9.3). It also forms aggregates suspended in the cyanobacterial tufts, exhibiting several crystal morphologies and sizes.

Submicron-sized crystals about 10-20 nm in diameter, with a sub-spherical shape, are the smallest mineral units observed in all tufa neo-precipitates (Figs 9.3, 9.4, 9.5). Sub-spherical nano-crystal units agglutinate early to form rod-shaped crystal aggregates, 100-200 nm in size (Figs 9.3A, 9.4). These aggregates create two basic types of crystal polyhedrons. In one case, polyhedrons, apparently disphenoidal, in the range of 1-2 μm, originate directly by the aggregation of the early-formed rod-shaped crystals (Fig. 9.3B). In a second case, they grow in a geometrical order to form minute triads of calcite fibres, departing from a common cusp and forming an angle of ~100° between them. Triads of calcite vary in size and length of fibre from ~0.4 (short triads) to ~1 μm (long triads). They commonly occur closely stacked along their C-axes to form pyramidal to rhombohedral solids (Fig. 9.3C and D). All types of basic polyhedron coalesce to form larger crystals of calcite (mainly tetrahedrons) that represent the mineral structure of the biofilm, mainly in the form of the micro-columns and pinnacles (Fig. 9.3C and E). Some of the triad aggregates are not connected with the neo-formed mineral surface of the tufa deposit, but occur within and amongst the filament tufts (Fig. 9.3F). Finally, the long triads of calcite may occur stacked along a single line, forming needle-shaped crystals.

Neomorphic nano-scale precipitates are frequently observed in close association with both organic living and non-living components within the biofilm (Fig. 9.6). Inorganic substrates like grains (clay minerals, old carbonates, quartz) do not appear to be good locations for the neo-precipitation of minerals (Fig. 9.6A). Nano-scale mineral units begin their formation mainly by replacing a degrading organic matter substrate (Fig. 9.6B-D). EPS, dead bacterial cells or plants tissues are seen replaced by nano-scale crystals with or without the presence of degrading microorganisms (heterotrophic bacteria, actinomycetes, fungi). Living organisms like cyanobacteria are often sites of mineral formation. In this case neo-precipitates are crystalline aggregates (< 10 μm) along the external surface of the sheath of the filament in isolated sites (Fig. 9.3F).

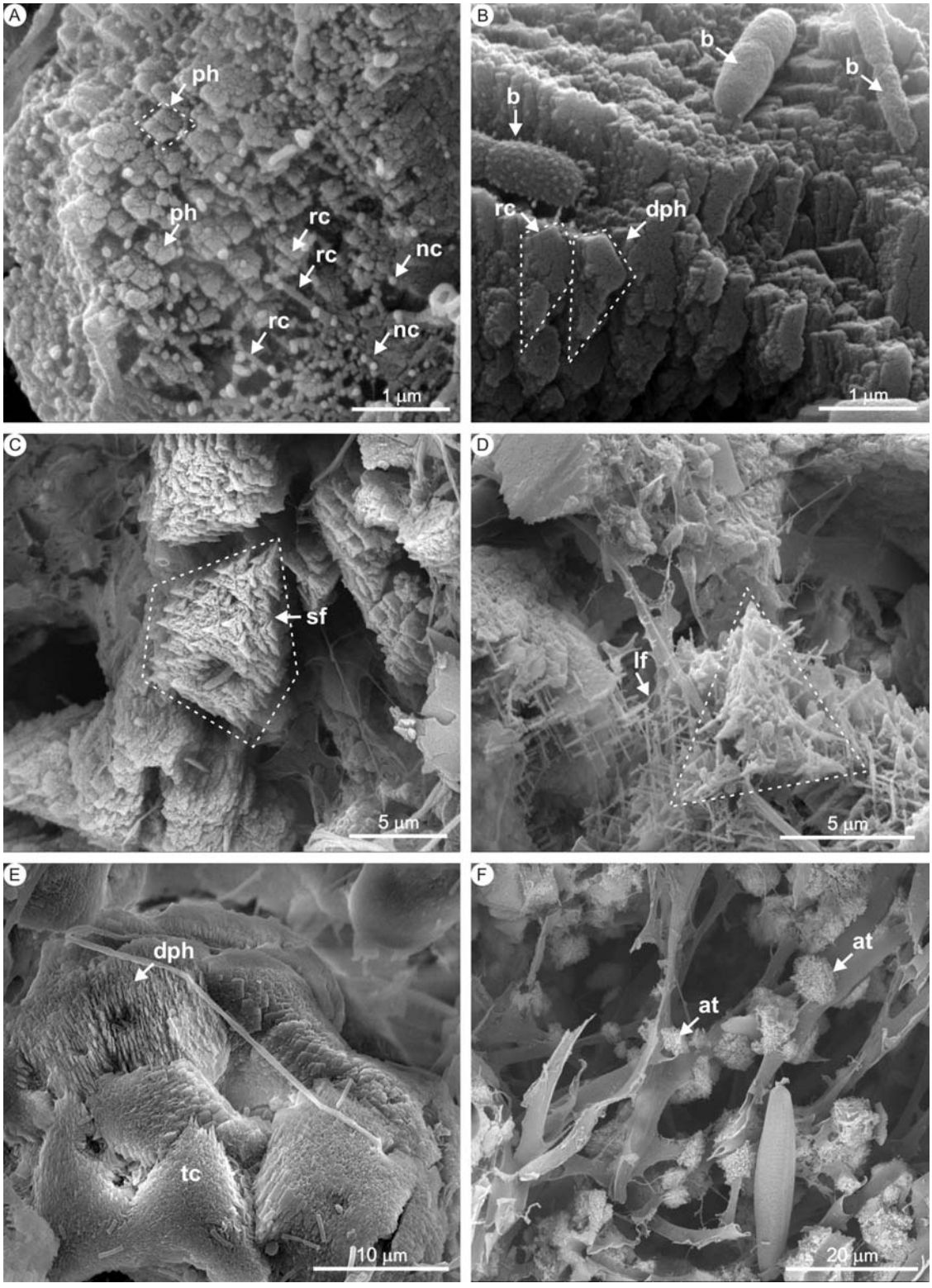

Fig. 9.3. Micro-nano-structure of neo-formed minerals in the Parmenta barrage system. A) Sub-spherical nano-crystals (nc) are the smallest mineral units observed, which aggregate to form rod-shaped crystals (rc), then coalescing to form polyhedrons (ph). Detail of Fig. 11A. B) Disphenoidal polyhedrons (dph) originate by the aggregation of the early-formed rod-shaped crystals (rc); note bacterial bodies (b). C) Triads of short calcite fibres (sf) and long calcite fibres (lf) (D) are closely stacked along their C-axes to form pyramidal to rhombohedral solids. E) Tetrahedral crystals of calcite (tc) formed by the aggregation of disphenoidal polyhedrons (dph) creating a micro-column colonized by the biofilm. F) Aggregates of triads (at) occurring within cyanobacterial filaments forming a tuft. Compare with Fig. 8.1D.

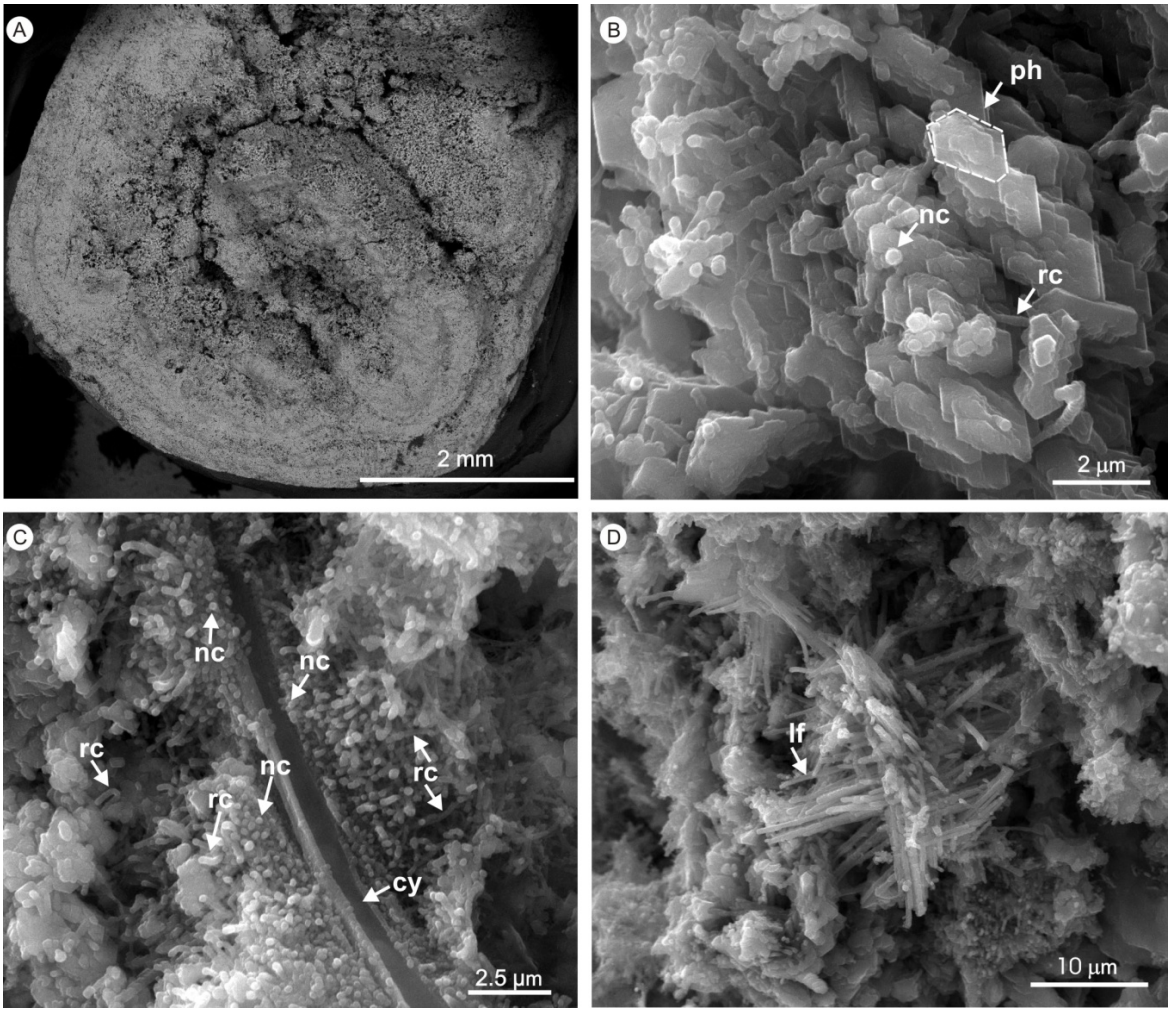

Fig. 9.4. Micro-nano-structure of neo-formed minerals in the terraced-slope system of Barnard Castle. A) SEM photomicrograph of internal fabric of a pisoid. B) Association of sub-spherical nano-crystals (nc), aggregating in rod-shaped crystals (rc), which coalesce to form polyhedrons (ph). C) Close-up of cyanobacterial sheath (cy) showing precipitated nano-crystals of calcite (nc) and rod-shaped crystals (rc). D) Elongate fibres of calcite (lf) around microbial filaments.

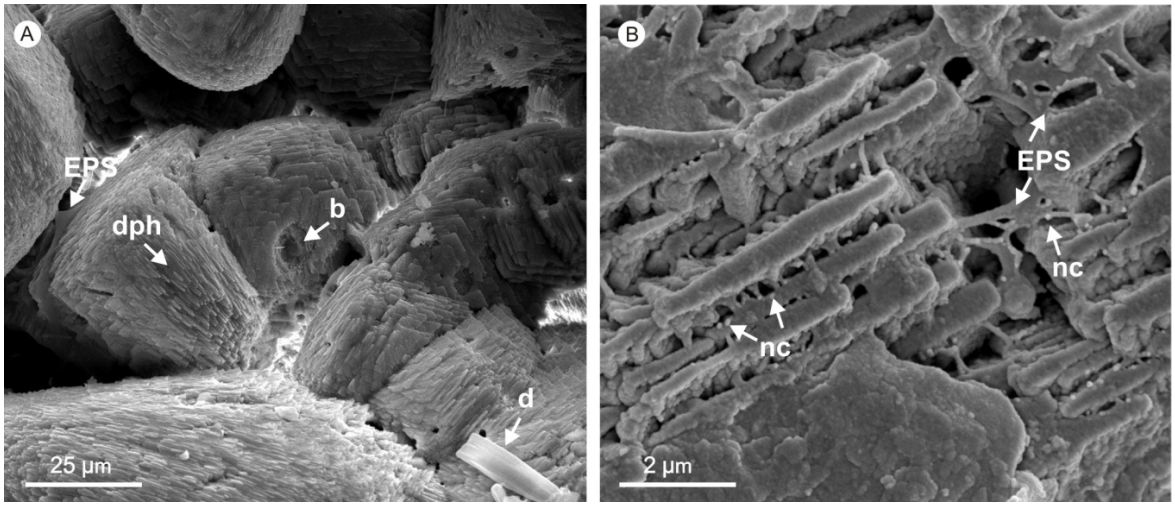

Fig. 9.5. Nano-structures of neo-precipitated calcite minerals in Thornley barrage system. A) Coalescing polyhedrons (dph); note scattered unicellular bacteria (b), diatom (d) and EPS sheet. B) Sub-spherical nano-crystals (nc) substituting EPS sheets. Untreated samples.

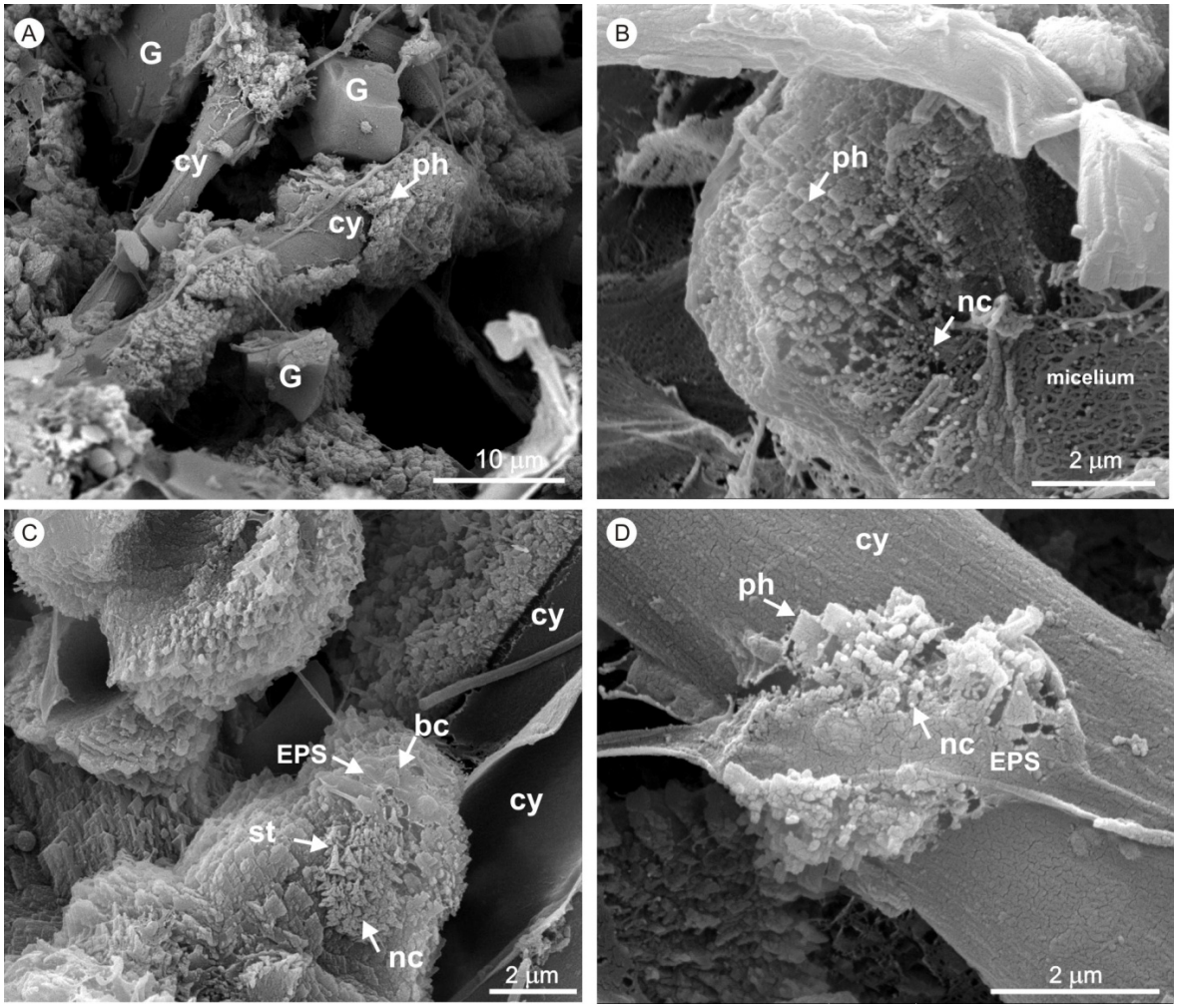

Fig. 9.6. Replacement of organic matter by mineral nano-crystals. A) Polyhedrons made of sub-spherical nanocrystals, replacing cyanobacterial filaments (cy). Note that detrital mineral grains (G) do not present any neo-precipitated minerals. B) Sub-spherical nano-crystal units (nc), aggregating successively to polyhedron aggregates (ph), replace degrading organic matter represented by possible actinobateria mycelia. C) Short triads (st) formed by the aggregation of sub-spherical nano-crystals (nc), replacing cyanobacteria (cy) and unicellular bacteria (bc) associated EPS. (D) Replacing of EPS sheet by sub-spherical nano-crystals (nc) and polyhedron aggregates (ph). Note the non-degraded cyanobacterial sheath (cy).

9.2 Petrographic features of neo-precipitates

Tufa neo-formed in both natural depositional sites and on inorganic substrates placed in the stream for this study were observed and compared through one monitoring year. Their general characteristics observed with SEM, in terms of mineral composition, biota and mineral-organic nano-structures, are similar. This confirms that the experiments are comparable to the natural system. Moreover, petrographic mineral components and fabrics of natural deposits are also similar to those observed in tufa formed on artificial substrates, with the important difference being that in the latter, it has been possible to observe the formation of the mineral fabrics and components in the different seasons.

With the purpose to compare petrographic with SEM observed features of neo-formed precipitated, in the Parmenta system it has been performed a simultaneous observation, through one monitoring year, of the thin section and the SEM-prepared sample.

After 1 month (winter) a thin ~0.1 mm-thick tufa crust formed on the artificial substrates emplaced in January (Fig. 9.7A and B). Under SEM the deposit is characterized by mushroom-shaped micro-columns composed of disphenoidal sub-crystal units, formed by the aggregation of the early-formed rod-shaped crystals. Columns are attached directly on the substrate and colonized by an already well-diversified biofilm community, dominated by unicellular prokaryotes and actinomycete-like bacteria, with minor diatoms and cyanobacteria. The same crust, observed with the petrographic microscope, is seen like a sparitic crust formed by coalescing fan-shaped limpid crystals of ~100 μm (Fig. 9.7A).

The tufa crust on the artificial substrates collected after 4 months (representing the deposition of part of the winter and the spring seasons) at the same site, reached a total thickness of ~350 μm (Fig. 9.7C and D). SEM view reveals a major upward growth of the micro-columns, which develop with pinnacle-shaped structures. At the nano-scale, short triads form pyramidal to rhombohedral crystals and dominate the ultrastructure of the crystals. This time-interval records a major expansion of cyanobacteria and diatoms. A new layer is visible in thin section, overlying the previous sparry crust, composed of microspar and subordinate micrite, deposited mostly around cyanobacterial filaments to form the elongated pinnacles. The resulting structure in thin-section is mainly a layer with a dendrolitic fabric with scattered patches of aphanitic micrite (Fig. 9.7C).

After 6 months (part of spring and summer) the crust was 450 μm in thickness (Fig. 9.7E and F). The general structure of the active depositional zone records a new trend of the micro-columns that now tend to expand laterally in their upper part. As a consequence of this, pinnacles are often connected to each other as a result of precipitation of calcite as elongate triads that cover almost uniformly the upper part of depositional zone. Calcite fibres are also precipitated within internal cavities of the crust (Fig. 9.8A). Cyanobacteria and diatoms continue to dominate the biofilm community. In thin-section a new, more or less continuous, layer of aphanitic-peloidal cloudy

micrite appears overlying the previous dendrolitic fabric (Fig. 9.7E). Cavities within the previous layers are apparently reduced in volume, compared with near-surface cavities, through syntaxial growth of crystals upon the walls.

After 9 months (summer-autumn) the total thickness of the crust was around 600 μm (Fig. 9.7G and H). During this time, the growth of the deposits continued with a similar structure at the depositional surface, and minor precipitation of new short-triads. The resulting petrographic fabric is characterized by a smaller amount of cloudy micrite and an increasing content of microspar organized into a peloidal/aphanitic fabric (Fig. 9.7G).

During the winter (December-January) 2009 an intense period of rainfall caused a major flood that destroyed most of the barrages and severely eroded the surface of the deposits.

Fig. 9.7. Comparison between the petrographic (left-hand pictures) and the SEM characteristics (right-hand pictures) of fresh tufa collected through the monitoring year. See text for comments. Bedrock (br), micro-columns (mc), interstitial spaces and inner cavities (isc), sparite crust (sc), dendrolitic fabric (df), sparite (sp), microsparite (ms), micrite (m), cyanobacterial filaments (cy). Petrographic pictures are thin sections under polarized light; SEM pictures are all fresh surfaces.

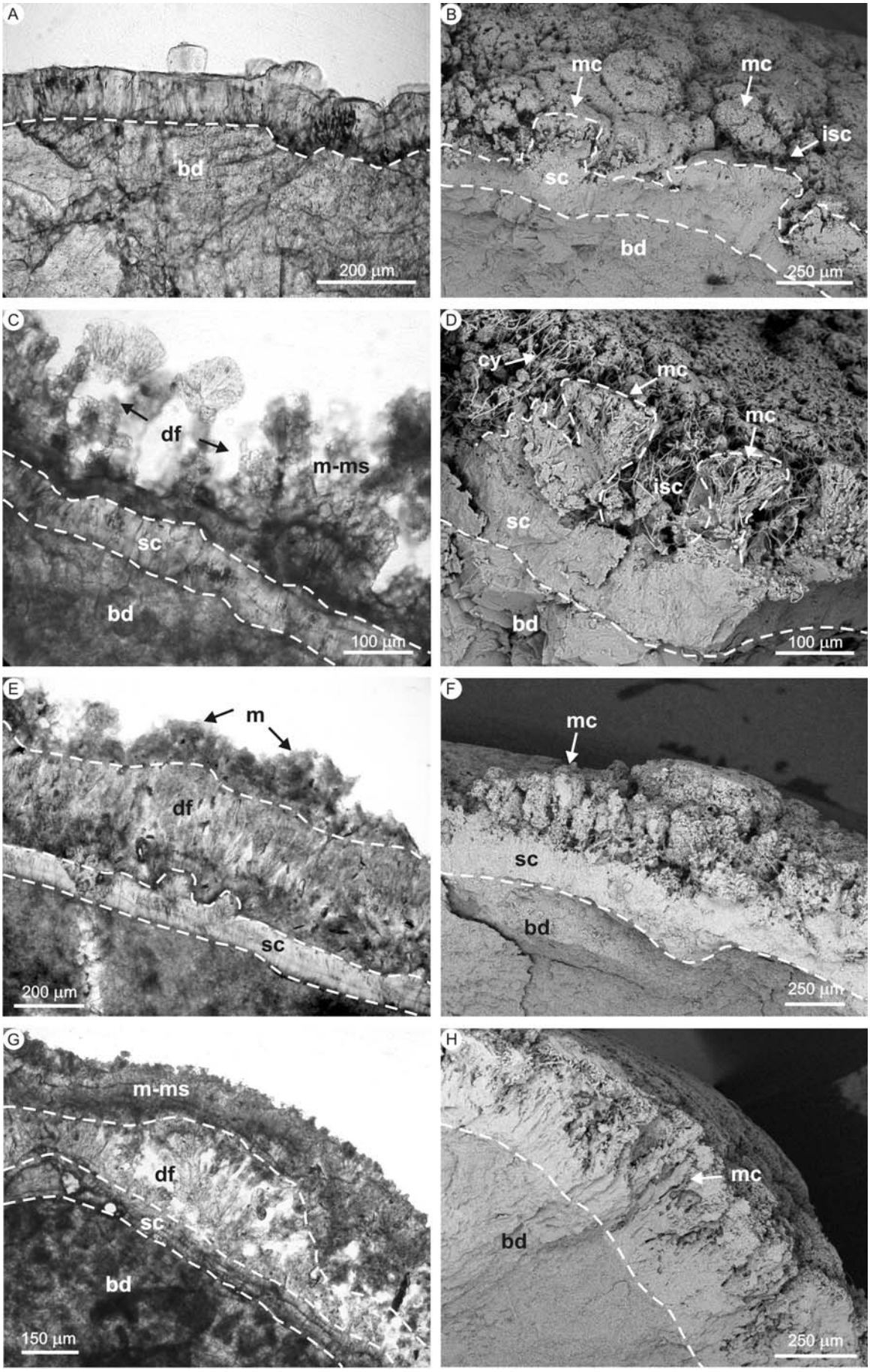
A
bd
200 µm
B
mc
mc
isc
sc
bd
250 µm
C
df
m-ms
sc
bd
100 µm
D
cy
mc
mc
isc
sc
bd
100 µm
E
m
df
sc
200 µm
F
mc
sc
bd
250 µm
G
m-ms
df
sc
bd
150 µm
H
mc
bd
250 µm

10. BIOFILM MEDIATION IN MINERAL GENESIS: DISCUSSION

Apart from the mechanisms that control the precipitation of minerals, the supersaturation of the water is an essential environmental condition for tufa formation. The absence of deposits in the Corvino River is explained by the constant SI < 0.5. In effect, it seems that the saturation index of water in respect of calcite has to be > 8-10 fold for spontaneous precipitation (Kempe & Kazmierczak, 1990; Mertz-Preiß & Riding, 1999; Arp et al., 2001b). Shiraishi et al. (2008a) demonstrated through in situ and ex situ measurements in a tufa-producing karst-water stream in Germany, that no spontaneous precipitation occurs on biofilm-free natural substrates, even under highly supersaturated conditions. In the Parmenta stream the calculated macro-environmental saturation state of water varies between 0.75 and 0.89, and this follows the seasonal variation of water temperature itself. For most of the year, this condition should inhibit the formation of any tufa deposit, but it has been observed to occur on the barrages although not in the pools. As a consequence of this, it could be that there is a particular factor(s), related to the biological component (the biofilm), that allows the formation of tufa deposits in the Parmenta stream.

Studies of the mechanisms of precipitation of calcite in freshwater tufa systems have focused on the in situ measurement of environmental parameters (CO_2, DIC, pH etc.), both in the macro-environment and at the micro-scale in the active depositional zone, including the biofilm-deposit interface. Furthermore, the study of the neo-precipitates is often limited by the traditional thin-section petrographic approach, which only recently has been concerned with the biological components (see Shiraishi et al., 2008a). On the other hand, SEM studies of tufa deposits (natural or produced in the lab) have been classically limited to the observation of already-formed minerals in relation to a single group of micro-organisms (mainly cyanobacteria). SEM analyses moreover generally lack any detailed description of the biofilm and its morphological and biological structure, especially in conjunction with the petrographic details. The actual locations of the early stage of mineral formation, such as where and how it takes place within the biofilm ultra-structure, are still unknown. To confirm the processes operating in a natural system, Pedley et al. (2009) recently reproduced a tufa-generating biofilm in the lab. They showed that the mineral only forms in association with an organic substrate (EPS and cyanobaterial sheaths) and that the early stages of the mineral appear diversified in relation to the organic substrates. This experimentalapproach revealed distinctive ultra-structures related to their origin.

The precipitation of calcite in the Parmenta system takes place more or less constantly within a complex space that can be called the 'active deposition zone' (ADZ) (Fig. 9.1), and we have observed continuous formation of neo-precipitates during the study period (Fig. 9.3). In this space, which extends for a few hundred microns, the physical preciptiation of mineral occurs along the external, strongly irregular, surface of micro-columns (or pinnacles) separated by interstitial channels, and within cavities, with or without connection to the external surface, which

characterize the internal structure of the columns. Further point sites of precipitation occur suspended within the masses of cyanobacterial tufts above the deposit surface (Fig. 9.3F). The microbial community forming the biofilm is closely connected with the ADZ, since no precipitation has been observed to take place in the absence of a biofilm. This indicates that precipitation originates as a consequence of the biological activities of the biofilm community, related with the presence of either living or non-living organic matter.

The characteristics of our ADZ allow a parallelism with the 'diffusive boundary layer' of Shiraishi et al. (2008b), in which chemical gradients are established reflecting biofilm activities. The latter isolate this layer from the flowing water and positively affect the photosynthesis-induced precipitation of mineral, as well as inhibiting inorganic precipitation (Shiraishi et al., 2008a). Moreover, Shiraishi et al. (2008a, Fig. 2, resin-embedded thin-sections) reported a columnar structure to the mineral component and related biofilm in their tufa, comparable with the general structure of our active depositional zone. Only recently, using advanced SEM techniques that allow high magnification of organic matter after sample preparation that avoids the destruction of the organic tissues in high vacuum, Turner & Jones (2005) documented the intimate association between organic substrates and minerals. They gave a partial view of the active depositional zone, and evidence for localized sites of precipitation. They observed in an active tufa system of Canada that on the nano-scale where mineral nucleates first appear as 100-200 nm thick dendritic calcite fibres, they form a 3D lattice-like domain of half shortened octahedrons (triads). This early stage of mineral precipitation formed only in association with EPS that discontinuously coats bryophytes and cyanobacteria.

Pedley et al. (2009) reported a detailed analysis of the sites of precipitation in a lab-reproduced tufa system, although their sample preparations lacked treatment for the preservation of the organic tissues. This is indispensable for a correct interpretation of the observed morphologies, as suggested by Fratesi et al. (2004). In any case, Pedley et al. (2009) suggested that where living cyanobacterial sheath substrates are available there is a rapid localized development of long-crystallite dendrite triads. Where a diverse living biofilm with abundant EPS is present, they reported both micro-peloid aggregates of spherulites and short-crystallite dendrite triads. To avoid any misinterpretation, in this study we used SEM and ESEM with chemically dried and untreated samples, respectively, in order to obtain ultra-high-magnifications (in a high-vacuum SEM) and control the tissue preservation (in a low-vacuum ESEM).

In the ADZ of the Parmenta tufa, sub-spherical nano-crystal units ('nanospheres', 10-20 nm in diameter) are the smallest neomorphic precipitate (Figs. 9.3A and 9.7). They commonly form by replacing non-living degrading organic matter or at point sites along the external surface of a living cyanobacterial sheath (Fig. 9.3F). In the first case, EPS, dead bacterial cells and plant tissues are seen to be replaced by nano-scale crystals with or without the presence of degrading

microorganisms (heterotrophic bacteria, actinomycetes, fungi), suggesting the existence of biotic and abiotic degradation processes of the organic matter (Fig. 9.6). Although we did not measure ion fluxes that can reveal the metabolic activities of micro-organisms, the complexity of the studied biofilm, evident even from a morphological observation, suggests the coexistence of several metabolic pathways within the observed biota. Recently the complexity of the tufa-associated biofilm has been demonstrated with molecular DNA analysis that confirms the coexistence of several trophic groups (Arp et al., 2010; Bissett et al., 2008). In fact, the studied biofilm could be compared with a micro-ecosystem like a microbial mat, in which occur autotrophs and organic matter degrading heterotrophs, as well as abiotic degradation of organic matter. It is well known that all these processes can activate organo-mineralization (see Dupraz et al., 2009 and references therein). Moreover the studied biofilm is characterized by a variation in relative abundance and distribution of the microbial taxa through the monitoring year. Cyanobacteria, that are often reported to be the main agents of organo-mineralization (Shiraishi et al., 2008a), as well as diatoms (Winsborough & Golubić, 1987; Winsborough, 2000), through the photosynthetic uptake of CO2 in the biofilm, are patchily distributed and only really abundant during the spring and early part of the summer season. During the remaining time, and away from the main areas of cyanobacterial growth (greenish-brown tufts), the biofilm is dominated by prokaryotic and eukaryotic heterotrophs (yellowish layer), as is to be expected for areas of degrading organic tissue (i.e. plant remains) (Dunn et al., 1997). Pedley & Rogerson (2010), observing lab-reproduced tufa biofilm, demonstrated the formation of biotic-mediated tufa in the absence photosynthetic processes but in association with EPS. Arp et al. (2010) suggested e that cyanobacterial photosynthesis is the fundamental biotic factor in the formation of tufa stromatolites,together with a major contribution from physicochemical processes;however, they did not exclude a role of heterotrophic activities in biomineralization in tufa formation.

The origin of mineral nanospheres which represent the first product of organo-mineralization in microbial carbonates has been explained from studies of examples formed in marine, non-marine and laboratory conditions. In continental freshwater carbonates, Folk (1993) showed that mineral nanospheres interpreted as mineralized nanobacteria compose the ultra-structure of hot-water travertines. Pedley et al. (2009) recognized nanospheres as the first product of mineralization, successively developing clusters composed of micropeloids in lab-produced tufa. In natural active tufa deposits it has been shown that the first products of organo-mineralization are nm-scale fibres (e.g. Turner and Jones, 2005). However, observing their ultra-high-magnification pictures (e.g. Fig. 5, Turner & Jones, 2005), the fibres do appear to be composed of coalescing nanospheres, just as seen in the Parmenta system. In lab experiments on the precipitation of Ca-carbonates in the presence of bacteria cultured in a polysaccharide-rich gel-like medium, Chekroun et al. (2004) found that in the presence of living and non-living bacterial cells, mineral precipitates form

amorphous-to-spherical or disphenoidal crystal aggregates that are all characterized by a nanospherical ultrastructure. This distinctive nanospherical or nanoglobular ultra-structure has also been found in many marine microbialites, both modern and ancient (Perri & Tucker, 2007; Bontognali et al., 2008; Sánchez-Román et al., 2008; Spadafora et al., 2010).

As observed in our studies, nanospheres agglutinate early to form firstly rod-shaped crystal aggregates (100-200 nm), which can evolve to form triads of fibres, or after an apparently random aggregation, disphenoidal solids (Fig. 9.3). Both triads of calcite (short or long) and disphenoidal solids coalesce to form larger calcite crystals (mainly tetrahedrons tens of microns in size) that represent the fundamental bricks for the construction of the micro-columns and pinnacles. Basic aggregates of neo-precipitates (disphenoids and triads) do not seem to form in association with one particular type of organic matter substrate. In fact, we observed that living cyanobacterial EPS sheath substrates mineralize through both disphenoidal micro-crystals and long-crystallite dendrite triads to form peloids and mineralized filaments. Other organic substrates, living or non-living, both EPS and cellular material, also do not have any specific calcifying crystal morphology. On the other hand, it has been suggested that long-crystallite dendrite triads only form in association with cyanobacterial sheath EPS (Turner & Jones, 2005; Pedley et al., 2009), whereas nm-scale spherulites (corresponding to our nano-spheres) and short dendrite triads only form through mineralization of generic EPS matter (Pedley et al., 2009). In modern marine stromatolites composed of early-stage microbial Mg-rich calcite followed by aragonite, Spadafora et al. (2010) have shown that the calcite crystals consist of aggregates of nano-scale triads with abundant relics of organic matter in the interstitial space, whereas the abiotic aragonite has a solid ultra-structure.

Although in our system nano-crystal morphologies of neo-precipitates are not strictly linked with the type of organic substrate, they do appear to be influenced by the seasonal environmental variations. We observed abundant disphenoidal microcrystal precipitates in the colder season. During the intermediate seasons these are gradually replaced by short triads, and finally by long triads in the warmest conditions. Since the main environmental factor varying in the Parmenta stream is the water temperature, which controls the calculated SI, we propose that the ultra-structure of the neo-precipitates mainly reflects the seasonal temperature variations. In lab culture experiments, Chekroun et al. (2004) have already demonstrated that supersaturated conditions in the absence of bacterial activities, but with organic matter present in the medium, induce the formation of long dendrite triads, whereas low supersaturated conditions trigger disphenoidal or dipyramidal nano-crystals morphology. Moreover, in the presence of bacterial activity and high supersaturation the same authors observed that bacterial cells were calcified by an amorphous calcium carbonate precursor, possibly comparable with the early-stage nano-sphere aggregates observed in our studies. In addition, Turner & Jones (2005) suggested that dendrites form in highly supersaturated conditions but only on an EPS film, whereas low supersaturation induces

subsequent abiotic solid crystal growth by diffusion, through the occlusion of the interstitial spaces between fibres by epitaxial rhombohedral crystal masses. The latter, however closely resemble our early-stage nano-sphere aggregates, as they are actually smaller than fibres (see Fig. 5D in Turner & Jones, 2005).

10.1 Biotic versus abiotic interpretation of the petrographic components

The petrographic fabrics described here consist of one or more petrographic components (micrite, microspar and spar) as seen in the particular two-dimensional spatial distribution of a thin-section, where it is possible (but not always) to identify the crystals' essential dimensions and degree of transparency (often mediated by the organic component and by the thickness of the section). Apart from the possibility of greater magnifications under SEM, the main feature to observe is the external morphology of the crystals. Moreover, the organic components are almost invisible in thin-section (if it is not treated properly), whereas they can be distinguished easily under the SEM if appropriate techniques are used. Up till now, petrographic observations and the subsequent interpretations of the fabrics and components in terms of genesis and distribution (with insights often inherited from studies of marine carbonates), have been the main starting point in the study of these continental carbonates.

As discussed above, a strict biological driving-force has been suggested for the origin of the micro-scale early-stage precipitates through SEM studies. At the same time other crystal phases examined under the SEM, notably the sparry cements, have been inferred to be abiotic in origin (Pedley, 1992; Turner & Jones, 2005; Pedley et al., 2009).

In order to obtain a comparison between the petrographic and the SEM characteristics of fresh tufa, we have examined all samples (particularly those on the artificial substrates positioned along the stream) collected throughout the monitoring year, with identical techniques and instruments (Fig. 9.7). Through this step-by-step comparison, we observed that the petrographic components: micrite, microspar and spar, can form within the same biofilm, in any or all depositional sites, with the same mechanisms of biotic-mediated precipitation and result in the formation of all the described basic nano-crystal mineral units.

After 1 month in wintertime, the thin ~0.1 mm sparitic crust, composed of coalescing fan-shaped columnar limpid crystals, is seen under the SEM to correspond to the micro-columns covered by a well-diversified biofilm community dominated by non-photosynthetic bacteria. Micro-columns are composed mainly of an ordered package of crystal nano-sphere aggregates (100-200 nm) forming disphenoidal solids, still visible even in the inner part of the columns. Residual living and non-living organic components fill some interstitial spaces between the basic

nano-crystal units. Under the optical microscope one can observe a sparry limpid layer, which is probably due to the close packing of the nano-crystal units with a low content of trapped organic matter. However, such a porous crystal ultra-structure observed in our sparite is actually far from being solid, contrasting with true physico-chemically controlled euhedral sparry precipitates (Braissant et al., 2003 fig.4a; Pedley et al., 2009).

Early deposited sparry calcite in tufa systems, even though often observed in close association with micrite in thin alternating layers, has traditionally been considered an inorganic product mainly due to physical CO_2 degassing, in the absence (not always demonstrated) of a biofilm during cold seasons (Pedley, 1992). Recently the abiotic genesis of the early sparry components in tufa deposits has been interpreted as the epitaxial filling of the interstitial space between the early-formed (biotic) dendrites as a result of diffusion (Turner & Jones, 2005) or by the overgrowth of rhombic (abiotic) crystals when previous (biotic) micritic crystals (or aggregates) exceed 10-12 μm in diameter (Pedley et al., 2009). Nevertheless, Braissant et al. (2003) demonstrated in lab experiments that Ca-carbonate sparry crystals can be organo-minerals, as they can form through mediation in the presence of EPS and amino acids within the fluid. Verrecchia et al. (1995) had already referred to the formation of sparry crystals in the sheaths of cyanobacteria in laminar calcrete crusts.

Within internal cavities of the tufa, we commonly observed the deposition of neo-precipitates that appear to have formed syntaxially over the already present crystals (Fig. 9.8A). Their origin is probably due to a connection of such cavities with the water body above, along with the frequently observed presence of residual organic matter (EPS) and heterotrophic degrading microorganisms that can both induce mineral formation. Such mineral precipitation that takes places far from the photic zone of the biofilm remains included in the ADZ as it is still connected with the deeper layers of the biofilm in which organic matter consumption is still operating. The effect of this is the closure of most of the cavities and interstitial spaces, which then give rise to a more solid appearance to the deeper layers of the deposit. However, the nano-spherical origin of the basic mineral units forming these layers is still preserved and very often inherited in their ultra-structure, as it is possible to observe at high magnification under SEM of fresh mineral surfaces (Fig. 9.8B).

In the tufa forming on artificial substrates and in the natural depositional sites during winter-spring time, contemporaneously with the acme of cyanobacteria and diatoms, variations in the growth-style of the micro-columns have been seen. They evolve into the elongate pinnacle-like structures, along with major development of short triads in the crystal nano-structure. These structural modifications, which follow the increase of SI, result in the appearance of microspar and subordinate micrite, and the disappearance of spar crystals. Individual cyanobacterial filaments mineralize to form the dendrolitic fabric with scattered patches of aphanitic micrite. As this new dendrolitic/micritic structure of the deposit is different from the previous sparry structure, the two

phases of deposition are easily distinguished. Each depositional time is recorded by a 100-150 μm thick layer.

The further increase of the saturation state of water, characteristic of spring-summer time, does not induce important variations in the biota but results in the widespread formation of elongate triads. Isolated pinnacles (around single cyanobacteria), are gradually substituted by the deposition of a new discontinuous layer of aphanitic-peloidal cloudy micrite, which overlies the previous dendrolitic fabric. In this neo-formed layer, filaments are still mineralized, but as the long dendrites are rich in residual organic matter in the interstitial spaces, they appear optically cloudy (in thin-section). With the SEM and ESEM it can be seen that the structure of the active depositional zone is essentially unchanged.

The decrease of the SI in summer-autumn confirms the link between the saturation state of water and the mineral products, as similar petrographic aphanitic-peloidal fabrics appear, but they are composed mainly of microspar. In fact, the ultra-structure of the crystals again becomes dominated by short triads similar to the winter-spring time.

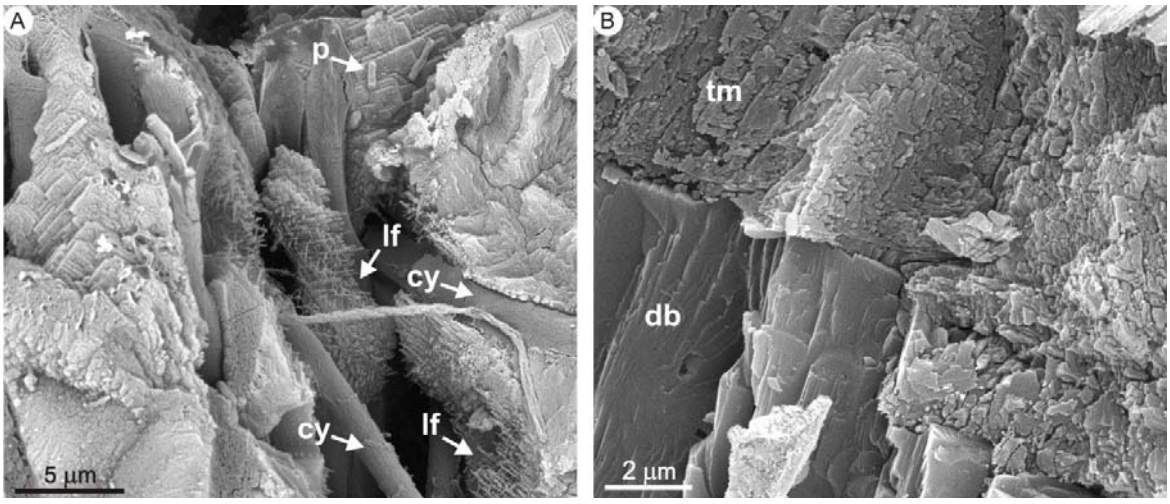

Fig. 9.8. A) Deposition within an internal cavity of neo-formed tufa of long triads of calcite (fc), syntaxially overgrown on already present crystals. Note cyanobacterial filaments (cy) and single-cell prokaryotes (p). B) Tufa calcite mineral (tm), with a nano-spherical crystal ultra-structure, deposited over dolomite (bd) substrate. SEM views fresh surfaces.

Each period of deposition is recorded with a 100-150 μm thick calcite layer, which forms over any type of substrate with a biofilm cover. A layered fabric is generated, independent of the petrographic component/s forming under the ambient environmental conditions (see earlier discussion). This basic micro-scale layered fabric of tufa deposits, independent of the depositional facies, is well known. Pedley (1992) reported that all types of tufa are composed essentially of micrite-sparite layers that respectively originate as a consequence of a slow rate of water flow and well-developed biofilm, and a high flow rate with a reduced biofilm layer. A more recent interpretation of the micrite-sparite couplets indicates that in the absence of an EPS substrate a sparry layer is formed, and if subsequently a biofilm develops, then micrite is precipitated (Pedley et al., 2009).

Finally the basic micro-scale layered fabric is present in any depositional facies, since if the biofilm colonizes all free surfaces of a strongly irregular substrate made of plant remains and/or autochthonous moss, then a vacuolar deposit is created. On the other hand if the biofilm develops on an even surface, a well laminated stromatolitic deposit is formed.

11. CONCLUSIONS

This research has concentrated on the study of the sedimentological and geochemical features of modern tufa deposits forming in different depositional environments, located in northern Calabria and in north-east England. The study of these active tufa systems has focused on the role of abiotic *vs* biotic factors involved in the precipitation process. The results obtained through a multidisciplinary and multi-scale study, of both tufa neo-precipitates and pre-existing deposits, have allowed an understanding of the morphological and biological structure of the biofilm and its ultra-structure, as well as identifying the sites of early-stage mineral nucleation at the interface of organic matter - mineral components.

In the studied sites, three main tufa depositional environments have been defined: the barrage system (Parmenta stream, NW Calabria and Thornley stream, NE England), terraced-slope system (Barnard Castle, NE England) and the overhanging-lobe system (Sunderland and Barnard Castle, NE England).

The barrage-type and terraced-slope tufa systems, independently from the dimensions of the deposits, are characterized by two basic gross morpho-facies: dams (forming pools) and lobes, whereas only lobes form in the overhanging-lobe systems. Such morpho-facies form as a consequence of the barrage morphology related to the nature of the underlying bedrock: low gradient slope favours large pools that separate distanced barriers (Thornley system), whereas, with the raising of the gradient, distance between dams and pools is reduced, as observed in the intermediate gradient slope of the Parmenta system, and in the higher angle slope of the terraced-slope system of Barnard Castle. Furthermore, the nature and morphology of the bedrock can induce some variations in the dimensions and shapes of the deposits. In fact, a staircase profile of the bedrock (generally due to the stratification) determes position, frequency and particularly dimension of the deposits as a function of the drop and the step size. For example, a small step with low drop induces small-size deposit, whereas a large-dimension step with high drop produces the overhanging-lobe type, which would represent an end-member of this system.

Depositional facies observed in all tufa systems are mainly represented by autochthonous deposits and secondarily by allochthonous deposits. The first group includes stromatolitic tufa crusts, phytohermal framestones (moss tufa and *Vaucheria* tufa) and phytoclastic tufa (mainly encrusted plant fragments); the second group is represented by pisoids and cave pearls. Observations suggest that the subdivision between phytohermal framestones and phytoclastic tufa, commonly used in the literature, is based on end-members depositional facies that have not been found isolated to form significant morpho-facies. In fact, they have been constantly found mixed to form porous deposits containing large voids, as for example mosses, *Vaucheria* tufts, and pustular tufa, that can be collectively termed vacuolar tufa.

Identical petrographic components are recognizable in all these depositional facies: micrite and microsparite, which are often associated with peloidal to aphanitic, laminar and dendrolitic fabrics, and a sparite, which can occur in layers composed of isolated to coalescent fan-shaped crystals forming botryoids and continuous crusts. All fabrics, occurring in all depositional facies, are organized into layers with a more or less well-developed cyclicity, which has its best expression in both autochthonous and allochthonous laminated deposits (stromatolitic tufa, laminated crusts and pisoids). Even pustular tufa, in which occur different crystalline phases (Mn-rich layers, fibrous calcite, aphanitic microspar), can show a sort of cyclicity.

Despite the variability of the studied tufa environments, in terms of water chemistry, climatic conditions, and geology of the catchment areas, all the deposits are composed of low Mg-calcite (Mg 1.0 - 3.5 mole %). The distribution of minor elements (Sr, Mn, Fe, S) is variable through the studied calcite tufa deposits. Calcite in the Parmenta tufa has a typical mean tufa Mg value and is enriched in Sr (0.5 - 0.8 mole%). The Mg values are attributed to the seasonal variation in water temperature of the Parmenta stream (8°-17°). The presence of sulphate evaporites and Sr-rich dolomites in the local bedrock influences the Sr values. In Thornley barrage tufa, the low Mg-calcite is locally enriched in Mn (0.2 – 1.8 mole%), Fe (0.2 – 1 mole%) and S (1.1 – 2.4 mole%) along micro-scale layers, representing a carbonate transitional phase, between the "normal" precipitation of low Mg-calcite and Mn-rich non-carbonate mineral layers (probably organo-minerals), following a possible variation of Eh–pH condition of the stream water. Moreover, the chemical composition of the Thornley stream water, which belongs to Ca-HCO_3-SO_4^{2-} system, influences the incorporation of S into calcite. Supply of the sulphate ions could be derived from organic matter degradation in the soil and/or pyrite oxidation within the coal measure beds that constituted the catchment area of the Thornley stream.

Scanning electron microscope (SEM and ESEM) observations of tufa neo-formed crusts revealed that the precipitation of calcite takes place more or less constantly within the active depositional zone (ADZ), which extends for a few hundred microns through the external surface of the deposit. Precipitation is attributed to the presence of a widespread biofilm (present in all studied sites) that occurs within and creates the ADZ, variably composed of epilithic and endolithic filamentous cyanobacteria, green algae, unicellular prokaryotes, Actinobacteria and fungi, with a variable amount of EPS. No precipitation takes place where the biofilm is absent, indicating that the biological activities of the biofilm are crucial, with its living organisms and non-living organic matter. A distinctive micro-morphology of porous micro-columns (50 - 150 μm in size), separated by interstitial channels, characterizes the ADZ and is present in all seasons. The precipitation of mineral occurs upon both external surfaces and within internal cavities of the ADZ. Further point-sites of precipitation occur suspended within the masses of cyanobacterial tufts and biofilm-EPS, above the depositional surface.

Sub-spherical nano-crystal units, 'nano-spheres' (10-20 nm in diameter), are the basic biotic neo-precipitate. They commonly form by replacing non-living degrading organic matter and at point-sites along the external surface of living cyanobacterial sheaths. Nano-spheres agglutinate early to form first rod-shaped crystal aggregates (100-200 nm), which evolve into triads of fibres, and after an apparently random aggregation, into disphenoidal solids. Both triads of calcite (short or long) and disphenoidal solids coalesce to form larger calcite crystals (mainly tetrahedrons tens of microns in size) that represent the fundamental bricks for the construction of micro-columns and pinnacles. Basic aggregates of neo-precipitates (disphenoids and triads) do not seem to form in association with any one particular type of organic matter substrate.

Comparison between the petrographic and the SEM characteristics of fresh tufa obtained during a monitoring year in the selected site of Parmenta, shows that each petrographic component and related ultra-structure in terms of basic crystal aggregates is related to the seasonal temperature variation. Abundant disphenoidal microcrystals precipitate in the colder season, and, during the intermediate seasons, these are gradually replaced by short triads, and finally by long triads in the warmest conditions. These three basic crystal aggregate types have a petrographic counterpart, respectively in the spar, microspar and micrite crystal habits. In this sense these terms have only a descriptive meaning, in the study of tufa, and probably in all microbial deposits, without a genetic significance.

Andrews J. E. (2006) Palaeoclimatic records from stable isotopes in riverine tufas: synthesis and review. *Earth Sci. Rev.,* **75**, 85–104.

Andrews, J.E., Riding, R. and **Dennis, P.F.** (1997): The stable isotope record of environmental and climatic signals in modern terrestrial microbial carbonates from Europe. *Palaeocr. Palaeoclimatot. Palaeoecol.,* **129**, 17l-189.

Andrews, J.E. and **Brasier, A.T.** (2005) Seasonal records of climatic change in annually laminated tufas: a short review and future prospects. *J. Quatern. Sci.,* **20**, 411–421.

Arenas, C., Gutiérrez, F., Osácar, C. and Sancho, C. (2000) Sedimentology and geochemistry of fluvio-lacustrine tufa deposits controlled by evaporite solution subsidence in the central Ebro Depression, NE Spain. *Sedimentology,* **47**, 883–909.

Arp, G., Reimer, A. and **Reitner, J.** (1999) Calcification in cyanobacterial biofilms of alkaline salt lakes. *European Journal of Phycology*, **34**, 393–403.

Arp G, Wedemeyer N, Reitner J. (2001a). Fluvial tufa formation in a hard-water creek (Deinschwanger Bach, Franconian Alb, Germany). *Facies*, **44**, 1–22.

Arp, G., Reimer, A. and **Reitner, J.** (2001b) Photosynthesis-induced biofilm calcification and calcium concentrations in Phanerozoic oceans. *Science*, **292**, 1701–1704.

Arp, G., Bissett, A., Brinkmann, A., Cousin. S., De Beer, D., Fried, T., Mohr, K.I., Neu, T.R., Reimer, A., Shiraishi, F., Stackebrandt, E. and **Zippel, B.** (2010) Tufa-forming biofilms of German karstwater streams: microorganisms, exopolymers, hydrochemistry and calcification. In: *Tufas and Speleothems: Unravelling the Microbial and Physical Controls* (Eds Pedley, H.M. and Rogerson, M) *Geological Society, London, Special Publications*, **336**, 83–118.

Bachofen, R. (1994) Cell structure and metabolism and its relation with the environment. In: *Chemical and biological regulation in aquatic system.* (Eds. Buffle J. and De Vitre R.R.), p. 231. Lewis Publishers, Boca Raton.

Badger, M. (2001) The roles of carbonic anhydrases in photosynthetic CO_2 concentrating mechanisms. *Photosynthesis Research*, **77**, 83–94.

Baker, A. (2001). Fluorescence excitation–emission matrix characterization of some sewage impacted rivers. *Environ. Sci. Technol.,* **35**, 948–953.

Baker, A. (2002) Spectrophotometric discrimination of river dissolved organic matter. *Hydrological Processes,* **16,** 3203–3213.

Baker, A., Inverarity, R., Charlton, M. and **Richmond, S.** (2003) Detecting river pollution using fluorescence spectrophotometry: Case studies from the Ouseburn, NE England. *Environmental Pollution*, **124**, 57–70.

Barabesi, C., Galizzi, A., Mastromei, G., Rossi, M., Tamburini, E., Perito, B. (2007). Bacillus subtilus gene cluster involved in calcium carbonate biomineralization. *J. Bacteriol.,* **189**, 228–235.

Bissett, A., De Beer, D., Schoon, R., Shiraishi, F., Reimer, A. and **Arp, G.** (2008) Microbial mediation of stromatolite formation in karst-water creeks. *Limnology and Oceanography*, **53**, 1159–1168.

Bontognali, T.R.R., Vasconcelos, C., Warthmann, R.J., Dupraz, C., Bernasconi, S.M. and **McKenzie, J.A.** (2008) Microbes produce nanobacteria-like structures, avoiding cell entombment. *Geology*, **36**, 663–666.

Bosak, T. and **Newman, D.K.** (2005). Microbial kinetic controls on calcite morphology in supersaturated solutions. *J. Sed. Res.,* **75,** 190–199.

Boulton, A., Findlay, S., Marmonier, P., Stanley, **E.** and **Valett, H.** (1998), The functional significance of the hyporeic zone in streams and rivers, *Annu. Rev. Ecol. Syst.,* **29**, 59– 81.

Boyde, A. (1972) Biological specimen preparation for the scanning electron microscope—an overview: *Scanning Electron Microscopy,* **1972** (Part II), 257–264.

Braissant, O., Cailleau, G., Duprez, C. and **Verrecchia, E.P.** (2003) Bacterially induced mineralization of calcium carbonate in terrestrial environments: the role of exopolysaccharides and amino acids. *J. Sed. Res.,* **73,** 485–490.

Bray, D.F., Bagu, J., and **Koegler, P.,** (1993) Comparison of hexamethyldisilazane (HMDS), Peldri II, and critical-point drying methods for scanning electron microscopy of biological specimens. *Microscopy Research and Technique,* **26**, 489–495.

Buccino, G., D'Argenio, B., Ferreri, V., Brancaccio, L., Ferreri, M., Panachi, C. and Stazione, D. (1978) I travertini della basse valle del Tanagro (Campania). Studio geomorphologico, sedimentologico e geochimico. *Boll. Soc. Geol. Ital.,* **97**, 617–646.

Buffle, J. (1990) *Complexation reactions in aquatic systems, an analytical approach.* Ellis Horwood, New York. pp.692.

Burne, R.V. and **Moore, L.S.** (1987) Microbialites: organosedimentary deposits of benthic microbial communities. *Palaios,* **2**, 241–254.

Carthew, K.D., Taylor, M.P. and **Drysdale, R.N.** (2003) Are current models of tufa sedimentary environments applicable to tropical systems? A case study from the Gregory River. *Sedimentary Geology*, **162**, 199–218.

Carthew, K.D., Taylor, M.P. and **Drysdale, R.N.** (2006) An environmental model of the fluvial tufas of the seasonally humid tropics, northern Australia. *Geomorphology*, **73**, 78–100.

Chafetz, H.S. and Folk, R.L. (1984) Travertines: depositional morphology and bacterially constructed constituents. *J. Sed. Petrol.,* **54**, 289–316.

Chafetz, H.S., Srdoč, D. and **Horvatiničic´, N.** (1994) Early diagenesis of Plitvice lakes waterfall and barrier travertine deposits. *Géogr. Phys. Quatern.,* **48**, 247–255.

Chekroun, K. B., Rodriguez-Navaro, C., Gonzalez-Munoz, M.T., Arias, J.M., Cultrone, J. and **Rodriguez-Gallego, M.** (2004) Precipitation and growth of calcium carbonate induced by *Myxococcus xanthus*: implications for recognition of bacterial carbonates. *J. Sed. Res.,* **74**, 868–876.

Cohen, A.L. (1979) Critical point drying—principles and practice. *Scanning Electron Microscopy*, **1979**, 303–324.

Decho, A.W. (1990) Microbial exopolymer secretions in ocean environments: their role(s) in food webs and marine processes. *Oceanography Marine Biology Annual Review*, **28**, 73–154.

Decho, A.W. (2010) Overview of biopolymer-induced mineralization: What goes on in biofilms?. *Ecological Engineering,* **36**, 137-144.

Douglas, S., Abbey, W., Mielke, R., Conrad, P. and **Kanik, I.** (2007) Textural and mineralogical biosignatures in an unusual microbialite from Death Valley, California. *Icarus*, **193**, 620–636.

Dunn, K.A., McLean, R.J.C., Upchurch, G.R. and **Folk, R.L.** (1997) Enhancement of leaf fossilization potential by bacterial biofilms. *Geology*, **25**, 1119–1122.

Dupraz, C., Visscher, P.T., Baumgartner, L.K. and **Reid, R.P.** (2004) Microbe–mineral interactions: early carbonate precipitation in a hypersaline lake (Eleuthera Island, Bahamas). *Sedimentology,* **51**, 745–765.

Dupraz, C. and **Visscher, P.T.** (2005) Microbial lithification in marine stromatolites and hypersaline mats. *Trends in Microbiology*, **13**, 429–438.

Dupraz, C., Reid , R.P., Braissant, O., Decho, A.W. Norman, R.S. and **Visscher, P.T.** (2009) Processes of carbonate precipitation in modern microbial mats. *Earth-Science Reviews,* **96**, 141–162.

Elkins, K.M. and **Nelson, D.J.** (2001) Fluorescence and FT-IR spectroscopic studies of Suwannee river fulvic acid complexation with aluminium, terbium and calcium. *Journal of Inorganic Biochemistry,* **87,** 81–96.

Ercole, C., Cacchio, P., Botta, A.L., Centi, V. and **Lepidi, A.** (2007) Bacterially induced mineralization of calcium carbonate: the role of exopolysaccharides and capsular polysaccharides. *Microscopy and Micoanalysis,* **13**, 42–50.

Evans, J.E. (1999). Recognition and implications of Eocene tufas and travertines in the Chadron formation, White River Group, Badlands of South Dakota. *Sedimentology*, **46**, 771– 789.

Fenwick, G. R. and **McLean, S. G. (1996)** Opportunity docks: a case study of earth science conservation in a urban development. In: *Geology on your doorstep. The role of urban geology in earth heritage*

conservation. (Ed. Bennett, M. R., Doyle, P., Larwood, J. G. and Prosser C. D). pp. 263. Geological Society.

Fernandez-Diaz, L., Putnis, A., Prieto, M., Putnis, C.V. (1996) The role of magnesium in the crystallization of calcite and aragonite in a porous medium. *Journal of Sedimentary Research,* **66**, 482–491.

Ferris, F.G. (2000). Microbe-metal interactions in sediments. In:. *Microbial Sediments* (Ed. R.E. Riding and S.M. Awramik). pp. 121-126. Springer-Verlang, Berlin.

Folk, R.L. (1993) SEM imaging of bacteria and nannobacteria in carbonate sediments and rocks: *J. Sedimentary Petrology,* **63**, 990–999.

Ford, T.D. and **Pedley, M**. (1996) A review of the tufa and travertine deposits of the World. *Earth-Science Reviews,* **41,** 117–175.

Fratesi, S.E., Lynch, F.L., Kirkland, B.L. and **Brown, L.R.** (2004) Effects of SEM preparation techniques on the appearance of bacteria and biofilms in the Carter Sandstone. *J. Sedimentary Research,* **74**, 858–867.

Freytet, P. and **Plet, A.** (1996) Modern freshwater microbial carbonates: the Phormidium stromatolites (tufa-travertine) of southeastern Burgundy (Paris Basin, France). *Facies,* **34**, 219-238.

Freytet, P. and **Verrecchia, E.P.** (1998) Freshwater organisms that build stromatolites: a synopsis of biocrystallization by prokaryotic and eukaryotic algae. *Sedimentology,* **45**, 535–563.

Freytet, P. and **Verrecchia, E.P.** (1999) alcitic radial palisadic fabric in freshwater stromatolites: diagenetic and recrystallized feature or physicochemical sinter crusts?. *Sedimentology,* **45**, 535-563.

Fuchs, G., Thauer, R., Ziegler, H. and **Stichler, W.** (1979) Carbon isotope fractionation by *Methanobacterium thermoautotrophicum*. *Arch. Microbiol.,* **120**, 135-139.

Garcia-Pichel, F. (2002) Desert environments: biological soil crusts. In: *Encyclopedia of Environmental Microbiology.* (Eds. Bitton, G.), pp.1019–1023. John Wiley, New York.

Glover, C. and **Robertson, A.H.F.** (2003) Origin of tufa (coolwater carbonate) and related terraces in the Antalya area, SW Turkey. *Geol. J.,* **38,** 329–358.

Golubić, S. (1969) Cyclic and non-cyclic mechanisms in the formation of travertine. *Verh. Int. Ver. Theor. Ang. Limnol.,* **17**, 956–961.

Golubić, S., Violante, C., Plenković-Moraj, A. and **Grgasović, T.** (2008) Travertine and calcareous tufa deposits: insight into diagenesis. *Geologia Croatica,* **61**, 363-378.

Gradziński, M. (2010) Factors controlling growth of modern tufa: results of a field experiment. In: *Tufas and Speleothems: Unravelling the Microbial and Physical Controls* (Eds Pedley, H.M. and Rogerson, M) *Geological Society, London, Special Publications,* **336**, 143–191.

Guo, L. and **Riding, R.** (1998) Hot spring travertine facies and sequences, Late Pleistocene Rapolano Terme, Italy. *Sedimentology,* **45**, 163–180.

Hardikar, V.V. and **Matijevic, E.** (2001) Influence of ionic and nonionic dextrans on the formation of calcium hydroxide and calcium carbonate particles. *Colloids and Surfaces,* **186**, 23–31.

Hardy, R. and **Tucker, M. (1988)** *Techniques in Sedimentology* (Ed. M. Tucker), Blackwell Scientific Publications, Oxford. 394 pp.

Hazel and **Wilkinson** (2003) Fossil actinomycete filaments and fungal hyphae in dicotyledonous wood from the Eocene London Clay, Isle-of-Sheppey, Kent, England. *Botanical Journal of the Linnean Society,* **142,** 383–394.

Hudson, N.J., Baker, A. and **Reynolds, D**.(2007) Fluorescence analysis of dissolved organic matter in natural, waste and polluted waters – a review. *Rivers Res.*, **23**, 631–649.

Irion, G. and **Müller, G.** (1968) Mineralogy, petrology and chemical composition of some calcareous tufa from the Swäbische Alb, Germany. In: *Recent Developments in Carbonate Sedimentology in Central Europe* (Eds G. Müller and G.M. Friedman), pp. 157–171. Springer- Verlag, Berlin.

Janssen, A., Swennen, R., Podoor, N. and **Keppens, E.** (1999) Biological and diagenetic influence in recent and fossil tufa deposits from Belgium. *Sedimentary Geology,* **126**, 75–95.

Julia, R. (1983) Travertines. In: *Carbonate Depositional Environments* (Eds P.A. Schole, D.G. Bebout and C. Moore), AAPG Mem., **33**, 64–72.

Kano, A. and **Fujii, H.** (2000) Origin of gross morphology and internal texture of tufas of Shirokawa Town, Heime Prefecture, southwest Japan. *J. Geol. Soc. Japan,* **106**, 397-412.

Kano, A., Matsuoka, J., Kojo, T. and **Fujii, H.** (2003) Origin of annual laminations in tufa deposits, southwest Japan. *Palaeogeog., Palaeoclimatol., Palaeoecol.,* **191**, 243–262.

Kawai, T., Kano, A., Matsuoka, J., and **Ihara, T.** (2006) Seasonal variation in water chemistry and depositional processes in a tufa-bearing stream in SW-Japan, based on 5 years of monthly observations. *Chem. Geol*. **232**, 33–53.

Kempe S. and **Kazmierczak J.** (1990) Calcium carbonate supersaturation and the formation of in situ calcified stromatolites. In: *Facets of Modern Biogeochemistry*. (Eds. Ittekkot V.A., Kempe S., Michaelis W., Spitzy A.), pp. 255–278. Springer-Verlag, Berlin.

Kempe, S. and **Kazmierczak, J.** (1994) The role of alkalinity in the evolution of ocean chemistry, organization of living systems, and biocalcification processes. *Bull. Inst. Océanogr.* (Monaco) **13**, 61–117.

Konhauser K. (2007) *Introduction to Geomicrobiology*, Blackwell Publication. 425 pp.

Lian, B., Hu, Q., Chen, J., Ji, J. and **Teng, H.H**. (2007) Carbonate biomineralization induced by soil bacterium *Bacillus megaterium*. *Geoch. et Cosmoch. Acta*, **70**, 5522–5535.

Little, B., Wagner, P., Ray, R., Pope, R., and **Scheetz, R.** (1991) Biofilms: an ESEM evaluation of artifacts introduced during SEM preparation. *Journal of Industrial Microbiology*, **8**, 213–222.

Love, K. M. and **Chafetz, H.S.** (1988) Diagenesis of laminated travertine crusts, Arbuckle Mountains, Oklahoma. *J. Sed., Petrol.,* **58**, 441-445.

Marquardt, J. and **Palinska K. A.** (2007) Genotypic and phenotypic diversity of cyanobacteria assigned to the genus *Phormidium* (Oscillatoriales) from different habitats and geographical sites. *Arch. Microbiol.,* **187**, 397–413.

Martin-Algarra, A., Martin-Martin, M., Andreo, B., Julia, R. and Gonzalez-Gomez, C. (2003) Sedimentary patterns in perched springline travertines near Granada (Spain) as indicators of the paleohydrological and palaeoclimatical evolution of a karst massif. *Sed. Geol.*, **161**, 217–228.

Mastandrea, A., Perri, E., Russo, F., Spadafora, A. and **Tucker, M.E.** (2006) Microbial primary dolomite from a Norian carbonate platform (Northern Calabria, Southern Italy). *Sedimentology,* **53**, 465-480.

Merz, M.U.E. (1992) The biology of carbonate precipitation by cyanobacteria. *Facies*, **26**, 81–102.

Merz-Preiß, M. and Riding, R. (1999) Cyanobacterial tufa calcification in two freshwater streams: ambient environment, chemical thresholds and biological processes. *Sedimentary Geology,* **126,** 103–124.

Nealson, K.H. (1983) The microbial manganese cycle. In: *Microbial Geochemistry* (Ed. W.E. Krumbein), Blackwell, Oxford. 330 pp.

Ordóñez, S. and Garcia del Cura, M.A. (1983) Recent and Tertiary fluvial carbonates in Central Spain. In: *Ancient and Modern Fluvial Systems* (Eds J.D. Collinson and J. Lewin), Int. Assoc. Sedimentol. Spec. Publ., 6, 485–497.

Ordóñez, S., González-Martin, J.A., Garcia del Cura, M.A. and **Pedley, H.M.** (2005) Temperate and semi-arid tufas in the Pleistocene to Recent fluvial barrage system in the Mediterranean area: The Ruidera Lakes Natural Park (Central Spain). *Geomorphology*, **69**, 332–350.

Paerl, H.W., Steppe, T.F. and **Reid, R.P.** (2001) Bacterially-mediated precipitation in marine stromatolites. *Environmental Microbiology,* **3**, 123–130.

Patel-Sorrentino, N., Mounier, S., Lucas, Y. and **Benaim, J.Y.** (2004) Effects of UV-visible irradiation on natural organic matter from the Amazon basin. *Science of the Total Environment,* **321**, 231–239.

Pedley, H.M. (1990) Classification and environmental models of cool freshwater tufas. Sed. Geol., 68, 143–154.

Pedley, M. (1992) Freshwater (Phytoherm) reefs: the role of biofilms and their bearing on marine reef cementation. *Sed. Geol.,* **79**, 255–274.

Pedley, M. (2000) Ambient temperature freshwater microbial tufas. In: Microbial Sediments (Eds R. Riding and S.M. Awramik), pp. 179–186, Springer, Berlin.

Pedley, M. (2003) Tufas and Travertines. In: *Encyclopedia of Sediments and Sedimentary Rocks* (Ed. G.V. Middleton), pp. 753–755. Kluwer Academic Publishers, Dordrecht.

Pedley, H.M. (2009) Tufas and travertines of the Mediterranean region: a testing ground for freshwater carbonate concepts and developments. *Sedimentology,* **56,** 221–246.

Pedley, M., Ordóñez, S., Gonzalez-Martin, J.A. and Garcia del Cura, M.A. (1996) Does climate control the morphological fabric of freshwater carbonates? A comparative study of Holocene barrage tufas from Spain and Britain. *Palaeogeogr. Palaeoclimatol. Palaeoecol.,* **121**, 239–257.

Pedley, M., Gonzalez-Martin, J.A., Ordóñez, S. and Garcia del Cura, M.A. (2003) Sedimentology of Quaternary perched springline and paludal tufas: criteria for recognition, with examples from Guadalajara Province, Spain. *Sedimentology,* **50**, 23–44.

Pedley, H.M., Rogerson M. and **Middleton R.** (2009) Freshwater calcite precipitates from in vitro mesocosm flume experiments: a case for biomediation of tufas. *Sedimentology,* **56**, 511-527.

Pedley, H.M. and **Rogerson, M.** (2010) In vitro investigations of the impact of different temperature and flow velocity conditions on tufa microfabric. In: *Tufas and Speleothems: Unravelling the Microbial and Physical Controls* (Eds Pedley, H.M. and Rogerson, M) *Geological Society, London, Special Publications*, **336**, 193–210.

Pentecost, A. (1990) Calcification processes in algae and cyanobacteria. In: *Calcareus Algea and Stromatolites*. (Eds. R. Riding), pp. 3-20. Springer- Verlag, Berlin.

Pentecost, A. (1993) British travertines: a review. *Proc. Geol. Assoc.,* **104**, 23–39.

Pentecost, A. (2005) *Travertine*. Springer, Berlin, 445 pp.

Pentecost, A. and **Lord, T.C.** (1988) Postglacial tufas and travertines from the Craven district of Yorkshire. *Cave Sci.,* **15**, 15-19.

Pentecost, A. and **Spiro, B** (1990) Sable carbon and oxygen isotope composition of calcite associated with modern freshwater cyanobacteria and algae. *Geomicrobiol. J.,* **8**, 17-26.

Pentecost, A. and **Viles, H.A.** (1994) A review and reassessment of travertine classification. *Géogr. Phys. Quaternaire,* **48**, 305-314.

Pentecost, A., Viles, H.A., Goudie, A.S. and **Keen, D.H.** (2000) The travertine dams of Slade Brook, Gloucestershire: their formation and conservation. *Geology Today,* Jan., 2000.

Pentecost, A. and **Zhang, ZH**. (2008) Microfossils and geochemistry of some modern, Holocene and Pleistocene travertines from North Yorkshire and Derbyshire. *Proc. Yorkshire Geol. Soc.,* **57**, 79-94.

Perri, E. and **Tucker, M.** (2007) Bacterial fossils and microbial dolomite in Triassic stromatolites. *Geology,* **35**, 207–210.

Perri, E., Mastandrea, A., Neri, C. and **Russo, F.** (2003) A micrite-dominated Norian carbonate platform from Northern Calabria (Southern Italy). *Facies,* **49**, 101-118.

Reid, R.P. and **MacIntyre, I.G.** (2000) Microboring versus recrystallization: further insight into the micritization process. *Journal of Sedimentary Research,* **70**, 24–28.

Reitner, J. (1993) Modern cryptic microbialite/metazoan facies from Lizard Island (Great Barrier Reef, Australia) formation and concepts. *Facies,* **29**, 2–40.

Reitner, J., Gautret, P., Marin, F. and **Neuweiler, F.** (1995) Automicrites in modern marine microbialite. Formation model via organic matrices (Lizard Island, Great Barrier Reef, Australia). *Bull. Inst. Océanogr. (Monaco) Numéro Spécial*, **14**, 237–264.

Riding, R. (1991) Classification of microbial carbonates. In: *Calcareous Algae and Stromatolites*. (Eds. Riding, R), pp. 21–51. Springer-Verlag, New York.

Riding, R. (2000) Microbial carbonates: the geological record of calcified bacterial–algal mats and biofilms. *Sedimentology*, **47**, 179–214.

Rodriguez-Navarro, C., Jimenez-Lopez, C., Rodriguez-Navarro, A., Gonzales-Munoz, M.T. and **Rogriguez-Gallego, M.** (2007). Bacterially mediated mineralization of vaterite. *Geoch. et Cosmoch. Act.,* **71**, 1197–1213.

Rogerson, M., Pedley, H.M., Wadhawan, J.D. and **Middleton, R.** (2008) New insights into biological influence on the geochemistry of freshwater carbonate deposits. *Geochimica et Cosmochimica Acta,* **72,** 4976–4987.

Rogerson, M., Pedley, H.M. and **Middleton, R.** (2010) Microbial influence on macroenvironment chemical conditions in alkaline (tufa) streams: perspectives from in vitro experiments. In: *Tufas and Speleothems: Unravelling the Microbial and Physical Controls* (Eds Pedley, H.M. and Rogerson, M) *Geological Society, London, Special Publications,* **336**, 65–81.

Sánchez-Román, M., Vasconcelos, C., Schmid, T., Dittrich, M., McKenzie, J.A., Zenobi, R. and **Rivadeneyra, M.A.** (2008) Aerobic microbial dolomite at the nanometer scale: Implications for the geologic record. *Geology,* **36**, 879–882.

Schagerl, M. and **Kerschbaumer, M.** (2009) Autecology and morphology of selected *Vaucheria* species (Xanthophyceae). *Aquat Ecol.,* **43**,295–303.)

Schidlowski, M. (2000) Carbon isotopes and microbial sediments. In: *Microbial Sediments* (Ed. R.E. Riding and S.M. Awramik). pp. 84-95. Springer-Verlang, Berlin.

Shiraishi, F., Bissett, A., de Beer, D., Reimer, A. and **Arp, G.** (2008a) Photosynthesis, Respiration and Exopolymer Calcium-Binding in Biofilm Calcification (Westerhöfer and Deinschwanger Creek, Germany). *Geomicrobiology Journal,* **25**, 83 – 94.

Shiraishi, F., Reimer, A., Bissett, A., de Beer, D. and **Arp, G.** (2008b) Microbial effects on biofilm calcification, ambient water chemistry and stable isotope records in a highly supersaturated setting (Westerhöfer Bach, Germany). *Palaeogeogr. Palaeoclimatol. Palaeoecol.,* 262, 91-106**.**

Soetaert, K., Hofmann, A.F., Middelburg, J.J., Meysman, F.J.R. and **Greenwood, J. (**2007) The effect of biogeochemical processes on pH. *Mar. Chem.,* **105**, 30–51.

Sprachta, S., Camoin, G., Golubic, S. and **Le Campion, T.** (2001) Microbialites in a modern lagoonal environment: nature and distribution, Tikehau atoll (French Polynesia). *Palaeog., Palaeocl., Palaeoecol.,* **175**, 103–124.

Spadafora, A., Perri, E., Mckenzie, J.A. and **Vasconcelos, C.** (2010) Microbial biomineralization processes forming modern Ca:Mg carbonate stromatolites. *Sedimentology,* **57**, 27–40.

Spiro, B. and **Pentecost, A.** (1991) One day in the life of a stream- a diurnal inorganic carbon mass balance for a travertine-depositing stream (Waterfall Beck, Yorkshire), *Geomicrobiol. J.,* **9**, 1-11.

Stedmon, C.A., Markager, S. and **Bro, R.** (2003) Tracing dissolved organic matter in aquatic environments using a new approach to fluorescence spectroscopy. *Marine Chemistry,* **82**, 239–254.

Stumm,W. and **Morgan, J.J.** (1996) *Aquatic Chemistry*. John Wiley & Sons, NewYork.1022 pp.

Thompson, J.B., Schultze-Lam, S., Beveridge, J. and Des Marais, D.J. (1997) Whithing events: biogenic origin due to the photosynthetic activity of cyanobacterial picoplankton. *Limnology and Oceanography*, **42**, 133–141.

Trichet, J. and **Défarge, C.** (1995) Non-biologically supported organomineralization. *Bull. Inst. Océanogr. (Monaco) Numéro Spécial,* **14**, 203–236.

Tucker, M.E. (1991) Sequence stratigraphy of carbonate evaporite basins: models and applications to the Upper Permian (Zechstein) of northeast England and adjoining North Sea. *J. Geol. Soc. London,* **148**, 1019–1036.

Tucker, M.E. (2001) *Sedimentary Petrology*. Blackwell Science, Oxford, 262 pp.

Tucker, M. and **Wright, P.** (1990) *Carbonate Sedimentology*. Blackwell Science, Oxford, 482 pp.

Tucker, M.E., Gallagher, J. and **Leng, M**. (2009) Are beds in shelf carbonates millennial-scale cycles? An example from the mid-Carboniferous of NE England. *Sed. Geol.,* **214**, 19–34.

Turner, E.C. and **Jones, B**. (2005) Microscopic calcite dendrites in cold-water tufa: implications for nucleation of micrite and cement. *Sedimentology,* **52,** 1043–1066.

Vasconcelos, C.,Warthmann, R., McKenzie, J., Visscher, P.T., Bittermann, A.G. and **van Lith, Y.** (2006) Lithifying microbial mats in Lagoa Vermelha, Brazil: Modern Precambrian relics?. *Sedimentary Geology*, **185**, 175–183.

Verrecchia, E., A. Yair, G.H. Kidron and **Verrecchia, K.,** (1995). Physical properties of the psammophile cryptogamic crust and their consequence to water regim of sandy soil, north-western Negev Desert. *Israel. J. Arid Environ*., 29, 179-223.

Viles, H.A. and **Goudie, A.S.** (1990a). Tufas, travertines and allied carbonate deposits. *Progr. Phys. Geogr.*, **14**, 19– 41.

Viles, H.A. and **Goudie, A.S.** (1990b). Reconnaissance studies of the tufa deposits of the Napier Range, NW Australia. *Earth Surf. Proc. and Landf.,* **15**, 425–443.

Viles, H.A., Taylor, M.P., Nicoll, K. and **Neumann, S.** (2007) Facies evidence of hydroclimatic regime shifts in tufa depositional sequences from the arid Naukluft Mountains, Namibia. *Sedimentary Geololgy,***195**, 39-53.

Visscher, P.T., Reid, R.P., Bebout, B.M., Hoeft, S.E., Macintyre, I.G. and **Thompson Jr., J.** (1998) Formation of lithified micritic laminae in modern marine stromatolites (Bahamas): the role of sulfur cycling. *American Mineralogist,* **83**, 1482–1491.

Visscher, P.T., Reid, R.P. and **Bebout, B.M.** (2000) Microscale observations of sulfate reduction: correlation of microbial activity with lithified micritic laminae in modern marine stromatolites. *Geology*, **28**, 919–922.

Violante, C., Ferreri, V., D'Argenio, B. and Golubić, S. (1994) Quaternary travertines at Rocchetta a Volturno (Isernia, Central Italy). Facies analysis and sedimentary model of an organogenic carbonate system. In: *Pre-Meeting Fieldtrip Guidebook, A1* (Eds G. Carannante and R. Tonielli), pp. 3–23. Int. Assoc. Sedimentol., Ischia'94, 15th Regional Meeting, Italy. De Frede, Naples, Italy.

Winsborough B.M. and **Golubic S.** (1987) The role of diatoms in stromatolite growth: two examples from modern freshwater settings. *J. Phycol.*, **23**, 195-201

Winsborough, B.M. (2000) Diatoms and benthic microbial carbonates. In: *Microbial Sediments* (Eds R. E. Riding and S.M. Awramik), pp. 76–83, Springer-Verlang, Berlin.

Zavarzin, G.A. (2002) Microbial geochemical calcium cycle. *Microbiology*, **71**, 5–22.